Aus dem Institut für Systemische Neurowissenschaften
der Heinrich-Heine-Universität Düsseldorf
Direktor: Univ.-Prof. Dr. med. Simon B. Eickhoff

Within- and between-network functional connectivity in Parkinson's disease as potential biomarkers - systematic analysis and potential challenges

Dissertation

zur Erlangung des Grades eines Doktors der Medizin
der Medizinischen Fakultät der Heinrich-Heine-Universität Düsseldorf

vorgelegt von
Miriam Dodegge
2025

Als Inauguraldissertation gedruckt mit Genehmigung der Medizinischen Fakultät der Heinrich-Heine-Universität Düsseldorf

gez.:
Dekan: Prof. Dr. med. Nikolaj Klöcker
Erstgutachter: Univ.-Prof. Dr. med. Simon B. Eickhoff
Zweitgutachter: Univ.-Prof. Dr. med. Dipl.-Inform. Julian Caspers

Für meine Eltern

Summary (German)

Die Parkinson-Krankheit (PD) ist eine der häufigsten neurodegenerativen Erkrankungen, jedoch ist die diagnostische Genauigkeit durch das Fehlen sensitiver und spezifischer Biomarker begrenzt. Ein vielversprechender Ansatz zur Entwicklung von Biomarkern ist die Analyse PD-spezifischer Veränderungen der neuronalen funktionellen Konnektivität im Ruhezustand (rsFC) mithilfe der funktionellen Magnetresonanztomographie (fMRT). Verschiedene Studien berichteten über Veränderungen in der funktionellen Konnektivität (FC) im Default Mode Network (DMN, u.a. mit selbstbezogenen Gedanken und Tagträumen assoziiert) und in Task-positiven Networks (TPNs, bei der Ausführung von Aufgaben aktiv). Die Literatur ist jedoch häufig widersprüchlich.

Ziel der vorliegenden Studie war die Evaluierung der rsFC von metaanalytisch definierten Netzwerken als potenzielle Biomarker für PD und die Identifizierung möglicher Ansatzpunkte für die Biomarker-Forschung. Dabei wurde die FC des DMN, eines gesamten Gehirnnetzwerks (WBN) und von 11 metaanalytisch definierten TPNs in zwei unabhängigen Datensätzen mit insgesamt 66 PD-Patienten und 67 gesunden Kontrollpersonen systematisch untersucht. Dabei kamen einfache Mittelwerte der FC und graphentheoretische Kennzahlen zum Einsatz. Beide Datensätze wurden unabhängig voneinander analysiert, um die Replizierbarkeit der Ergebnisse zu überprüfen.

Im ersten Datensatz zeigte sich, dass das DMN bei PD-Patienten weniger stark und effizient vernetzt war. Die mittlere FC, die *global efficiency* und die *diffusion efficiency* des DMN waren verringert und mehrere Messgrößen korrelierten negativ mit der motorischen Symptomlast. Auch innerhalb mehrerer TPNs (u.a. zwei motorische Netzwerke) war die FC reduziert. Die Analyse der Interaktionen zwischen DMN und TPNs/WBN ergab Hinweise auf einen weniger effizienten Informationsfluss, z.B. zwischen dem DMN und dem *motor execution* Netzwerk bzw. dem *vigilant attention* Netzwerk. Darüber hinaus wurden veränderte Integrations- und Segregationsmuster des DMN bei PD festgestellt. Nur ein kleiner Teil der Ergebnisse aus dem ersten Datensatz wurde im zweiten Datensatz repliziert, vermutlich aufgrund der heterogenen Natur der PD. Insgesamt gab es Hinweise darauf, dass rsFC-Analysen von metaanalytischen Netzwerken ein möglicher Ausgangspunkt für die von Biomarker-Entwicklung bei PD sein könnten. Allerdings wirft die geringe Übereinstimmung der Ergebnisse in den beiden Datensätzen Fragen zur Zuverlässigkeit der Befunde auf. Zusammen mit früheren Studienergebnissen legt die Studie nahe, dass eine vertiefte Untersuchung von PD-Subtypen erforderlich ist, um das Potenzial von FC-basierten Biomarkern für die Parkinson-Diagnostik weiter zu erforschen und zu bewerten.

Summary (English)

Parkinson's disease (PD) is among the most prevalent neurodegenerative diseases. However, due to a lack of sensitive and specific biomarkers, diagnostic accuracy remains relatively low. One promising avenue for the development of biomarkers is the analysis of functional magnetic resonance imaging (fMRI) to detect PD specific changes in neural resting-state functional connectivity (rsFC) patterns. Previous studies found alterations of functional connectivity (FC) in the default mode network (DMN, associated with self-referential thoughts and mind-wandering) and in task-positive networks (TPN, involved in externally directed tasks), however the literature is often contradictory.

The aim of the study was to help to elucidate whether rsFC of meta-analytic networks has the potential to serve as a diagnostic biomarker in PD, and to identify potential starting points for further biomarker research. To this end, rs-fMRI data from two independent datasets from a total of 66 PD patients and 67 healthy controls (HC) were analyzed. Within- and between-network FC of the DMN, a whole-brain network (WBN) and 11 meta-analytically defined TPNs, covering a large set of cognitive functions, were systematically assessed via variations of simple mean FC and graph-theoretical measures. Both datasets were investigated independently to evaluate replicability of results.

In the first dataset, there were signs of a less strongly and less efficiently connected DMN in PD compared to HC. The average FC, global efficiency and diffusion efficiency of the DMN were decreased, and several measures correlated negatively with motor symptom severity. FC was also decreased within several TPNs, including the two investigated motor networks. The analysis of the interaction of the DMN and the TPNs/WBN revealed signs of a less efficient information flow between networks (e.g., between DMN and motor execution network or DMN and vigilant attention network). Furthermore, there were signs of altered integration and segregation patterns of the DMN in PD. Intriguingly, only a small portion of the results from the first dataset was replicated in the second dataset, probably due to the heterogeneous nature of PD. Overall, there is some evidence for the suitability of rsFC measures as a starting point for the development of new biomarkers in PD. However, the small overlap of results between the two datasets raises concerns about the reliability and generalizability of PD-related FC alterations. Overall, taken together with previous findings, the study indicates the need for further investigations into PD subtypes to fully explore and evaluate the potential to develop FC-derived biomarkers in PD.

List of abbreviations

ALE	activation likelihood estimation
ANCOVA	analysis of covariance
ATP	adenosine triphosphate
BET	mean node betweenness centrality vector
bnFC	average between-network functional connectivity
BOLD-signal	blood oxygen level dependent signal
CEN	central executive network
cf.	confer to
CogAC	cognitive action control network
CogAR	cognitive action regulation network
combFC	average combined network functional connectivity
DAT	dopamine transporter
Data-DU	dataset assessed in Düsseldorf
Data-PR	dataset assessed in Prague
DE	mean global diffusion efficiency
D-Hb	deoxygenated hemoglobin
DMN	default mode network
dMPFC	dorsal medial prefrontal cortex
ECC	mean nodal eccentricity
e.g.	*exempli gratia,* for example
eMDN	extended multiple demand network
EmoSF	emotional scene and face processing network
eSAD	extended social-affective default network
FDR	false discovery rate
FC	functional connectivity
fMRI	functional magnetic resonance imaging
FoV	field of view
GE	global efficiency
H&Y	Hoehn & Yahr disease stage
HC	healthy control
Hz	hertz

ICA	independent component analysis
IPC	inferior parietal cortex
MCI	mild cognitive impairment
MDN	multiple demand network
MDS	Movement Disorders Society
MDS-UPDRS-III OFF	motor part (part III) of the Movement Disorders Society Unified PD rating scale in medical off-state
mm	millimeter
mm^3	cubic millimeter
MNI	Montreal Neurological Institute
MoCa	Montreal Cognitive Assessment
MotorEx	motor execution network
MotorPerc	perceptuo-motor network
MPFC	medial prefrontal cortex
MPRAGE	magnetization-prepared rapid gradient echo
MPTP	1-methyl-4-phenyl-1,2,3,6- tetrahydropyridine
MRI	magnetic resonance imaging
ms	millisecond
MultiTask	multitasking network
O-Hb	oxygenated hemoglobin
PD	Parkinson’s disease
PCC	posterior cingulate cortex
PPC	mean positive participation coefficient
REM	rapid-eye-movement
Rew	reward-related decision-making network
ROI	region of interest
rsFC	resting-state functional connectivity
SD	standard deviation
SMA	supplementary motor area
ST	mean nodal strength of positive/negative weights
T	tesla
TE	echo time

thrX	no functional connectivity threshold level applied
thr0	functional connectivity threshold at 0
thr25	functional connectivity threshold at 0.25
TI	inversion time
TPN	task-positive network
TR	repetition time
UPDRS	Unified PD rating scale
UPDRS-III OFF	motor part (part III) of the Unified PD rating scale in medical off-state
VigAtt	vigilant attention network
vMPFC	ventral medial prefrontal cortex
WBN	whole-brain network
WM	working memory network
wnFC	average within-network functional connectivity

Table of contents

1 Introduction

1.1 Parkinson's disease

Parkinson's disease (PD) is a progressive neurodegenerative disease, primarily characterized as a motor disorder. The disease is caused by a loss of dopaminergic neurons in the *pars compacta* of the *substantia nigra*, a brain region crucial for the initiation and coordination of movements. Pathophysiologically, alpha-synuclein aggregates, called Lewy-bodies, are responsible for the neural loss, first occurring in the upper brainstem, then spreading throughout the brain over time (Braak *et al.* 2003; Goedert *et al.* 2013).

1.1.1 Epidemiology

Parkinson's disease affects approximately 1 % of the population above the age of 60 (Tysnes & Storstein 2017). Men seem to be more at risk than women (Tolosa *et al.* 2021). The disease onset usually occurs at 65 to 70 years, but earlier onsets are possible, especially in genetically predisposed individuals (Tysnes & Storstein 2017). When the condition was first described by James Parkinson in 1817 as "shaking palsy" (Parkinson 2002), it was a rare disease. However, over the course of the last two centuries, it has become more common and the prevalence is still rising (Ben-Shlomo *et al.* 2024; Dorsey *et al.* 2018). Between 1990 and 2016, an increase in deaths (161 %), disability-adjusted life-years (148 %) and prevalence (145 %) of PD has been reported (GBD 2016 Neurology Collaborators 2019). This increase is caused by increasing global life expectancy as well as environmental factors. Researchers predict that this increase will continue in the next generation (Dorsey *et al.* 2018; GBD 2016 Parkinson's Disease Collaborators 2018). PD is now one of the leading causes of neurological disability (Dorsey *et al.* 2018; GBD 2016 Neurology Collaborators 2019). These numbers illustrate that an increase in research efforts is needed to meet the challenges that arise with increasing PD prevalence.

1.1.2 Pathophysiology and etiology

The pathological hallmark of PD are aggregates of misfolded proteins, called Lewy bodies, discovered by Fritz Heinrich Lewy in 1912 (Engelhardt & Gomes 2017). In 1990, alpha-synuclein was identified as the major component of these neural inclusions leading to cell loss, especially in the *substantia nigra* (Braak *et al.* 2003; Goedert *et al.* 2013; Tolosa *et al.* 2021). To date, the post-mortem proof of the presence of Lewy bodies is the only way to definitively diagnose PD (Bloem *et al.* 2021). In 2003, Braak and colleagues proposed a staging scheme of PD based on their discovery that Lewy bodies seem to follow a systematic pattern of spread throughout the brain (Braak *et al.* 2003). They found that in early stages, Lewy bodies were present in the dorsal motor nucleus of the glossopharyngeal and vagal nerves as well as in the anterior olfactory nucleus. From here, the misfolded protein-aggregates spread to other brain regions in a presumably prion-like fashion (Braak *et al.* 2003; Goedert *et al.* 2013; Steiner *et al.* 2018). This, however, does not apply to all PD cases, underlining the heterogeneous nature of the disease.

Genetic predispositions also play an important role in PD etiology (Blauwendraat *et al.* 2020; Bloem *et al.* 2021). Mutations in several genes have been found to be associated with PD. These mutations can be differentiated into two different categories: (1) High risk mutations, being rather rare but showing a high penetrance and often occurring in familial PD and (2) low risk mutations, being rather common but showing smaller effects, often present in what seems to be sporadic PD (Blauwendraat *et al.* 2020; Bloem *et al.* 2021). Although these mutations increase the risk of developing PD, research suggests that other factors are needed to initiate the disease. The most important risk factor is age. Additionally, environmental factors, such as the exposure to pesticides, smoking (risk factors) or caffeine consumption (protective factor), play a role (Blauwendraat *et al.* 2020; Bloem *et al.* 2021).

Recent research has propagated the existence of a gut-brain axis, proposing an important role of the gastrointestinal system in the etiology of PD (Klann *et al.* 2021).

1.1.3 Clinical symptoms

By definition, Parkinson's disease is marked by the presence of bradykinesia in combination with either rigidity or rest tremor with a frequency of 4 to 6 Hz. Together, these symptoms are called parkinsonism (Gibb & Lees 1988; Jankovic 2008; Postuma *et al.* 2015). These cardinal symptoms are often accompanied by a loss of postural stability, usually occurring later in the course of the disease (Jankovic 2008). These motor symptoms result from the loss of neurons within the substantia nigra, impairing the basal ganglia circuit, normally involved in the initiation of motor functions. Secondary motor symptoms are for example hypomimia, dysarthria, micrographia or the freezing phenomenon, where patients literally freeze in the middle of motion (Jankovic 2008).

With regard to the importance of motor disability, PD is classified primarily as a motor disease. However, non-motor symptoms also play an important role. Among these are autonomic dysfunction, a cognitive impairment that can develop into dementia, sleep disorders, anosmia and muscle pain (Jankovic 2008). The PD defining symptoms often are preceded by a prodromal stage with predominantly autonomic symptoms, often preceding the motor symptoms by several years. Among these symptoms, hyposmia, constipation, depression and idiopathic rapid-eye-movement (REM) sleep behavior disorder are the most common (Mahlknecht *et al.* 2015). Idiopathic REM sleep behavior disorder, characterized by excessive movements during REM sleep, a sleeping phase that is usually characterized by atonia, seems to be the best predictor for the development of PD, or other synucleinopathies (Mahlknecht *et al.* 2015).

Autopsy studies suggest the existence of an asymptomatic stage in which Lewy bodies are present in the brain, but none of the abovementioned symptoms is experienced by the patient. It is estimated that motor symptoms begin when as much as 40 % of the substantia nigra is degenerated (Mahlknecht *et al.* 2015).

Cardinal symptoms	Bradykinesia
	Rigidity
	Rest tremor (4 to 6 Hz)
	Postural instability

Secondary motor symptoms	Hyposmia Dysarthria Micrographia Festination Freezing of gait
Non-motor symptoms	Autonomic dysfunction Cognitive impairment Dementia REM sleep disorder Anosmia Pain Urinary urgency Constipation Sexual dysfunction Hypotension Anxiety Depression Color vision impairment Dysexecutive syndrome
Frequent prodromal symptoms	Hyposmia Constipation Depression Idiopathic REM sleep behavior disorder

Table 1. Symptoms of Parkinson's disease. Modified after (Jankovic 2008; Tolosa *et al.* 2021)

1.1.4 Diagnosis

Until today, PD diagnosis relies on the evaluation of a patient's symptoms by a clinician. This reliance on the expertise of the examining clinician entails subjectivity and makes diagnosis difficult, especially in early disease stages (Bloem *et al.* 2021; Postuma *et al.* 2015). Therefore, there is a large research interest in developing biomarkers to improve the diagnostic accuracy for PD,

especially in early stages, to provide better and earlier treatments for the affected patients.

The diagnostic challenge resides in the overlap of PD symptoms with other neurodegenerative diseases. Among the most common misdiagnosed differential diagnoses are atypical parkinsonian syndromes, essential tremor, Alzheimer's disease or secondary parkinsonisms (e.g., drug induced, vascular or infectious) (Tolosa *et al.* 2021).

The UK Parkinson's Disease Society Brain Bank clinical diagnostic criteria propose a three-step approach for the clinical diagnosis of PD (for detailed criteria, see Table 2). In the first step, the presence of parkinsonism (bradykinesia plus either rest tremor or rigidity, or both) is assessed. In the second step, the clinician checks for exclusion criteria, namely symptoms or aspects in patient history that make secondary parkinsonism or an atypical Parkinsonian syndrome (such as corticobasal degeneration, supranuclear palsy and multiple system atrophy) more probable. If no other probable explanation for the parkinsonism is found, the clinician screens for supportive symptoms for the diagnosis of PD, such as unilateral onset, response to levodopa (cf. Table 2), of which at least 3 must be present to allow the diagnosis of PD (compare Gibb & Lees 1988; Hughes *et al.* 1992). Following this pattern, the accuracy of PD diagnosis is estimated to be around 80 % based on autopsy studies (Hughes *et al.* 1992; Rizzo *et al.* 2016; Schrag *et al.* 2002).

Step 1	Presence of parkinsonism, defined as bradykinesia combined with at least one of the listed symptoms	Rigidity Rest tremor (frequency: 4 to 6 Hz) Postural instability, not otherwise explained
Step 2	Checking for listed exclusion criteria, hinting at different etiology	History of head injury History of strokes History of encephalitis Oculogyric crisis Remission of symptoms Intake of neuroleptic medication

		Only one body side attained after 3 years Early autonomic dysfunction Early signs of severe dementia with speech and memory impairment or apraxia No response to high-dose levodopa > 1 affected relative Supranuclear gaze paresis Signs of cerebellar impairment Babinski sign Tumor or *hydrocephalus communicans* in neuroimaging MPTP exposure
Step 3	Presence of listed supportive criteria for Parkinson's disease; ≥ 3 for definite diagnosis	Unilateral onset Presence of rest tremor Progression of the disease Persistent asymmetry of the symptoms in Progressive disease Good response to treatment with levodopa (70 to 100 %) Response to levodopa over the course of min. 5 years Disease progression > 10 years Presence of severe levodopa-induced dyskinesia

Table 2. UK Parkinson's Disease Society Brain Bank clinical diagnostic criteria. Modified after (Deuschl *et al.* 2016; Gibb & Lees 1988; Hughes *et al.* 1992), MTPT = 1-methyl-4-phenyl-1,2,3,6-tetrahydropyridine.

To improve diagnostic accuracy, the goal is to standardize clinical assessment, in order to improve inter-rater reliability and the diagnostic process for less experienced clinicians. Hence, the recently validated Movement Disorders Society (MDS) clinical diagnostic criteria for PD suggest a four-step approach, based on

the UK Parkinson's Disease Society Brain Bank clinical diagnostic criteria (Postuma *et al.* 2015). Through the standardized symptom assessment, the criteria make a distinction in two levels of diagnostic certainty: (1) "Clinically Established PD", maximizing specificity and (2) "Clinically Probable PD", creating a balance between high specificity and sensitivity (Postuma *et al.* 2015). The criteria define absolute exclusion criteria which rule out a PD diagnosis. Additionally, they provide a list of red flags and supportive criteria. Red flags describe symptoms that make a PD diagnosis less probable and have to be outweighed by supportive criteria in order to allow the diagnosis of "Clinically Probable PD".

The clinical diagnosis can be supported by imaging strategies. A normal structural MRI favors PD over atypical parkinsonian syndromes, where specific structural changes can often be seen (Tolosa *et al.* 2021). Additionally, the diagnosis can be supported by dopamine transporter (DAT) imaging, which can detect dopaminergic degeneration (Brücke & Brücke 2022). A normal DAT scan rules out a PD diagnosis and favors differential diagnoses such as essential tremor (Brücke & Brücke 2022; Postuma *et al.* 2015).

As the diagnostic accuracy of PD still remains relatively low, different avenues for the development of new biomarkers for PD diagnosis are being explored. One promising research avenue is the analysis of functional brain networks, such as the well studied default mode network (DMN), assessed via functional magnetic resonance imaging (fMRI) in order to detect PD specific connectivity patterns. In the present study, a variety of functional brain networks assessed via fMRI was analyzed in two cohorts of PD patients and healthy controls. The neuroscientific and methodological foundations of these analyses will be explained in the following paragraphs.

1.2 Neural connectivity

1.2.1 Structural connectivity

The brain is arguably the most complex organ of the human body. It has a mostly invariant structure, composed of different types of neurons, however it can perform an enormous variation of tasks (Park & Friston 2013). The diverse functionalities range from unconscious activities, like controlling crucial biological functions such as breathing and body temperature, to highly complex conscious work such as

solving math problems and navigating through large cities. In contrast to other organs, the brain is able to learn complex new skills to adapt to environmental challenges. An immense research effort is put into answering the question of how such complex and dynamic functions are possible based on the mostly fixed neural structure (Park & Friston 2013). The neural structure resembles a complex network of myriads of neurons, organized in gray and white matter. The axons emerging from the perikarya in the gray matter travel to other cortical or subcortical brain regions, building the white matter. Neurons that are located next to each other communicate using electrical or chemical signals that they exchange via synapses. These structural connections are also called structural connectivity (Sporns 2013).

Historically, neurological disorders were distinguished into “cortical syndromes”, resulting from gray matter lesions, and “conduction syndromes", caused by white matter lesions (Geschwind 1965). Since then, disconnection of brain regions by damage to the cortico-cortical fibers has been studied as a possible explanation for various neurologic symptoms. In the following decades, interruptions of such cortico-cortical fibers have also been studied in more complex behavioral symptoms, e.g., in the context of Alzheimer’s disease (Hof & Bouras 1991). Similarly, different symptoms in PD (motor as well as non-motor symptoms) have been investigated with regard to interrupted and hence disconnected cortico-cortical and cortico-striato-thalamo-cortical fibers (Cronin-Golomb 2010). In comparison to the perception of PD simply as a basal ganglia or midbrain dysfunction, the definition of PD as a disconnection syndrome helps to understand complex cognitive symptoms. Even though the disease starts in the basal ganglia, the pathology also affects brain regions that have afferent or efferent connections to the basal ganglia. For example, patients with accentuation of motor symptoms in the left body side (with predominant pathology in the right midbrain) more often develop visual memory deficits. Vice versa, patients with right-sided symptoms (corresponding to left midbrain pathology) more often exhibit deficits in verbal memory (Amick *et al.* 2006; Cronin-Golomb 2010).

1.2.2 Functional connectivity

In contrast to the obvious structural connectivity between brain regions, functional connectivity refers to the temporal synergy between spatially distant brain regions

(Friston 1994) and can be quantified by correlations between activity signals, e.g., measured by magnetic resonance imaging, electroencephalography or magnetoencephalography (van den Heuvel & Hulshoff Pol 2010). If the activity pattern of two brain regions shows a high temporal correlation, these regions can be considered as functionally connected. Functional connectivity (FC) can be observed in regions that are at the same time structurally connected, but also between brain regions without a strong structural connection (Eickhoff & Müller 2015). In general, functional and structural connectivity are highly correlated (van den Heuvel & Sporns 2013; Zimmermann *et al.* 2019). A set of brain regions that exhibit similar activity patterns form a functional brain network (Sporns 2013).
One brain region can participate in different networks, depending on the required functionality (Dragomir & Omurtag 2023; Sporns & Betzel 2016). Functional connectivity can be found during the performance of cognitive tasks (task-based FC) but also when an individual is at rest (resting-state FC, cf. section 1.3.2). Both forms of functional connectivity have been extensively studied in healthy individuals and in patients with various neurological and psychiatric diseases and can be measured with the help of fMRI, which will be introduced in the following paragraph.

1.3 Functional magnetic resonance imaging

1.3.1 Principles of functional magnetic resonance imaging

Functional magnetic resonance imaging is an imaging technique which can measure brain activation by detecting differences in regional cerebral oxygen consumption (Glover 2011). It is a popular tool for the investigation of functional connectivity. The principle of fMRI-imaging is based on the phenomenon that an activated brain region has an increased energy need in comparison to an inactivated brain region. In the blood, oxygen is transported by hemoglobin, which exists in an oxygenated (O-Hb) and a deoxygenated form (D-Hb). O-Hb is diamagnetic and can not be magnetically differentiated from the surrounding brain tissue. D-Hb however has different magnetic properties (Pauling & Coryell 1936). It is paramagnetic and therefore can be detected by the scanner (Thulborn *et al.* 1982). If the neural activity in a specific brain region increases (e.g., to perform a motor task), the involved neurons need more energy. To meet the increased

energy-demand, locally stored oxygen is used to gain energy through oxygenation of glucose, a process called glycolysis, in order to produce energy rich adenosine triphosphate (ATP; Dienel 2019). As oxygen consumption increases, the ratio of O-Hb (decrease) and D-Hb (increase) changes, indicating a transient oxygen deficit. The increased oxygen consumption triggers an increase in regional blood flow within seconds, leading again to a change in the ratio of O-Hb (increase) and D-Hb (decrease) (Glover 2011). The altered ratio of O-Hb and D-Hb results in a magnetic field. This in turn triggers alterations in T2 and T2* relaxation times in the MRI-scanner, reflecting the initial brain activation (Glover 2011). The detected signal is called the blood oxygen level dependent (BOLD) signal and was first discovered in rats and then in humans by Ogawa and colleagues (Ogawa *et al.* 1990a, 1990b).

fMRI imaging can be performed on a standard MRI scanner, is a non-invasive technique and is considered a safe technique that can be used in children and adults alike (Gore 2003). It therefore quickly became a popular tool and is for example used for surgical planning, therapy monitoring or as a biomarker (Glover 2011). While the spatial resolution of fMRI is good compared to other neuro-imaging-techniques such as magnetoencephalography (a resolution below 3 cubic millimeters is possible (Farahani *et al.* 2019)), the temporal resolution is rather poor, because the hemodynamic response triggered by brain activation is delayed (Lv *et al.* 2018). Furthermore, the BOLD signal can be influenced by pathologies such as structural brain abnormalities, e.g., after an ischemic stroke or by alterations in blood flow in patients with arteriosclerotic vascular changes (Lake *et al.* 2016).

1.3.2 Resting-state functional magnetic resonance imaging

In the beginning, fMRI was used to map brain activity following a specific task or stimulus, targeting a specific brain function, e.g., motor system, visual system, auditory system (task-based fMRI). Biswal and colleagues later discovered consistent spontaneous low frequency BOLD signal fluctuations (0.01 to 0.08 Hz) in the resting-state that showed correlations in functionally related brain regions even in the absence of an active task (e.g., bilateral sensorimotor cortices, (Biswal *et al.* 1995; Biswal 2012; Smitha *et al.* 2017)). To acquire resting-state fMRI data, individuals are asked to lie in the scanner and simply rest with their eyes closed or

fixating a pre-defined point, without focusing on anything specific and without falling asleep for the duration of 5 or more minutes (Power *et al.* 2014; Smitha *et al.* 2017).

With the development of the resting-state fMRI-technique, image acquisition in the clinical setting became easier because the patients don't need to be able to follow task instructions (Lv *et al.* 2018). Therefore, resting-state fMRI-scanning can also be used for children, unconscious individuals or patients with disabling diseases that would make following a specific task paradigm difficult (Smitha *et al.* 2017). This advantage also applies to PD patients who can struggle with motor tasks and tasks targeting cognitive functions, depending on the present disease stage.

It was found that functional networks that can be seen during task-based fMRI (so-called task-positive networks, TPN) also appear during resting-state fMRI (Power *et al.* 2014). One of the first networks that was consistently observed in rs-fMRI data was the default mode network (DMN), which explicitly shows increased activity in the resting-state (cf. section 1.4.1; Power *et al.* 2014). Following the discovery of the DMN, an increasing amount of studies aimed at reproducing findings (i.e., functional networks) from task-based fMRI studies using resting-state fMRI (Power *et al.* 2014). The discovery of resting-state FC simplified FC research, because multiple networks could be analyzed simultaneously, requiring only one scanning session. In task-based fMRI, on the contrary, two different tasks and scanning sessions would be necessary to investigate two different functions (e.g., motor function vs. somatosensory function; Smitha *et al.* 2017). With fMRI, even analyzes at the whole-brain level became possible, providing valuable insights into the functional architecture of the brain as a whole (Baggio & Junqué 2019).

1.4 Functional brain networks

As mentioned above, the brain can be viewed as a large, complex network of brain regions interacting with each other. This interaction can be investigated at different levels. Functional connectivity assessed by fMRI relies on the grouped activation signals of several hundreds to thousands of neurons. A functional connection is calculated as the correlation between BOLD signal time series from groups of neurons (Bassett & Sporns 2017) (cf. Fig. 1). Several brain regions showing these

correlations in a specific context, e.g., a specific task or in the resting state, form a functional network. Multiple functional brain networks have been reliably found across individuals and can be examined in different contexts. Most of these functional networks are what Bassett and Sporns call “co-activation networks”, containing brain regions that are activated by the same task or sensory input (Bassett & Sporns 2017). Functional brain networks can change due to pathological processes. They simultaneously reflect underlying pathophysiological mechanisms as well as the change in behavior that can be observed externally (Bassett & Sporns 2017). The analysis of functional networks could be a valuable approach to develop biomarkers for disease diagnosis or therapy monitoring (Baggio *et al.* 2015b).

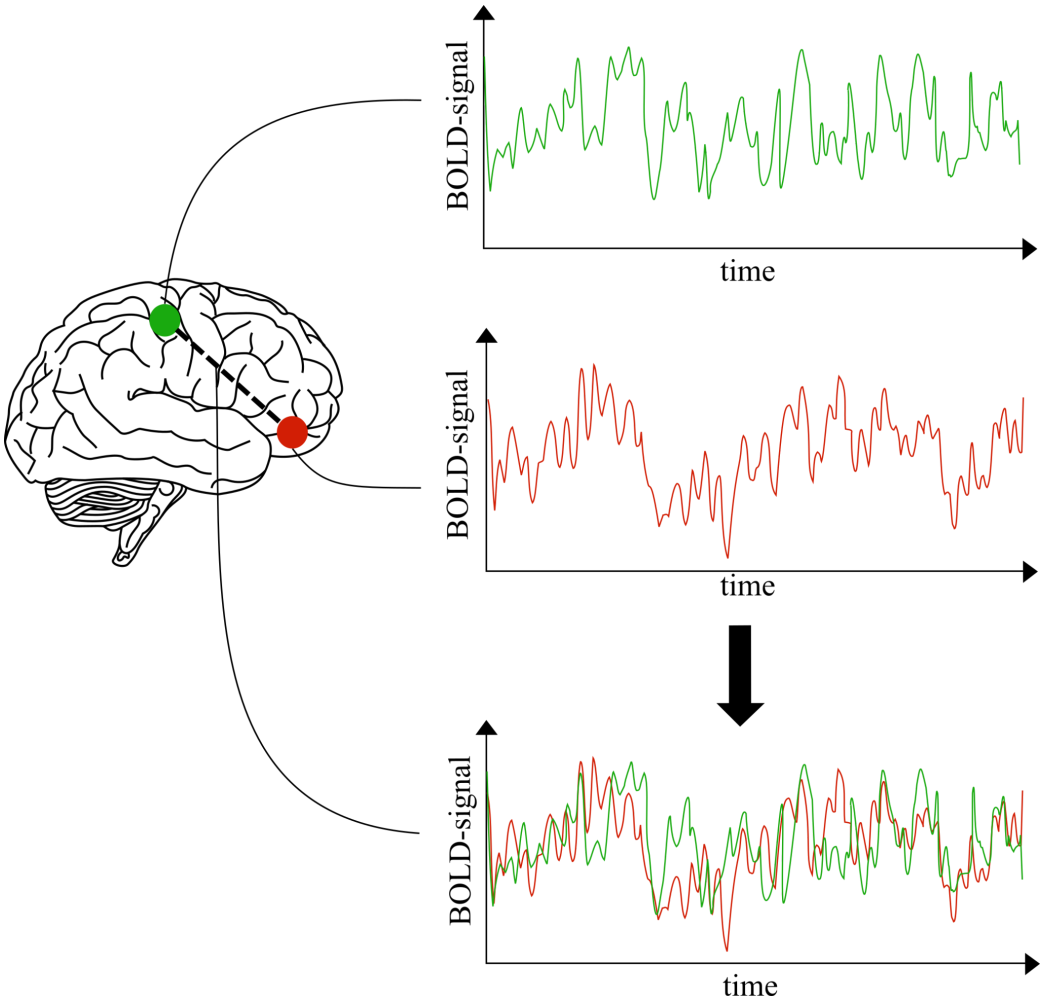

Fig. 1: Principle of functional connectivity: BOLD-time series correlation. For each region of interest (ROI), the BOLD-time series over time is assessed. Then, pairwise Pearson’s correlation of different ROIs is calculated as a measure of functional connectivity between brain regions. The higher the correlation coefficient, the higher the functional connectivity between these regions. BOLD = blood oxygen level dependent signal.

1.4.1. Default mode network

One functional network that has caught a high interest, both in the context of diseases and healthy subjects, is the default mode network (DMN). The DMN consists of several brain regions that exhibit a particularly high activity during rest, when the brain is not involved in any specific task. It was discovered by Shulman and colleagues in a meta-analysis of positron emission tomography (PET) (Shulman *et al.* 1997). They observed a set of brain regions that consistently showed less activation during the execution of externally directed tasks (Shulman *et al.* 1997). In 2001, Raichle and colleagues coined the term “default mode of brain function” and suggested that the involved areas and their activity were an indicator of intrinsic brain activity (Raichle 2015). There are several components within the DMN: the ventral and dorsal medial prefrontal cortex (vMPFC and dMPFC), the posterior cingulate cortex (PCC) with the neighboring precuneus, the inferior parietal lobule, the lateral temporal cortex and the hippocampal formation (Buckner *et al.* 2008; Raichle 2015). The functions of the DMN are manifold and include self-related thoughts like autobiographical memory, planning of future events, thinking about past events, mind wandering and theory-of-mind (Andrews-Hanna *et al.* 2010; Buckner *et al.* 2008; Mantini & Vanduffel 2013; Raichle 2015). Moreover, the DMN also plays a role in externally directed tasks, e.g., by interacting with different TPNs (Spreng 2012). Because of its central role in cognitive functions and the association of its dysfunction with various neurological and psychiatric diseases, the DMN was used as the central or core network for the present study.

1.4.2 Analysis of functional brain networks

In order to interpret disease-driven changes in functional network architecture, e.g., of the DMN, the properties of a network need to be quantified using measures that can be compared between subjects, populations or over time. One popular approach in network science is graph theory, originally derived from mathematics (Bullmore & Sporns 2009). In graph theory, networks are represented as nodes that are connected by edges (Rubinov & Sporns 2010; Sporns 2018).
This approach can be applied to all kinds of networks, from subway systems and telephone networks to functional neuronal networks. In fMRI-derived networks, the nodes correspond to brain regions and the edges to the correlations between

BOLD time series (Farahani *et al.* 2019). All possible pairwise internodal correlations within a network can be represented in an association matrix. Starting from this matrix, a graph is then created (Bullmore & Sporns 2009). The graph can either be binary or weighted, by attributing the correlation coefficient of two nodes to the corresponding edge (Bullmore & Sporns 2009).

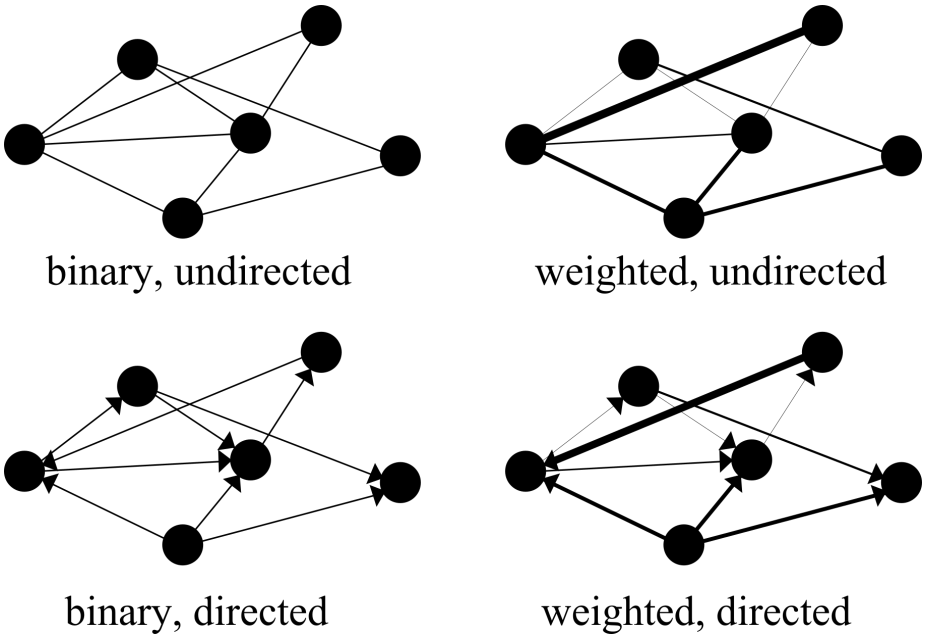

Fig. 2: Schematics of different types of graphs. In graph theory, a network is represented by nodes and edges. The strength of the connections between two nodes can be taken into account by the attribution of a weight. The result is a weighted graph, in contrast to a binary graph, that only indicates that there is or is not a connection above a defined threshold between two regions. Depending on whether the direction of information flow is taken into account, a directed or undirected graph results. In the present study, weighted undirected graphs were analyzed.

However, not all correlations might be meaningful, e.g., some could be the byproduct of noise sources or random correlations and produce false positives (Drakesmith *et al.* 2015). Therefore, it is common practice to threshold the association matrix and retain only higher, potentially meaningful correlations for the ensuing calculations. Unfortunately, there are no generally accepted rules as to which threshold level is best or if thresholds should be used at all. Furthermore, there is an ongoing discussion about the meaning of negative correlations. This issue is addressed in the present study by the use of three different FC thresholds.

Once a graph is defined, different descriptive network metrics can be computed to describe the network properties and make them comparable across subjects or groups. In the present study, the functional connectivity of predefined functional networks was examined. To this end, the average BOLD time series of brain regions participating in a given network were extracted from fMRI data of PD patients and healthy control subjects in two different cohorts. Using Pearson's correlation coefficient, a correlation matrix was obtained which resulted in a weighted, undirected functional network that was further analyzed using average functional connectivity measures and other graph theory measures.

Graph theory measures aim at revealing specific network properties at a global (network) or local (nodal) level. Frequently used measures are for example the clustering coefficient or the shortest path and related measures like the characteristic path length or global efficiency (Rubinov & Sporns 2010). The clustering coefficient for example reflects clustered connectivity around network nodes by assessing if neighbors of a given node A are also neighbors of each other. The shortest path is defined as the minimal number of steps needed to get from node A to node B (Rubinov & Sporns 2010). The average shortest path length for all possible pairs of nodes is called characteristic path length and is a measure of integration of a network (Rubinov & Sporns 2010). Integration describes the capacity to integrate information originated in different and distant network areas (Farahani *et al.* 2019). Meanwhile, segregation describes the formation of specialized communities or modules within a network (Farahani *et al.* 2019). Local measures (such as betweenness centrality or participation coefficient, cf. methods) on the contrary can help to understand the role of a single brain region within the network (Farahani *et al.* 2019).

1.5 Functional connectivity as potential biomarker in Parkinson's disease

1.5.1 Resting-state functional connectivity as biomarker

As pointed out before, the accuracy of PD diagnosis has yet to be improved. Thus, there is a growing interest in the development of diagnostic biomarkers. Disease-specific FC patterns are studied as potential biomarkers for several

diseases, e.g., Alzheimer's disease, schizophrenia, Huntington's disease, dementia with Lewy Bodies, multiple system atrophy, frontotemporal dementia and also Parkinson's disease (González-Madruga *et al.* 2022; Hohenfeld *et al.* 2018; Sheffield & Barch 2016).

The Biomarkers Definition Working Group defines a biomarker as "a characteristic that is objectively measured and evaluated as an indicator of normal biological processes, pathogenic processes, or pharmacologic responses to a therapeutic intervention" (Biomarkers Definitions Working Group. 2001). In general, biomarkers can be used to diagnose a medical condition, to stage an already diagnosed disease or to estimate the prognosis and treatment response. In PD, biomarkers could help to reliably diagnose the disease, even in early stages, monitor disease progression and differentiate between PD and similar conditions like atypical parkinsonian syndromes (Yamashita *et al.* 2023). Additionally, biomarkers can increase the objectivity of the diagnosis, so far relying on the subjective assessment by a clinician (Yamashita *et al.* 2023). Different properties of ideal biomarkers in pharmacological research have been defined by Lesko and Atkinson (Lesko & Atkinson 2001). These properties can also serve as a guidance for biomarkers in other contexts. After Lesko & Atkinson, the properties of biomarkers should include clinical relevance, sensitivity and specificity, reliability, practicality and simplicity (Lesko & Atkinson 2001). These properties should also be fulfilled for PD biomarkers derived from the analysis of rsFC.

Clinical relevance means that the potential biomarker should reflect a pathophysiological process, which requires a deep understanding of the underlying pathomechanism of a disease (Lesko & Atkinson 2001). In the context of PD, rsFC can both help to understand pathomechanisms and at the same time reflect the changes in the functional architecture to differentiate between PD-patients and healthy subjects.

A sensitive rsFC biomarker should be able to detect even small changes in the functional architecture of the brain in PD to allow early diagnosis and to avoid false negatives and thus increase diagnostic accuracy. At the same time, a useful biomarker should be able to differentiate between PD and other diseases or healthy individuals (specificity). It has been shown, that rsFC in principle has these potentials (cf. section 1.2.6, functional networks in PD).

Lesko and Atkinson define reliability as the “ability to measure [the biomarker] with acceptable accuracy, precision, robustness, and reproducibility” (Lesko & Atkinson 2001). A lack of reliability is the greatest challenge when it comes to rsFC-derived biomarkers in PD. In general, fMRI signals are robust, and many findings could be repeatedly reproduced across different populations (Bandettini 2009). However, in PD but also in other neurological diseases, specific FC alterations frequently cannot be replicated in other datasets acquired at different sites. In rsFC measured by fMRI, low frequency alterations in BOLD-signal are analyzed. These can be “hidden” or altered by noise signals, for example caused by respiration, heart activity, head motion or thermal noise (Caballero-Gaudes & Reynolds 2017; Glover 2011). Therefore, prior to BOLD-signal-analysis, potential noise signals have to be removed in a process called preprocessing. To date, no standard preprocessing pipeline has been established (Douw *et al.* 2019). Hence, results of FC-studies could be influenced by the choice of denoising technique, decreasing the comparability across studies and reducing the replicability of results (Baggio *et al.* 2015b). This issue is addressed in the present study by the use of an identical analysis pipeline applied to the two independent datasets.

A powerful advantage of fMRI imaging for the assessment of rsFC is its practicality, as it is noninvasive and does not require the injection of a contrast medium (Kim *et al.* 2021). It therefore poses little risk to patients or research participants, and there are only a few contraindications that prevent subjects from undergoing fMRI scanning. Additionally, fMRI acquisition is relatively simple compared to other imaging techniques that might require the administration of contrast agents or radioactive markers. MRI-scanners are widely available and image requisition in the resting-state does only require a small amount of compliance of the scanned subjects.

Since the analysis of rsFC can deliver detailed insights into the pathophysiology of PD and is a promising avenue for the discovery of new and improved biomarkers, an increasing amount of studies investigates rsFC in PD and uncovered disease specific changes in single functional connections between brain regions but also in previously defined functional networks, which help broaden our understanding of both the healthy brain and the brain affected by various neurological or psychiatric diseases.

1.5.2 Functional networks in Parkinson's disease

Although many studies were able to detect different rsFC alterations in PD patients, the literature does not paint a clear picture and is partly contradictory. To date, most studies on functional networks in PD analyze within-network FC, often focusing on specific connections rather than network-based properties. More recently, several studies also investigated the coupling of different networks (between-network FC).

The network that was most studied in the context of PD is the DMN. Several studies found dysfunctions in FC of the DMN in PD patients, with different results. On the one hand, decreased within-DMN FC was observed in PD patients (e.g., Baggio *et al.* 2015a; Jellinger 2023; Wolters *et al.* 2019). Disbrow and colleagues observed decreased FC between the PCC, medial prefrontal cortex (MPFC) and inferior parietal cortex (IPC) within the DMN (Disbrow *et al.* 2014). Another study found decreased FC of the right medial temporal lobe and the bilateral inferior parietal cortex within the DMN (Tessitore *et al.* 2012). In several studies, decreased DMN connectivity was associated with the presence of mild cognitive impairment (MCI, e.g., Disbrow *et al.* 2014; Jellinger 2023; Wolters *et al.* 2019) and with performance in cognitive tasks in cognitively unimpaired patients, suggesting that DMN connectivity is disrupted even before the emergence of cognitive impairment (Jellinger 2023; Tessitore *et al.* 2012). Another study found decreased FC in the dorsal part of the DMN in cognitively unimpaired patients with akinetic rigidity subtype PD (Hou *et al.* 2017). At the same time, they found increased FC in the anterior part of the DMN. Increased FC within the DMN was further described by Campbell and colleagues (Campbell *et al.* 2015). Alterations in DMN were also found in association with visual hallucinations (Yao *et al.* 2014) and in akinetic-rigidity dominant PD compared to tremor dominant PD (Karunanayaka *et al.* 2016). Finally, some studies did not find any significant changes in DMN FC (e.g., Helmich *et al.* 2010). As the DMN plays an outstanding role in the functional architecture of the brain and has been the subject of various FC studies in the context of PD and other neuropsychological diseases, it was chosen as the central network for the present study.

In addition to the DMN, other functional networks have been studied in the context of PD. In contrast to the DMN, which is sometimes termed the task-negative

network, other functional networks are often termed as task-positive networks (TPNs) (Power *et al.* 2014), because of their relation to different externally focused cognitive functions or tasks. However, there is no clear definition or nomenclature of task-positive networks (for instance, there is not “the” working memory network), complicating the comparison of results across studies. However, functional networks for the same functions often comprise similar brain regions (Baggio *et al.* 2015b). As PD is primarily classified as a motor disease, a relatively large amount of studies focused on the investigation of motor related networks and found decreased (Campbell *et al.* 2015; Caspers *et al.* 2021; Peraza *et al.* 2017) as well as increased (de Schipper *et al.* 2018) FC between motor regions. Furthermore, functional aberrations (mostly a decrease of FC) were described for cortico-striato-thalamo-cortical circuits (e.g., Hacker *et al.* 2012; Helmich *et al.* 2010; Kwak *et al.* 2010). Moreover, FC alterations in networks involved in attention processes have consistently been observed and associated with different PD symptoms (Baggio *et al.* 2015a; Bezdicek *et al.* 2018; Maidan *et al.* 2019; Yeager *et al.* 2024). On the contrary, a study investigating the executive control network in PD did not find any significant differences in comparison to healthy controls (Disbrow *et al.* 2014).

Besides the analysis of within-network FC, the interest in between-network FC is growing as well. Complex interactions between the DMN and other, usually anticorrelated task-positive networks (TPNs) is crucial for the execution of complex cognitive tasks (Fox *et al.* 2005; Spreng 2012; Spreng *et al.* 2013). It has been hypothesized that dopamine modulates the interaction of different cognitive networks like the DMN, the dorsal attention network and the frontoparietal network (Dang *et al.* 2012). In a state of dopamine depletion and in the case of a highly complex disease like PD, the investigation of the coupling between networks is therefore interesting.

In the context of PD, between-network FC was found to be an indicator for the presence of specific symptoms, e.g., freezing of gait (Bharti *et al.* 2020), difficulties in executive functions (Boon *et al.* 2020) or attention (Boord *et al.* 2017) and impulsivity (Koh *et al.* 2020). Moreover, reduced connectivity between the ventral and dorsal attention networks was found in PD patients with hallucinations (Shine *et al.* 2014). Another study found a correlation between cognitive impairment and reduced coupling between the DMN and the dorsal attention network, as well as

between the dorsal attention network and right frontal insular regions, that are thought to be involved in network switches necessary for attention or executive functions (Baggio *et al.* 2015a). Furthermore, coupling of the right central executive network (CEN) and the salience network as well as coupling of the DMN and CEN were found to be altered in PD patients without dementia (Putcha *et al.* 2015). The same group found a correlation of cognitive functions and coupling of the DMN and the salience network (Putcha *et al.* 2016). Recently, a study found an association of motor and cognitive symptom severity with altered interaction between the sensorimotor network and the dorsal attention network, as well as between the ventral attention network and frontoparietal network (Delgado-Alvarado *et al.* 2023). In another study, PD patients were differentiated from healthy controls (HC) using a machine-learning algorithm based on between-network FC (Rubbert *et al.* 2019), underlining its diagnostic potential.

Several studies have used a graph theoretical approach for the analysis of resting-state fMRI in PD research. FC alterations were found at the global and nodal level. It was for example found that network efficiency was decreased in PD, combined with a higher clustering coefficient and higher characteristic path length (Göttlich *et al.* 2013; Wei *et al.* 2014). Another study found a decreased global efficiency and increased characteristic path length as well, but paired with a decreased clustering coefficient (Suo *et al.* 2017). It was further found that global efficiency was reduced even in early-state patients under treatment (Sang *et al.* 2015). At the nodal level, nodal centrality was decreased in the sensorimotor cortex, in regions of the DMN and in temporal-occipital regions (Suo *et al.* 2017). Berman and colleagues found that the small-world architecture (high clustering coefficient and short path length) of several functional networks is modulated by dopaminergic treatment (Berman *et al.* 2016). Graph theory results could also be attributed to different symptoms like impulse control disorder (Zhu *et al.* 2021).

1.5.3 Challenges and motivation

The literature on FC alterations in PD does not paint a clear picture yet. As pointed out above, network alterations have been linked to different PD symptoms, motor as well as non-motor. However, findings sometimes seem contradictory (Prodoehl *et al.* 2014) and cannot always be explained with the current understanding of PD pathophysiology. Results of FC studies vary between different patient groups, e.g.,

early vs. advanced disease stage, tremor-dominant vs. akinetic-rigid subtype or cognitive impairment vs. cognitively normal (Filippi *et al.* 2019), which makes it difficult to find disease specific patterns that apply to all PD patients but not to healthy subjects or patients with other, similar diseases.

Overall, it becomes clear that while a substantial effort has already been put into the identification of FC patterns in PD, there is a need for further research. As the majority of conducted studies in the literature focus on the FC of single brain regions, leading to contradictory results, systematic network-based approaches could prove useful to uncover characteristics that apply to all individuals with PD and could hence be used for the development of biomarkers. This work therefore systematically analyzes FC patterns of various predefined meta-analytic networks across two different datasets. Meta-analytic networks are based on task-activation data in healthy populations and contain brain regions that are consistently activated by specific task paradigms. They are thus well suited to investigate FC changes as a possible basis for different, heterogeneous symptoms (Chen *et al.* 2021), which could in turn be promising starting points for the future research for FC biomarkers. Furthermore, the same network coordinates can be applied across subjects and datasets and allow for comparisons. However, to date, there are only few studies that investigated meta-analytic networks in the context of diseases such as PD.

One of the biggest challenges of the analysis of FC via fMRI is the lack of reliability. Alterations often cannot be replicated in different, independent datasets. At the same time, there is no gold standard for pre-processing and analysis pipelines. Both factors highlight the need for more research using independent datasets from different sites, while applying the same analysis pipeline to further investigate the reasons for the lack of reliability.

1.6 Aims of thesis

As pointed out before, there is a substantial need for the development of novel biomarkers to improve and objectify PD diagnosis. The present work therefore aimed at evaluating the potential of the analysis of rsFC of meta-analytic networks as a diagnostic or disease monitoring biomarker in PD by answering the following research questions:

(1) Does the network-based analysis of resting-state functional connectivity of predefined meta-analytic networks have the potential to uncover altered functional connectivity patterns in Parkinson's disease?
(2) Which networks and FC measures should be considered for further biomarker research?
(3) Can reliability of resting-state fMRI analysis in Parkinson's disease be improved by using the same analysis pipeline on independent datasets?

In order to answer these questions and help to elucidate the fractionated and partly contradictory literature on FC patterns in PD, this study assessed within- and between-network FC of the DMN, a whole-brain network and 11 robust meta-analytically defined TPNs, involved in various cognitive functions, to reflect the variety of possible symptoms in PD. To this end, rs-fMRI data from two independent datasets from a total of 66 PD patients and 67 healthy controls were analyzed. Within- and between-network FC was assessed via variations of simple mean FC and graph-theoretical measures such as global efficiency, diffusion efficiency or positive participation coefficient.

As mentioned above, replicability of neuroimaging-based results across datasets is challenging (Lerma-Usabiaga *et al.* 2019), especially in the context of neuropsychiatric disorder (Badea *et al.* 2017; Douw *et al.* 2019; He *et al.* 2020; Specht 2019). This challenge was taken into account by applying the exact same analysis pipeline in both datasets to exclude any methodological influences in case of non-replicability of results.

2 Material and methods

2.1 Participants

In the present study, two separate datasets, Data-PR and Data-DU, were analyzed separately, following the same analysis steps. Subject characteristics are listed in Table 3.

Data-PR contained a total of 30 patients diagnosed with idiopathic PD and 30 HC, assessed in the General University Hospital in Prague, Czech Republic. Of the PD patients, 17 subjects were male, 13 female. The mean age was 64.6 ± 7.7 years. Of the HC, 15 subjects were male, 15 female. The mean age of HC was 63.5 ± 7.9 years. The PD patients were diagnosed by neurologists according to criteria as defined by the UK brain bank (Gibb & Lees 1988). Patients exhibiting psychotic symptoms or taking antipsychotic treatment were excluded from the dataset. Other exclusion criteria were a cognitive impairment with a Montreal Cognitive Assessment (MoCa)-Score > 1.5 SD below the Czech norm, patients after implantation of deep brain stimulation or jejunal levodopa application, the presence of other motor or cognitive diseases and patients not eligible for MRI scanning. Motor symptom severity was assessed using the motor part of the Unified PD rating scale in pharmacological OFF-state (UPDRS-III OFF) and was 30.6 ± 9.9 on average. Patients were scanned in pharmacological ON-state, following their individual drug regimens. All subjects gave their informed consent and data acquisition was approved by the ethics committee of the General University Hospital, Prague, Czech Republic.

Data-DU consisted of 36 patients with idiopathic PD and 37 HC taken from a pre-existing pool assessed by the University Hospital Düsseldorf, Germany (Caspers *et al.* 2017, 2021; Rubbert *et al.* 2019). Of the PD patients, 22 subjects were male and 14 female. The mean age was 61.7 ± 9.8 years. Of the HC, 21 subjects were male and 16 female. The mean age of HC was 60.5 ± 9.2 years. The PD patients were diagnosed by a board-certified neurologist. Exclusion criteria were the presence of a non-idiopathic parkinsonian syndrome, dementia or a major depression. Motor symptom severity was assessed by the attending neurologist using the motor part of the Movement Disorders Society (MDS-) UPDRS-III OFF and was 33.9 ± 10 on average. Patients were scanned in

pharmacological ON-state, following their individual drug regimens. All subjects gave their informed consent and data acquisition was approved by the ethics committee of the Medical Faculty of Heinrich-Heine-University, Düsseldorf, Germany.

Retrospective analysis of both datasets was approved by the ethics committee of the Heinrich-Heine-University, Düsseldorf, Germany.

	Patients	**Healthy controls**	**p-value**
Data-PR			
sample size	30	30	
gender (m/f)	17/13	15/15	0.6*
age	64.6 ± 7.7 (46–82)	63.5 ± 7.9 (46–83)	0.58**
UPDRS-III OFF	30.6 ± 9.9 (8–64)		
Hoehn & Yahr Stage	2.02 ± 0.54 (1–3)		
Data-DU			
sample size	36	37	
gender (m/f)	22/14	21/16	0.7*
age	61.7 ± 9.8 (44–80)	60.5 ± 9.2 (44–78)	0.59**
MDS-UPDRS-III OFF	33.9 ± 10 (15–55)		
Hoehn & Yahr Stage	2.59 ± 0.72 (1–4)		

Table 3. Sociodemographic data and clinical scores. Overview of subject characteristics in analyzed datasets. UPDRS-III: Motor part of the Unified Parkinson's disease rating scale; MDS: Movement Disorder Society; OFF: pharmacological OFF-state). Characteristics are displayed as mean ± standard deviation (lowest to highest value). Statistics: *gender was compared using a Chi^2-Test; **for age comparison, a two-sample t-test was conducted.

2.2 Ethic votes

Data-acquisition for the datasets was approved by the local Ethics Committees of the respective universities (General University Hospital Prague, Czech Republic and Heinrich-Heine-university Düsseldorf, Germany). Retrospective analysis of these datasets was approved by the local Ethics Committee at

Heinrich-Heine-University (Faculty of Medicine, Study numbers 4096, 4039, 5193 and 2018-317-RetroDEuA).

2.3 Data acquisition

For Data-PR, functional magnetic resonance imaging (rs-fMRI) was acquired using a 3 tesla (T) scanner (Siemens Skyra) with a 32-channel head coil. To obtain blood oxygen level dependent time series, a standard T2*-weighted echo-planar imaging sequence was used. One scan comprised 304 whole brain images and 30 slices with a repetition time (TR) of 2 seconds and an echo time (TE) of 30 ms. Voxel size was 3 mm^3. Structural information was obtained with a standard T1-weighted magnetization-prepared rapid gradient echo (MPRAGE) image scan with a voxel size of 1 mm^3.

Imaging for Data-DU was also performed with a 3T scanner (Siemens Trio, Erlangen, Germany). For BOLD times series, an echo-planar imaging sequence was used. One scan comprised 300 time points and 36 slices. Repetition time was 2.2 seconds, echo time 30 ms. Voxel size was 3.1 mm^3. Acquisition time was 11 minutes with a flip angle of 90° and a field of view (FoV) of 200 * 200 mm axial plane. Structural information was obtained with a standard T1-weighted MPRAGE image scan with a TR of 2.3 seconds, TE of 2.96 ms, inversion time (TI) of 900 ms, a flip angle of 8° and a FoV of 240 * 256 mm. The structural scan comprised 192 slices at a voxel size of 1 mm^3.

2.4 Preprocessing

In order to improve comparability across datasets, the exact same preprocessing pipeline was applied to both of them using SPM12 software and MATLAB (version 2019b, © MathWorks, Natwick USA) scripts. Data was realigned for motion correction. Rs-fMRI data was co-registered to structural data. Normalization parameters from structural scans were used to spatially normalize rs-fMRI data into Montreal Neurological Institute (MNI) space. Voxels other than gray matter were masked. Data was smoothed with a Gaussian kernel of 6 mm full width at half maximum. In order to allow magnetization for equilibrium, four dummy scans were discarded. Mean signals of white matter and cerebrospinal fluid were

regressed out together with 24-motion parameters, based on Friston-24 (Friston *et al.* 1996).

2.5 Choice and definition of functional networks

For this study, 13 *a priori* defined functional brain networks and their coupling were analyzed. In the center of the performed analyzes was the default mode network (DMN), here also termed the base network. We investigated functional connectivity behavior within the DMN as well as its coupling with 12 other functional networks. These comprised a whole-brain network (WBN) and 11 meta-analytically defined task-positive networks.

The WBN, as defined by Power and colleagues (Power *et al.* 2013), including 264 nodes participating in many different networks, was chosen because of its presumed potential to deliver insights into the coupling of the DMN with the brain as a whole.

To cover a diverse set of brain functions that play a role in PD, a wide variety of networks was chosen. The MNI coordinates are listed in the appendix.

2.5.1 Default mode network

We chose the DMN as the base network of our study because it also plays an important and central role in the architecture of the brain. As described above (c.f. introduction), it is involved in many cognitive processes and has been shown to be altered in various neurocognitive diseases, including PD.

In this study, coordinates for the regions of the DMN were taken from the literature. Core regions of the DMN were the posterior cingulate cortex, medial prefrontal cortex, lateral parietal cortex and the hippocampal formation (Van Dijk *et al.* 2010).

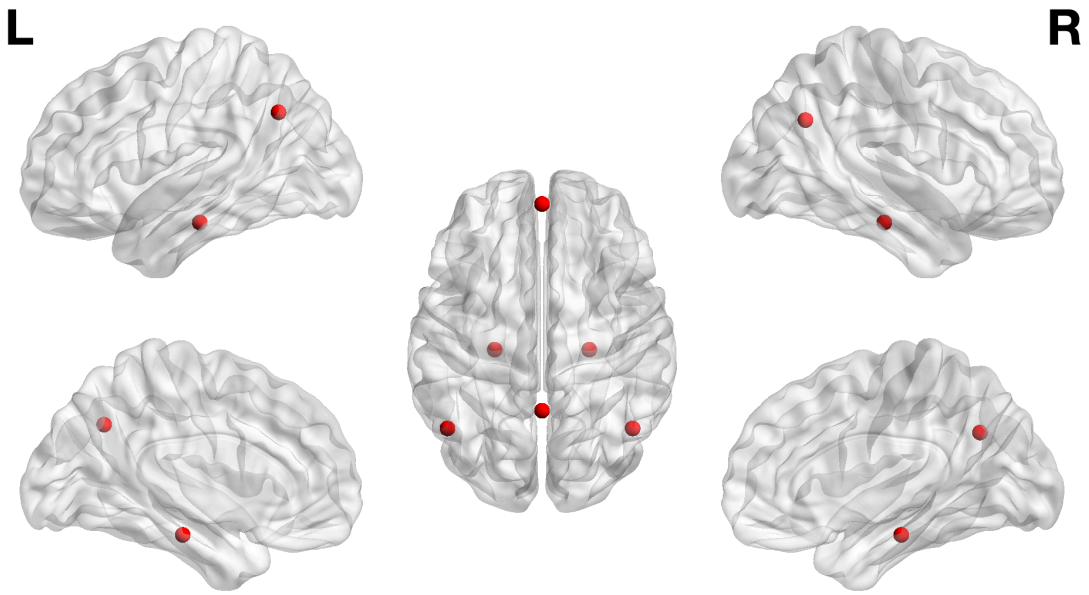

Fig. 3: Illustration of the default mode network. Created with BrainNet Viewer, Version 1.32 (Xia *et al.* 2013). MNI-coordinates as published by van Dijk and colleagues (Van Dijk *et al.* 2010).

2.5.2 Motor function

PD is primarily defined as a motor disorder. Therefore, two different motor networks were studied here: The motor execution network (MotorEx) (Witt *et al.* 2008) and the perceptuo-motor network (MotorPerc) (Heckner *et al.* 2021). Whereas MotorEx is based on an activation likelihood estimation (ALE)-meta-analysis (Eickhoff *et al.* 2009, 2012) of studies exclusively using finger-tapping tasks, MotorPerc is based on an ALE-meta-analysis including a wider variety of motor paradigms, such as isometric force, motor learning, writing and drawing, chewing, grasping or finger tapping. Regions included in MotorEx are located in the primary sensorimotor cortex, the supplementary motor area (SMA), the premotor cortex, inferior parietal cortex as well as the basal ganglia and the anterior cerebellum (Witt *et al.* 2008). Key regions of the MotorPerc network are the bilateral pre-supplementary SMA, the SMA, dorsal premotor cortex, primary motor and somatosensory cortex, intraparietal sulcus, the superior parietal lobule, the posterior inferior frontal gyrus, the anterior insula, putamen, thalamus and cerebellum (Heckner *et al.* 2021).

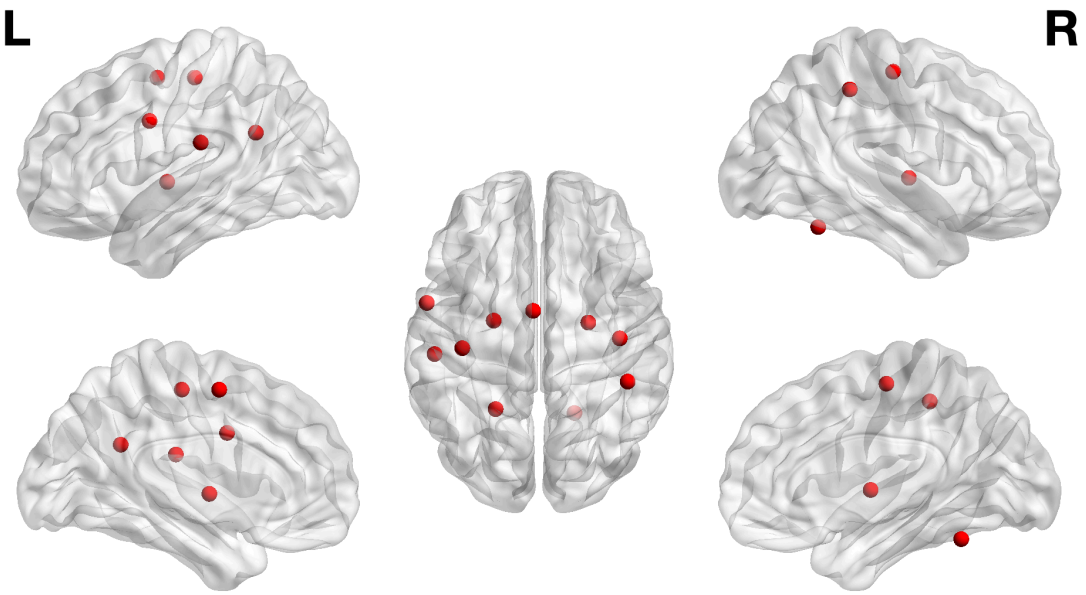

Fig. 4: Illustration of the motor execution network. Created with BrainNet Viewer, Version 1.32 (Xia *et al.* 2013). MNI-coordinates as published by Witt and colleagues (Witt *et al.* 2008).

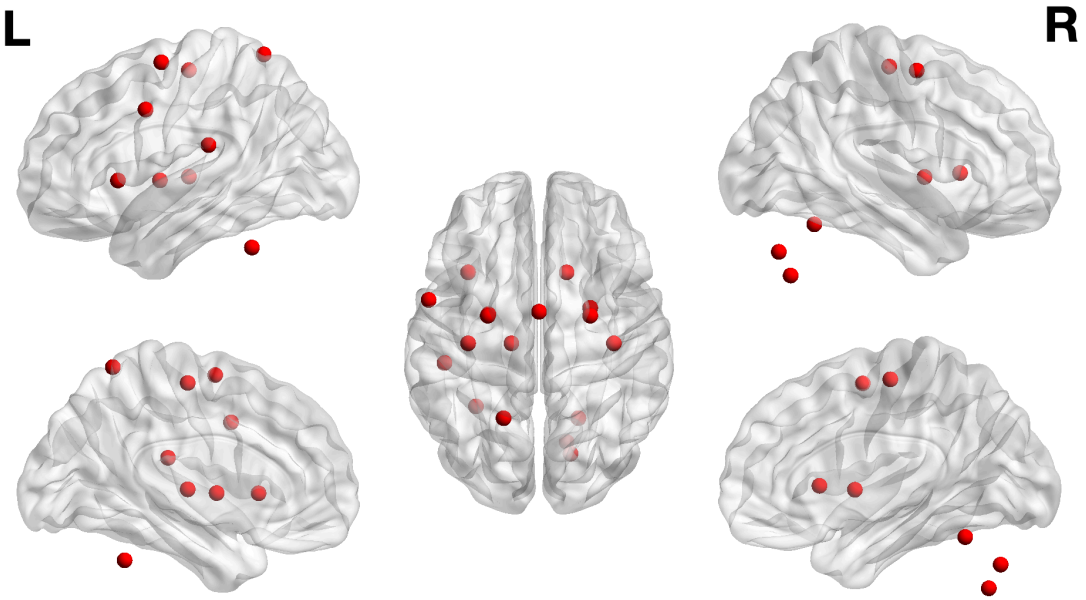

Fig. 5: Illustration of the perceptuo-motor network. Created with BrainNet Viewer, Version 1.32 (Xia *et al.* 2013). Several regions lie within the cerebellum, which is not included in the model. MNI-coordinates as published by Heckner and colleagues (Heckner *et al.* 2021).

2.5.3 Top-down control/Attention

Attention dysfunction is frequently seen in PD patients, even in early stages. It is also a predictive factor for the development of PD dementia (Woods & Tröster 2003). In general, attention as a complex brain function can be separated into two

mechanisms: top-down control and bottom-up control. Top-down control refers to the ability to actively direct attention to certain objects or subjects. Bottom-up control, however, is stimulus-driven. That is, if an external stimulus is perceived and identified as important, the currently performed task, action or thought can be disrupted to shift attention to the new stimulus (Corbetta & Shulman 2002). It was found that PD patients show an imbalance of attention control mechanisms: bottom-up attention control is dominant over top-down attention control (Bin Yoo *et al.* 2018; Cools *et al.* 2010; Flowers & Robertson 1995). To reflect attention deficits in PD, we included several functional networks involved in attention and action regulation.

The meta-analytical vigilant attention network (VigAtt) investigated in this study (Langner & Eickhoff 2013) includes brain regions involved in sustaining vigilant attention over more than 10 seconds. The concept of vigilant attention, defined as maintaining attention while performing monotonous tasks, was introduced by Robertson and Garavan (Robertson & Garavan 2004). The VigAtt network used in this study was defined using an ALE-meta-analysis. Experimental paradigms used in the assessment of vigilant attention are e.g., reaction time tasks, stimulus discrimination tasks (such as go/no-go tasks) or sustained target counting tasks (Langner & Eickhoff 2013). Brain regions that consistently showed activation during the aforementioned task paradigms were e.g., the dorsomedial, mid- and ventrolateral prefrontal cortex, the anterior insula, parietal regions as well as subcortical regions, as the cerebellar vermis, thalamus, putamen or midbrain (Langner & Eickhoff 2013).

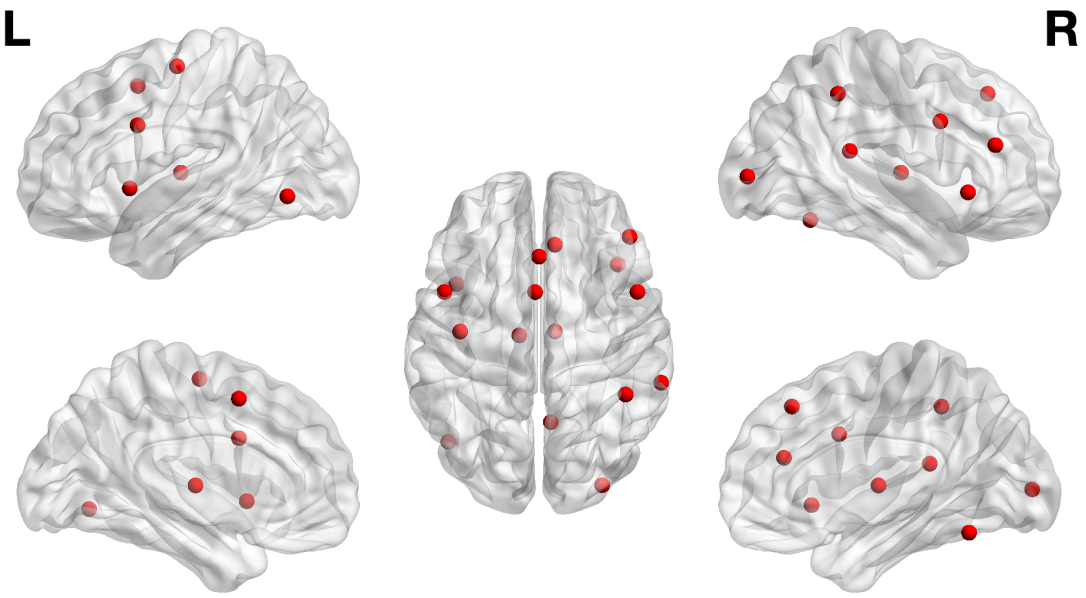

Fig. 6: Illustration of the vigilant attention network. Created with BrainNet Viewer, Version 1.32 (Xia *et al.* 2013). MNI-coordinates as published by Langner and Eickhoff (Langner & Eickhoff 2013).

The cognitive action control network (CogAC) contains brain regions needed to suppress routine actions in order to perform non-routine actions (Cieslik *et al.* 2015). These include the right anterior insula, the inferior frontal junction, the anterior midcingulate cortex and the pre-supplementary motor area (Cieslik *et al.* 2015). Definition of the CogAC network relied on a coordinate-based ALE-meta-analysis. The network represents different subcategories of cognitive action control, namely action withholding, action cancellation and interference control. Included task paradigms were the antisaccade, flanker, go/no-go, stop-signal, SRC, Stroop, and Simon tasks (Cieslik *et al.* 2015).

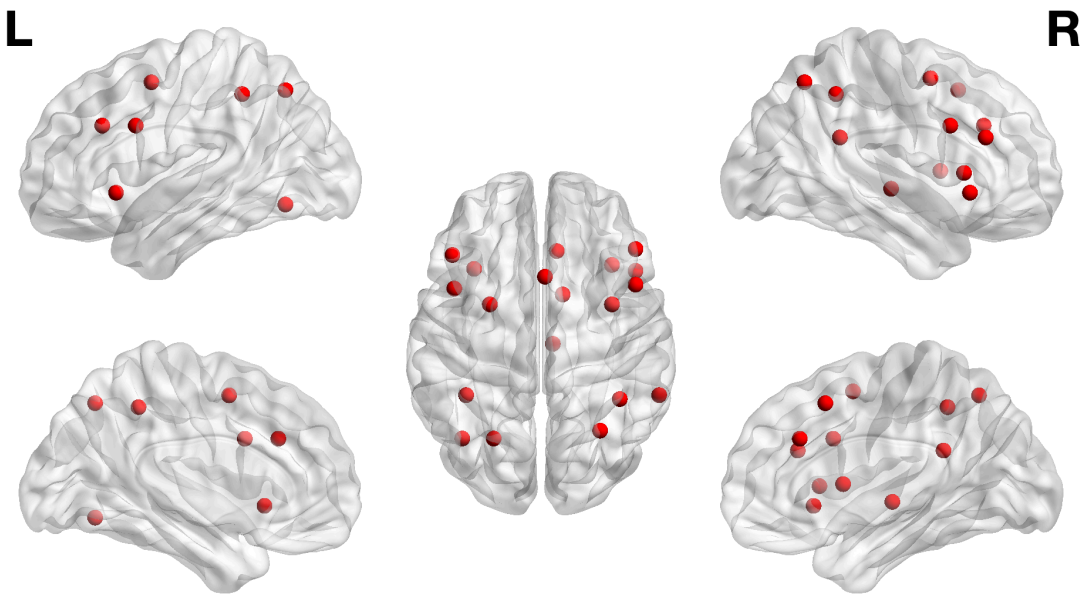

Fig. 7: Illustration of the cognitive action control network. Created with BrainNet Viewer, Version 1.32 (Xia *et al.* 2013). MNI-coordinates as published by Cieslik and colleagues (Cieslik *et al.* 2015).

Another network representing action control is the cognitive action regulation network (CogAR) (Langner *et al.* 2018). In the case of CogAR, cognitive action regulation is defined as “intentionally withholding or stopping a prepotent action, often in combination with performing a competing alternative action” (Langner *et al.* 2018). Situations requiring this kind of action control bear a conflict between different, competing responses: an inadequate but dominant response and an adequate but non-dominant response. The goal of action regulation is to favor the adequate, non-dominant response over the inadequate, dominant response. The ALE-meta-analysis for CogAR included the following tasks: Stroop, Flanker, Simon, Stimulus-response compatibility, other conflict tasks, Go/no-go, Stop-signal, Task switching, Wisconsin card sorting (Langner *et al.* 2018).

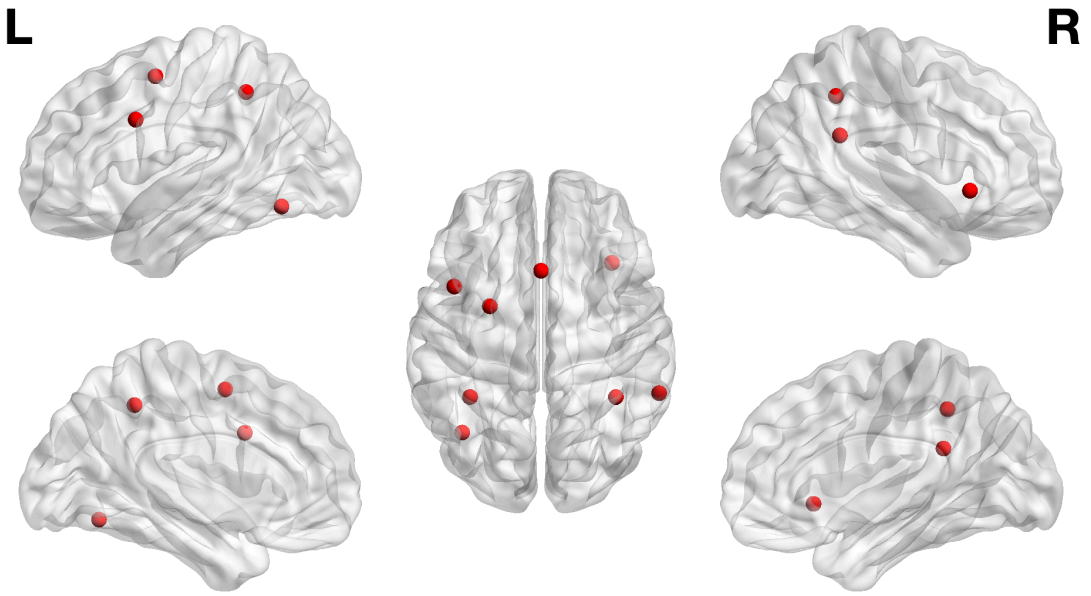

Fig. 8: Illustration of the cognitive action regulation network. Created with BrainNet Viewer, Version 1.32 (Xia *et al.* 2013). MNI-coordinates as published by Langner and colleagues (Langner *et al.* 2018).

2.5.4 Working memory

Along with attention deficits, impaired working memory is another sign of cognitive impairment in PD (Bin Yoo *et al.* 2018). Working memory allows humans to complete complex cognitive tasks, such as following and participating in a conversation, solving math problems or finding the way to work in the morning. In order to complete these tasks, working memory has the capacity to store information for a short period of time and to actively process the information (Ramos & Machado 2021). One of the most popular organizational models of working memory was developed by Baddeley & Hitch (1974), who postulated a distinction between verbal ("verbal loop") and spatial information ("visuospatial sketchpad"). In this model, attribution of incoming sensory information to one of the loops was mediated by a "central executive" (Baddeley & Hitch 1974; Rottschy *et al.* 2012). This model was later extended with the concept of an "episodic buffer", i.e., a system with the capacity for ultrashort-term storage of sensory input (Baddeley 2000). PD patients often show a deterioration of verbal working memory (Ramos & Machado 2021). In this study, we included a meta-analytically defined working memory network (WM), representing a core network of regions that are active across various different working memory tasks (Rottschy *et al.* 2012).

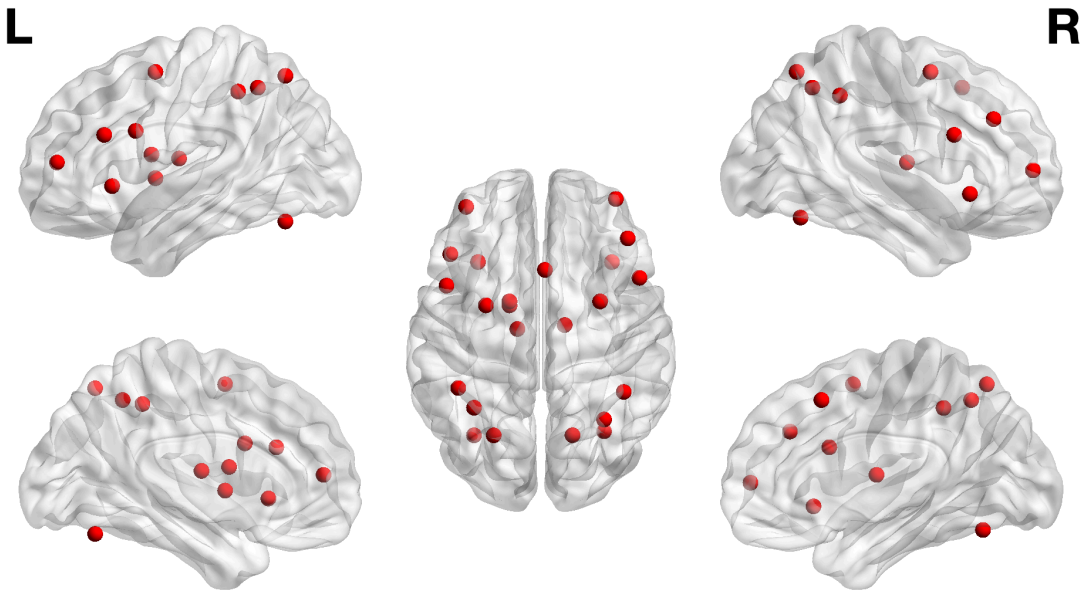

Fig. 9: Illustration of the working memory network. Created with BrainNet Viewer, Version 1.32 (Xia *et al.* 2013). MNI-coordinates as published by Rottschy and colleagues (Rottschy *et al.* 2012).

2.5.5 Multiple tasks

Performing two tasks simultaneously or rapidly switching between tasks is cognitively demanding and results in a delay of responses to external stimuli, as shown in many studies (e.g., Kiesel *et al.* 2010; Koch *et al.* 2018; Pashler 1994). Both, the ability of managing two tasks at once (like talking on the phone while cooking) and rapid task-switching decrease with age. It has been hypothesized that the same neural mechanisms underlie dual-tasking and task-switching and the deterioration of both with increasing age (Verhaeghen *et al.* 2003). Multitasking can be impaired in individuals with neurodegenerative diseases. In PD, especially patients with cognitive impairment experience difficulties with multitasking and hence with the completion of complex everyday tasks. For example, walking while talking can become difficult for affected individuals (Raffegeau *et al.* 2019; Schmitter-Edgecombe *et al.* 2024).

The multitasking network (MultiTask) analyzed in the present study relies on two ALE-meta-analyses on either dual-tasking or task-switching. The core network activated by both types of cognitive action included the bilateral intraparietal sulcus, left dorsal premotor cortex and the right anterior insula (Worringer *et al.* 2019).

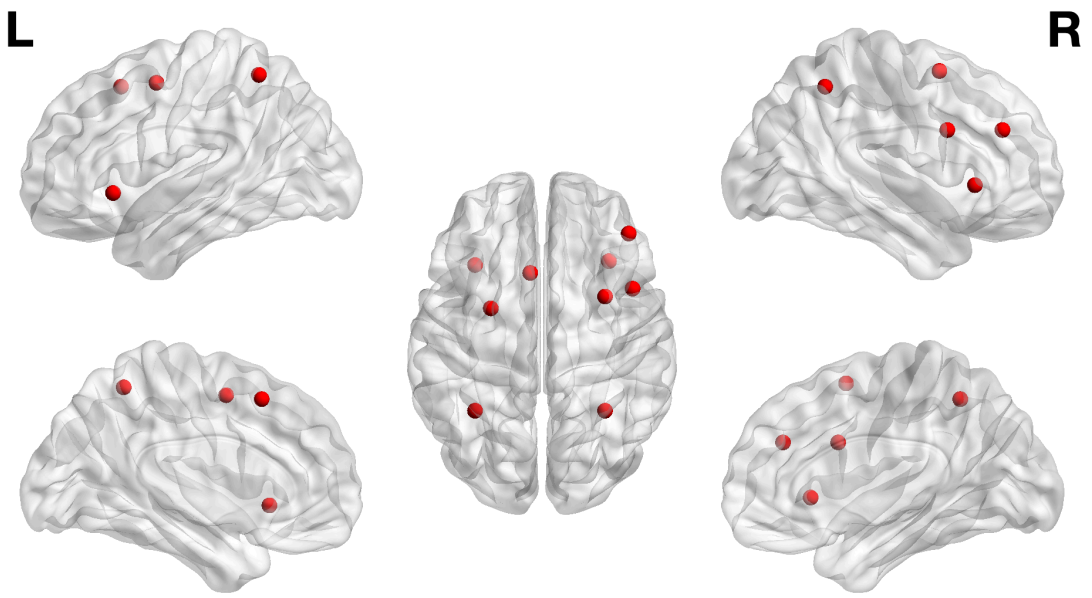

Fig. 10: Illustration of the multitasking network. Created with BrainNet Viewer, Version 1.32 (Xia *et al.* 2013). MNI-coordinates as published by Worringer and colleagues (Worringer *et al.* 2019).

2.5.6 Executive functions

The term ‘executive functions’ refers to a set of cognitive functions that allow higher-order cognitive processes such as solving problems, making decisions or planning (Diamond 2013). Among these functions are the abilities such as to hold and manipulate information in order to use it for another task (working memory), resisting temptations (inhibition) and paying attention to external or internal stimuli (attention). PD patients often experience a decline in executive functions in the context of the frequently observed cognitive impairment.

As seen before, neural networks for distinct executive functions (i.e., working memory, vigilant attention) have been described. However, it was observed that a set of brain regions is consistently activated across different executive functions. Consequently, a multiple-demand network (MDN) has been proposed, including brain regions that consistently contribute to different executive functions, like mid-dorsolateral regions (i.e., middle and posterior parts of the inferior frontal sulcus), mid-ventrolateral regions (around the frontal operculum to anterior insula) and dorsal anterior cingulate regions (Duncan & Owen 2000). Based on the concept of a common neural correlate for executive functions, an extended multiple demand network (eMDN) was proposed by Camilleri and colleagues (Camilleri *et al.* 2018), containing other brain regions that are active in several

executive functions but were not included in the MDN. Core regions of the eMDN are the bilateral inferior frontal junction (reaching into the inferior frontal gyrus), the bilateral anterior insula, and the bilateral pre-supplementary motor area (reaching into the anterior midcingulate cortex) (Camilleri *et al.* 2018).

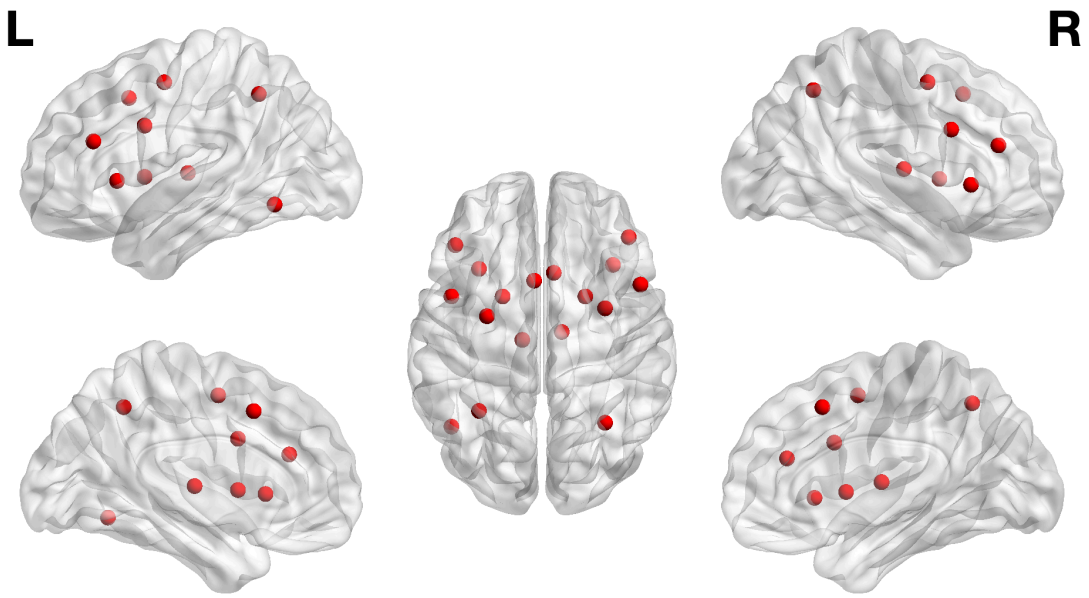

Fig. 11: Illustration of the extended multiple demand network. Created with BrainNet Viewer, Version 1.32 (Xia *et al.* 2013). MNI-coordinates as published by Camilleri and colleagues (Camilleri *et al.* 2018).

2.5.7 Social and emotional processing

Disturbances in emotional processing often occur in PD patients. These concern the emotional experience (e.g., reduced arousal in response to emotional pictures) as well as perception and expression of emotions on faces or in voices (for a review, cf. Péron *et al.* 2012).

To take impairment of emotional and social processing into account, we added two different functional networks to our analysis. The emotional scene and face processing network (EmoSF) is based on an ALE-meta-analysis of studies using expressive faces and natural scene photographs as emotional stimuli (Sabatinelli *et al.* 2011). Among the core regions of this network is the amygdala, which was activated by both emotional faces and scenes. Other regions that consistently showed activation across stimuli were located in the medial prefrontal cortex, inferior frontal cortex, inferior temporal cortex and extrastriate occipital cortex (Sabatinelli *et al.* 2011).

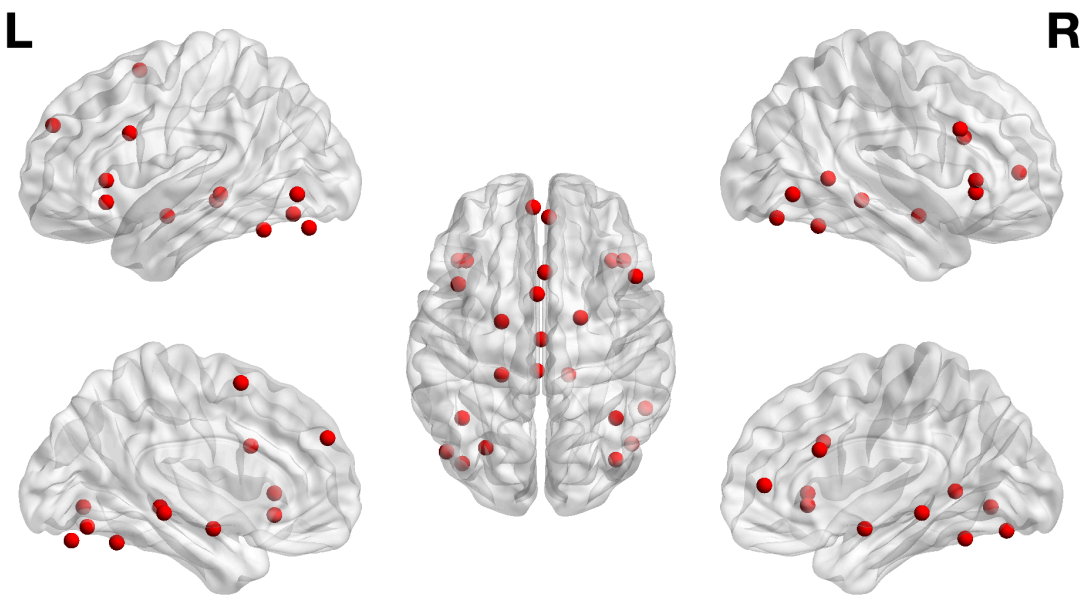

Fig. 12: Illustration of the emotional scene and face processing network. Created with BrainNet Viewer, Version 1.32 (Xia *et al.* 2013). Several regions lie within the cerebellum, which is not included in the model. MNI-coordinates as published by Sabatinelli and colleagues (Sabatinelli *et al.* 2011).

The other network involved in emotional processing that was analyzed for the present study is the extended social-affective default network (eSAD, (Amft *et al.* 2015), which includes regions of the DMN involved in social and affective processes as well as related areas. The eSAD network comprises regions such as the amygdala and the hippocampus, associated with emotional and memory processes. It further includes brain regions associated with motivation and reward or autobiographical information (Amft *et al.* 2015) and is thus involved in a broad variety of cognitive functions that might be impaired in PD.

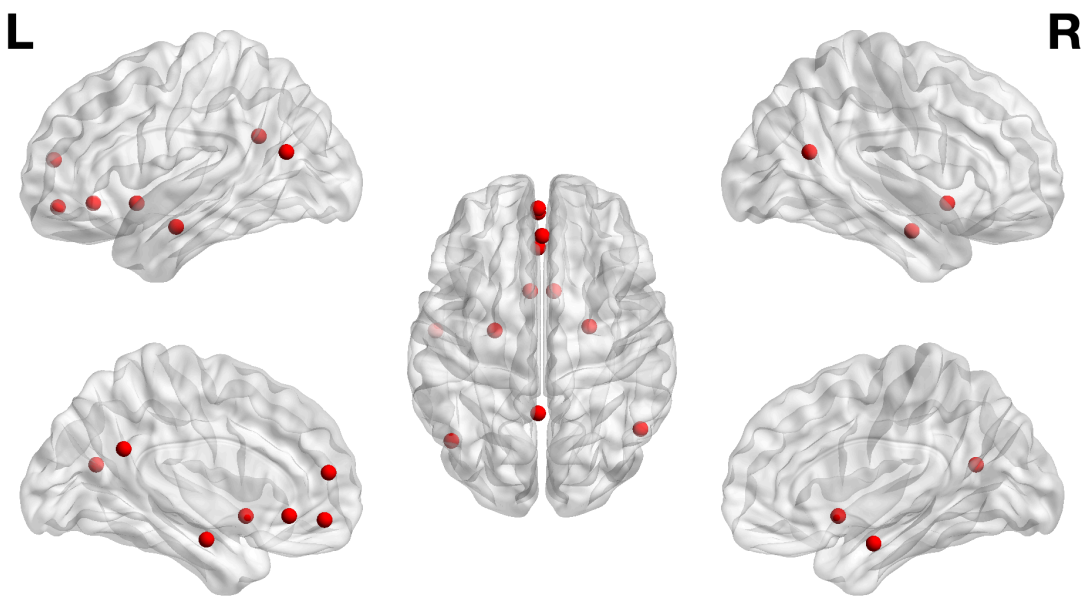

Fig. 13: Illustration of the extended social-affective default network. Created with BrainNet Viewer, Version 1.32 (Xia *et al.* 2013). MNI-coordinates as published by Amft and colleagues (Amft *et al.* 2015).

2.5.8 Reward-related processes

As PD affects the dopaminergic pathways in the brain which are also involved in reward-related behavior, a meta-analytically defined network involved in reward-related decision-making (Rew) was included in this study as well. A common reward-related symptom in PD is, e.g., impulse control disorder, often caused by dopamine replacement therapy (Drew *et al.* 2020). Regions of the Rew network include the nucleus accumbens, caudate, putamen, thalamus, orbitofrontal cortex, bilateral anterior insula, cingulate cortex (anterior and posterior), inferior parietal lobule and prefrontal cortex (Liu *et al.* 2011)

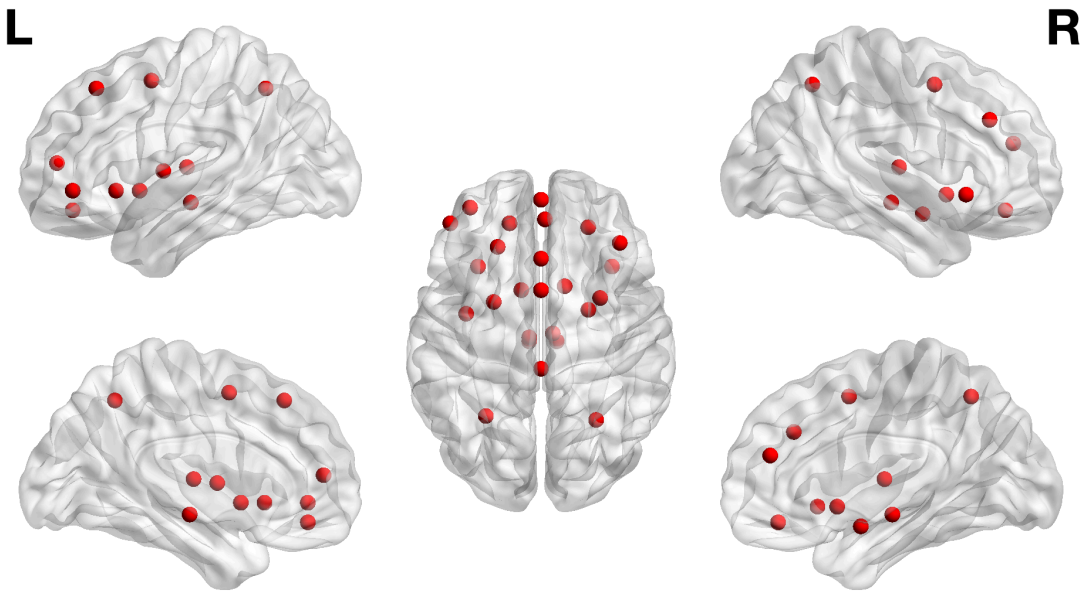

Fig. 14: Illustration of the reward-related decision-making network. Created with BrainNet Viewer, Version 1.32 (Xia *et al.* 2013). MNI-coordinates as published by Liu and colleagues (Liu *et al.* 2011).

2.6 Calculation of resting-state functional connectivity

The location of the network regions were described by MNI coordinates. Each region within the network was defined as a network node. To obtain a characteristic BOLD time series for a node, the time series of each voxel within a 6 mm sphere around the center of each region were extracted and averaged. The weights of the edges between the network nodes were defined as the correlation between the time series of the two respective nodes. The weights were calculated as Pearson's correlation coefficient.

2.7 Measures of network connectivity

To systematically quantify within- and between-network FC of the included networks, three different variations of simple average FC as well as several graph-theory based measures suitable for the analysis of human brain networks were calculated.

2.7.1 Average functional connectivity measures

As this work focuses on the interaction of the DMN with other networks and the brain as a whole, first, the average within-network FC (wnFC; cf. Fig. 15a) of each network separately as mean FC between all pairs of nodes of the network was calculated. Second, the average FC of different network-combinations was calculated. To this end, the DMN was paired with each of the TPNs and with the WBN and again mean FC between all pairs of nodes of the network-combination was calculated (combFC; cf. Fig. 15b). Finally, the average between-network FC (bnFC) was of interest. To this end, the same network combinations as for combFC were analyzed, but focusing on the between-network edges, excluding any within-network connections (cf. Fig. 15c).

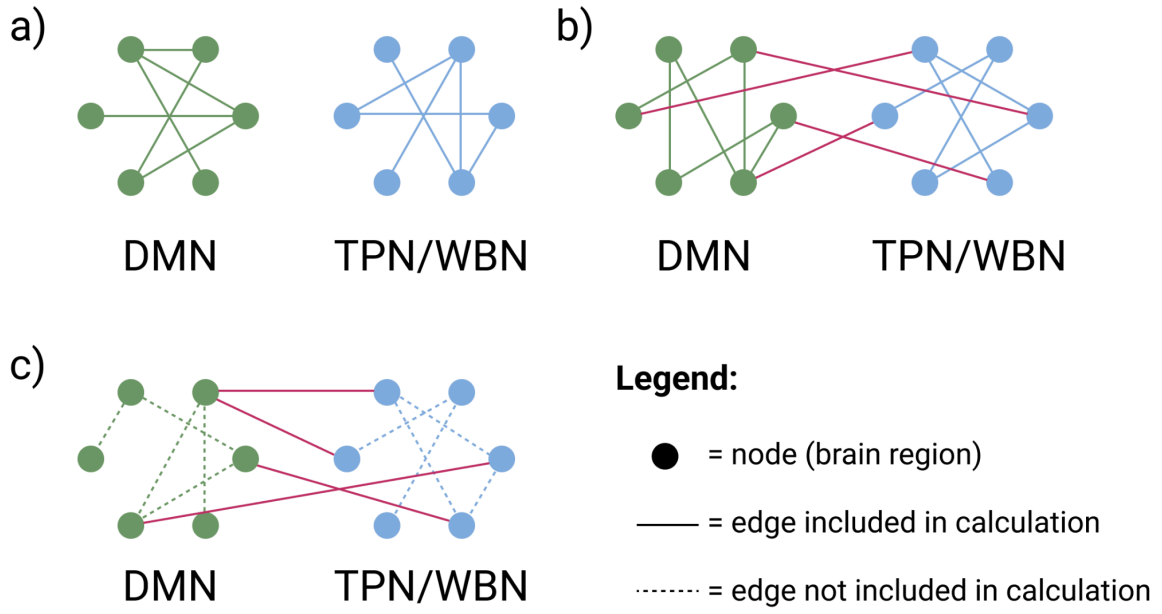

Fig. 15: Schematic of average functional connectivity measures. Bold lines were included into the calculations of a given measure, dotted lines were excluded. a) Average within-network functional connectivity (wnFC) of the default mode network (DMN), the task-positive networks (TPNs), and the whole-brain network (WBN). b) Average functional connectivity of the DMN taken together with each TPN or the WBN separately (combFC). c) Average between-network functional connectivity of the DMN taken together with each TPN or the WBN separately (bnFC).

2.7.2 Graph theory measures

To further characterize the integration and segregation of the DMN with TPNs and the WBN, several graph theory measures were computed using the Brain Connectivity Toolbox (Sporns 2018; https://sites.google.com/site/bctnet/).

Global efficiency

The Global efficiency (GE) of a network is a measure that describes how efficiently information is exchanged between the different nodes of a given network (Fagiolo 2007; Latora & Marchiori 2001; Onnela *et al.* 2005; Rubinov & Sporns 2010). It is defined as the average of the inverse shortest path length. Weighted GE is calculated as (Ek *et al.* 2015; Latora & Marchiori 2001; Rubinov & Sporns 2010):

$$E^W = \frac{1}{n} \sum_{i \in N} \frac{\sum_{j \in N,\, j \neq i} \left(d_{ij}^w\right)^{-1}}{n-1}$$

where:

- n = number of nodes within the given network
- d_{ij} = distance between two nodes (i and j)

Higher weights correspond to a shorter path length. Values for GE range between 0 and 1, where 1 indicates the highest possible efficiency as observed in a fully connected network. Paths between disconnected nodes are defined as having a length of ∞. Contrary to the characteristic path length, global efficiency is more influenced by short paths and therefore might be a suitable measure to characterize network integration (Achard & Bullmore 2007; Rubinov & Sporns 2010). GE can be used in the context of functional networks, however it has to be noted that functional networks have in general weaker connections between nodes and therefore have a lower global efficiency than structural and effective networks (Rubinov & Sporns 2010).

GE was calculated for the DMN alone, for each combination of DMN and TPN and the DMN combined with the whole-brain network.

Mean global diffusion efficiency

The mean global diffusion efficiency (DE) is the average of the inverse of the mean first passage time, which is itself defined as the average amount of steps or time it takes to move from node *i* to node *j* of a given network, while choosing a random path. It is calculated as (Goñi *et al.* 2013):

$$E_{diff} = \frac{\sum_i \sum_j \frac{1}{t_{ij}}}{n(n-1)},\ i \neq j$$

where:

- t_{ij} = mean first-passage time of an undirected graph

To describe communication within a network, two concepts can be differentiated: routing or diffusion. Whereas routing describes directed, navigated movement of information to a specific target (for example characterized using GE), diffusion describes a more passive, random movement without a specific target. Passive diffusion can be observed in different types of networks, like social networks, and might play a role in neural networks as well (Goñi *et al.* 2013). The measures of diffusion efficiency were developed to complement known measures for routing efficiency (Goñi *et al.* 2013).

Mean nodal eccentricity

The mean nodal eccentricity (ECC) is defined as the average maximal path length between a node and any other node of a given network (https://sites.google.com/site/bctnet/list-of-measures):

$$e(v) = \max\{d(u,v) : u \in V\}$$

where:

- u, v = nodes of a given network

The minimal possible eccentricity corresponds to the radius of the network, whereas the maximal possible eccentricity is the diameter. Eccentricity is related to the characteristic path length, which is defined as the average shortest path length between all pairs of nodes within a given network (Rubinov & Sporns 2010).

Mean node betweenness centrality vector

The node betweenness centrality (BET) is defined as the portion of all possible shortest paths in a given network that involve the examined node. That means that a node with a high betweenness centrality takes part in many shortest paths. It

acts as an information bridge and is therefore central for information flow within the network.

Betweenness centrality was first described by Freeman (Freeman 1977) and is mathematically described as (Brandes 2001):

$$C_B(v) = \sum_{s \neq v \neq 1 \in V} \frac{\sigma_{st}(v)}{\sigma_{st}}$$

where:

- σ_{st} = total number of shortest paths from node s to node t
- $\sigma_{st}(v)$ = number of shortest paths that pass through v

Nodes with a high betweenness centrality are often hub nodes.

Mean positive participation coefficient

The positive participation coefficient (PPC) is defined as the distribution of positively weighted edges of a given node within its own community and with other communities.

For the present study, every investigated network was defined as one community and the PPC was then calculated for each node of the DMN, combined with the nodes of another community. Values of the PPC vary between 0 and 1, with values close to 1 indicating an equal distribution of edges between the communities and 0 indicating a restriction of edges to one community (Guimerà & Nunes Amaral 2005).

$$P_i = 1 - \sum_{s=1}^{N_m} \left(\frac{K_{is}}{k_,} \right)^2$$

where:

- K_{is} = number of links of a node *i* in a module *s*
- k_i = total degree of node *i*

Mean nodal strength of positive/negative weights

The nodal strength (ST) is defined as the sum of the weights of all edges that are connected to a given node (Fornito 2016). It is the weighted analogue of a node's degree, which is simply defined as the number of edges one specific node has. Mathematically, normalized (average) strength of a node is described as (Fornito 2016):

$$s'_i = \frac{1}{N-1} \sum_{j \neq i} w_{ij}$$

where:

- w_{ij} = weight of the edge between the nodes *i* and *j*

2.7.3 Functional connectivity filters

In graph theory, it is a common procedure to apply filters to FC by only including edges above a certain weight into the calculations. However, little is known about the impact of the use of such thresholds and to date, no standard threshold level exists. In the present work, three different threshold levels were applied. At the first threshold level, named thrX, both negative and positive edges were retained, if allowed by the respective measure. Second, a threshold level of 0, named thr0, was applied, retaining only edges with a positive correlation coefficient. All negative correlations were set to 0. Third, a threshold level at 0.25, named thr25, was applied, including only higher correlations between node time series in the calculation. All correlations below 0.25 were set to 0.

2.8 Statistics

Analogous to the FC calculation, all statistical tests were conducted on both datasets separately.

2.8.1 Patient parameters

To compare the age distribution of the PD and HC groups, a two-sample t-test was conducted. Gender distribution among groups was compared via the Chi^2-test.

Differences between motor symptom severity ((MDS-)UPDRS-III OFF) and disease stage (Hoehn & Yahr, H&Y) were evaluated using two-sample t-tests. This test was conducted despite the use of different versions of the UPDRS in the two datasets, as it was demonstrated that there is a high correlation between the two scales (Merello *et al.* 2011).

2.8.2 Functional connectivity measures

Statistical analyzes were conducted separately for each measure (i.e., three variations of average FC and six different graph theory derived measures) and each of the 13 networks and DMN-TPN/-WBN-combinations respectively. The data were first tested for group differences between PD patients and healthy controls, followed by testing for correlations of each measure with motor disease severity in PD patients.

Group differences in FC measures between PD and HC groups were analyzed by using the analysis of covariance (ANCOVA) procedure. Age and gender were included as covariates. For each measure and each network or network combination, a separate ANCOVA was conducted. False discovery rate (FDR) procedure was used to correct for multiple comparisons, to account for the number of included networks and resulting network combinations (Benjamini & Hochberg 1995).

For the examination of the relationships between FC measures and clinical symptom severity, Pearson's partial correlations were calculated. To this end, the FC measures were correlated with (MDS-)UPDRS-III OFF. Age and gender were included as covariates. Significance levels were again adjusted for multiple testing using the FDR procedure.

3 Results

3.1 Participants

No differences in age and gender distribution between PD patient and HC groups were detected in either dataset ($p > 0.05$). Furthermore, the age and gender distribution of both datasets was similar ($p > 0.5$). When comparing the motor symptom severity in PD patients of both datasets, measured by (MDS-)UPDRS-III OFF, no significant differences could be found ($p > 0.05$). The only significant difference between the patient characteristics of both datasets was a higher average Hoehn & Yahr stage in Data-DU ($p < 0.05$).

3.2 Data-PR

3.2.1 Group differences

For every measure and every network, a group-wise comparison was performed between PD and HC. Among the networks that showed significant group differences between the two groups were the DMN, both motor networks (MotorPerc and MotorEx), the vigilant attention network (VigAtt) and the whole-brain network (WBN). Of all the tested measures, significant group differences were found for wnFC, combFC, and the graph theory measures GE and DE. Concerning the FC thresholds (thrX, thr0 and thr25), it was observed, that more significant results appeared without a threshold (thrX), while the exclusion of negative edges (thr0) and rising the FC threshold to 0.25 (thr25) gradually lead to a reduction of significant differences. All FDR-corrected *p*-values can be found in the appendix.

WnFC of both motor networks was significantly reduced in PD patients at all three FC thresholds (see Fig. 16). Besides the DMN, wnFC of different TPNs, namely CogAC, CogAR, Rew, VigAtt, as well as in the WBN was significantly reduced in PD patients. In contrast to wnFC-changes in the motor networks, the mentioned networks only showed significant differences at FC threshold levels thrX (no threshold) and thr0 (only positive edges retained).

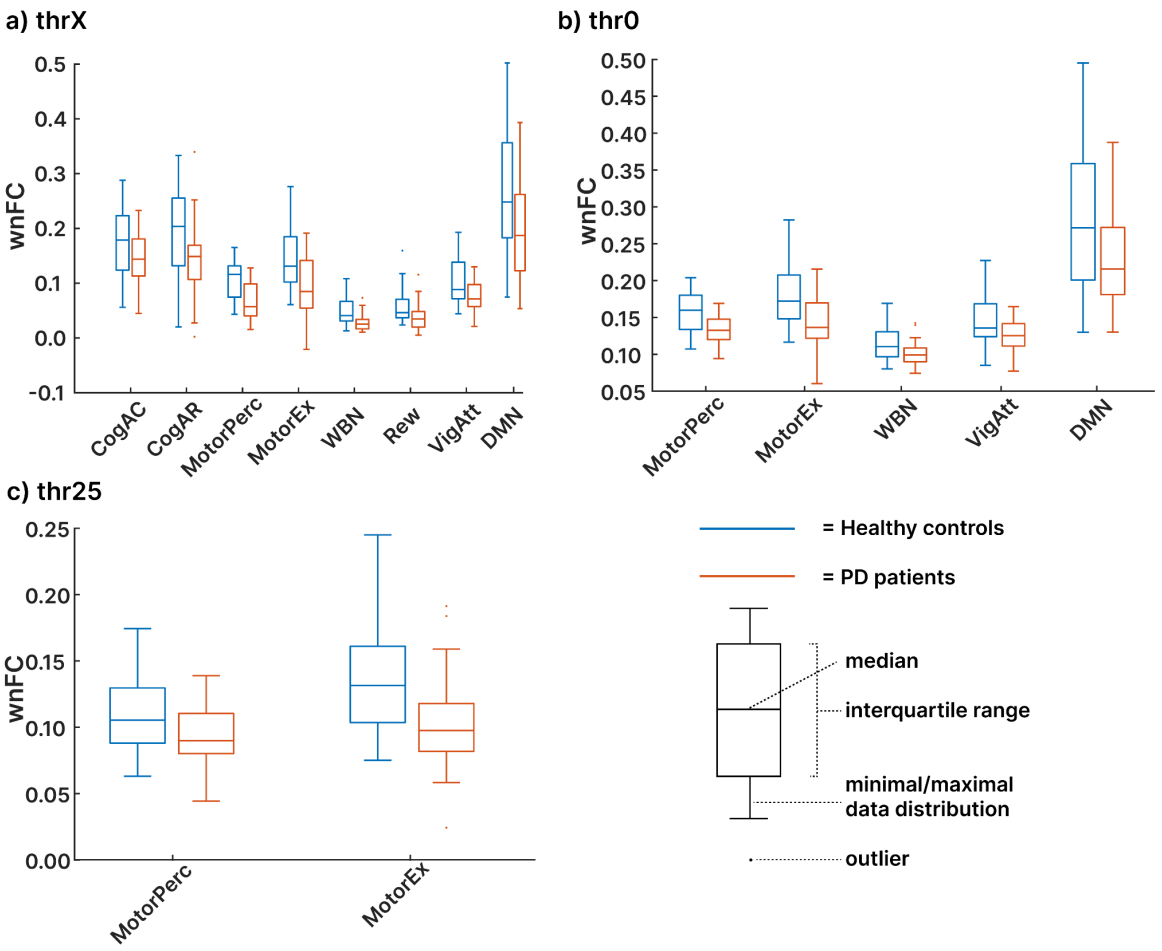

Fig. 16. Group differences in wnFC in Data-PR. Displayed are boxplots showing the data distribution for networks with significant differences in average within-network functional connectivity (wnFC). Conducted statistical analysis: Analysis of covariance (covariates: gender, age), false-discovery-rate-corrected *p*-level 0.05. Computation at 3 functional connectivity threshold levels (thr): thrX = all weights included, thr0 = positive edges retained, thr25 = weights above 0.25 retained. Networks: Default mode network (DMN), cognitive action control network (CogAC), cognitive action regulation network (CogAR), perceptuo-motor network (MotorPerc), motor execution network (MotorEx), whole-brain network (WBN), reward-related decision-making network (Rew), vigilant attention network (VigAtt).

When analyzing the average FC of the DMN combined with each of the TPNs and the WBN (combFC), a decrease was observed for the combinations of the DMN with CogAC, CogAR, MotorEx, MotorPerc, Rew, VigAtt, eMDN and the WBN (see Fig. 17). All the mentioned network combinations (DMN-TPN/WBN) showed significant differences at thrX, some also at thr0.

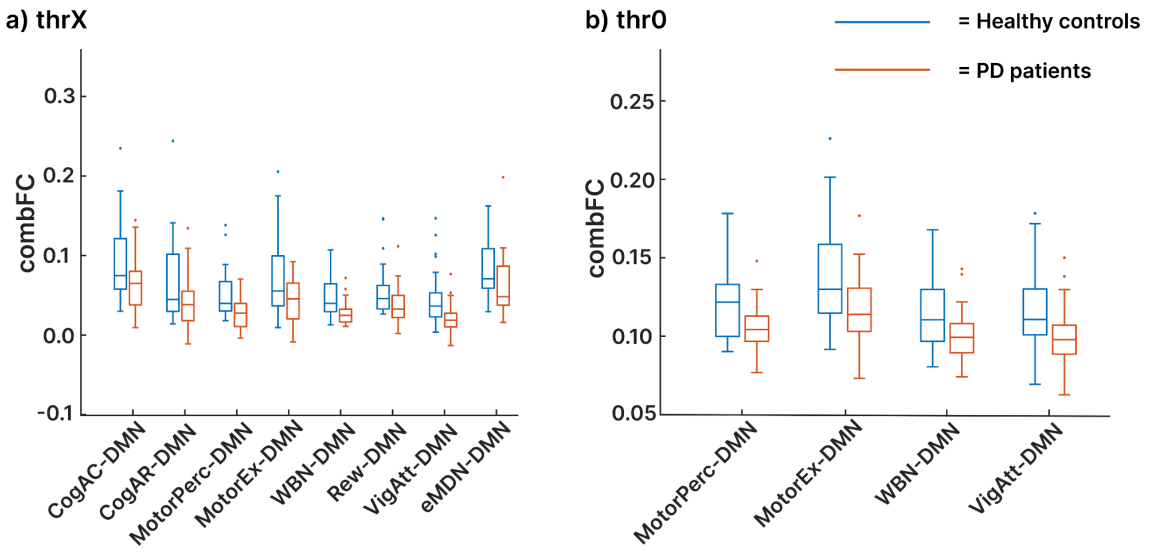

Fig. 17: Group differences in combFC in Data-PR. Displayed are boxplots showing the data distribution for networks with significant differences in average combined functional connectivity (combFC). Conducted statistical analysis: Analysis of covariance (covariates: gender, age), false-discovery-rate-corrected *p*-level 0.05. Computation at 3 functional connectivity threshold levels (thr): thrX = all weights included, thr0 = positive edges retained, thr25 = weights above 0.25 retained. Networks: Default mode network (DMN), cognitive action control network (CogAC), cognitive action regulation network (CogAR), perceptuo-motor network (MotorPerc), motor execution network (MotorEx), whole-brain network (WBN), reward-related decision-making network (Rew), vigilant attention network (VigAtt), extended multiple demand network (eMDN).

No significant group differences of pure between-network average FC (bnFC) were observed.

Concerning the analyzed graph theory measures, significant group differences were found for GE and DE. Except for PPC and ST, the analyses for the graph theory measures were only performed at thr0 and thr25, as per definition not all the measures allow negative weights.

The GE of the DMN as well as of the DMN combined with the MotorEx and VigAtt networks was reduced in PD patients at thr0 (cf. Fig. 18). At thr25, none of these differences were significant.

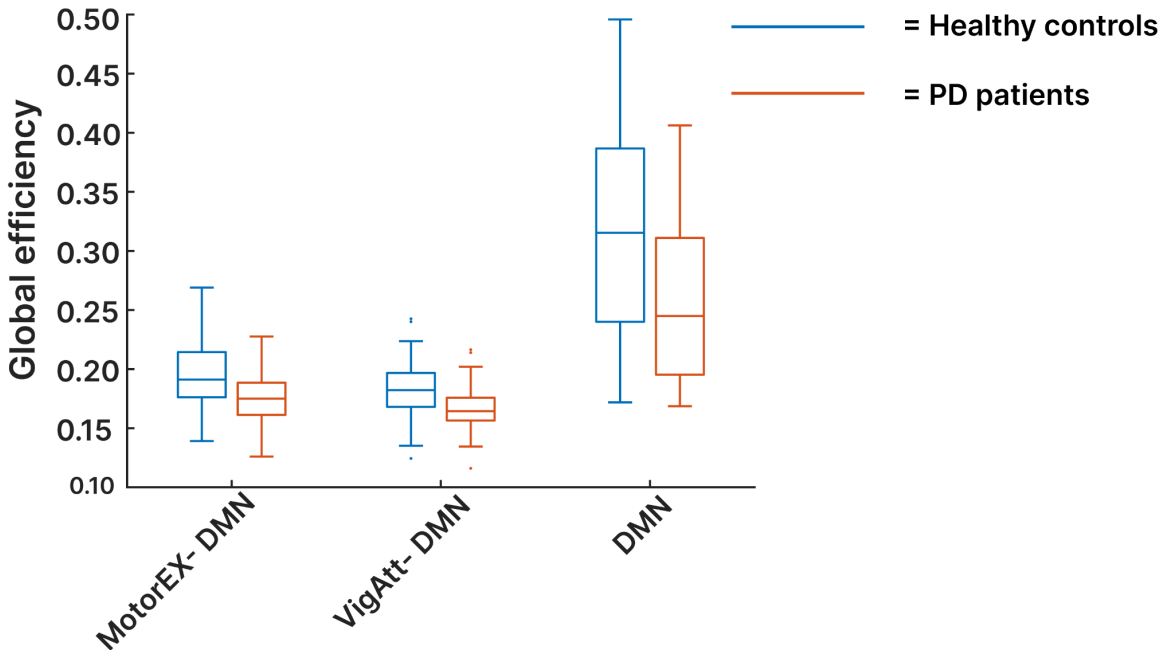

Fig. 18: Group differences in GE in Data-PR. Displayed are boxplots showing the data distribution for networks with significant differences in global efficiency (GE). Conducted statistical analysis: Analysis of covariance (covariates: gender, age), false-discovery-rate-corrected *p*-level 0.05. Displayed are results from analysis at FC threshold level thr0 (only positive edges retained). Networks: Default mode network (DMN), motor execution network (MotorEx), vigilant attention network (VigAtt).

In PD patients, DE was significantly reduced in several network combinations at thr0, namely the DMN and the combinations of DMN with CogAC, MotorPerc, Rew, VigAtt, WM, eMDN, eSAD and WBN (cf. Fig. 19). At thr25, only the group differences in network combinations of DMN with WBN and eSAD remained significant.

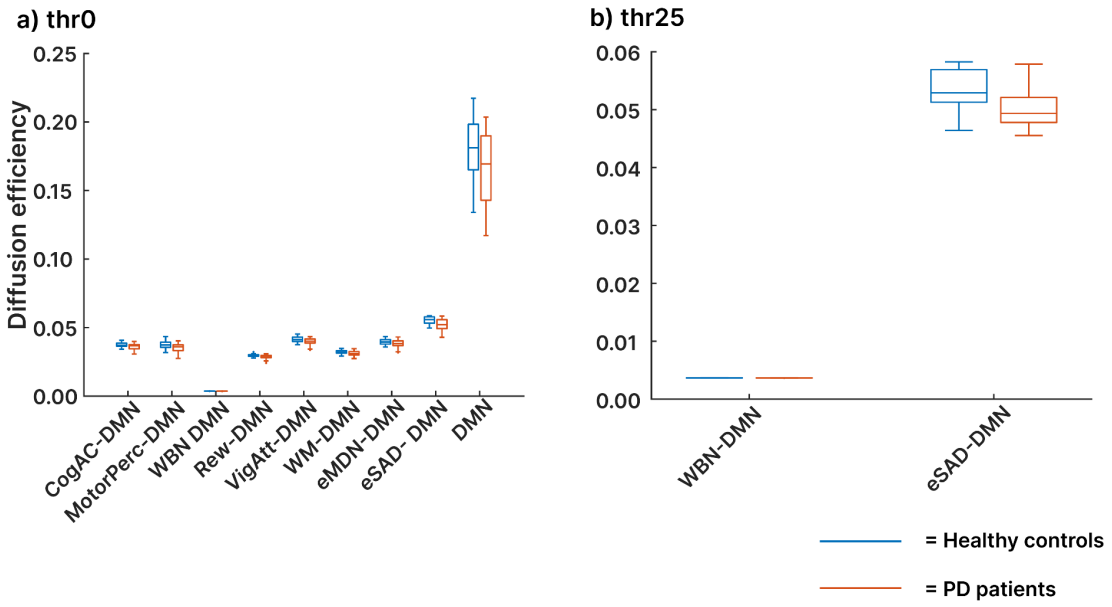

Fig. 19: Group differences in DE in Data-PR. Displayed are boxplots showing the data distribution for networks with significant differences in diffusion efficiency (DE). Conducted statistical analysis: Analysis of covariance (covariates: gender, age), false-discovery-rate-corrected *p*-level 0.05. Displayed are results from analysis at FC threshold level thr0 (only positive edges retained) and thr25 (only edges with weights > 0.25). Networks: Default mode network (DMN), cognitive action control network (CogAC), perceptuo-motor network (MotorPerc), whole-brain network (WBN), reward-related decision-making network (Rew), vigilant attention network (VigAtt), working memory network (WM), extended multiple demand network (eMDN), extended social-affective default network (eSAD).

3.2.2 Correlations with motor symptom severity

All different FC metrics were correlated with motor symptom severity. In general, stronger correlations were observed at a higher FC threshold. Among the networks that showed significant group differences were the DMN, MotorPerc and MultiTask. Of all tested measures, the highest number of significant correlations was observed for wnFC (of DMN), ST, PPC and GE.

First, a negative correlation between wnFC of the DMN and motor symptom severity was found at thr0 and thr25 (thr0: r = -0.53; thr25: r = -0.57, both $p < 0.05$, cf. Fig. 20).

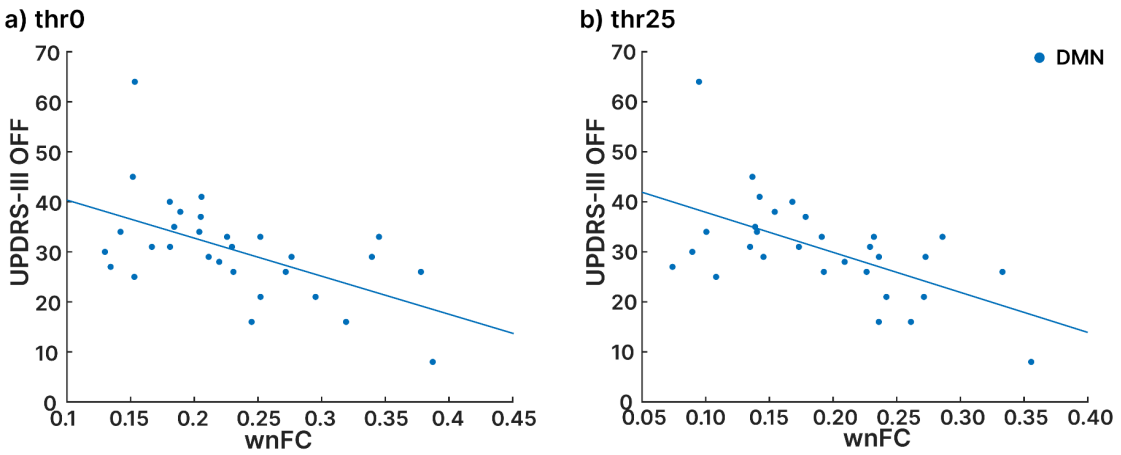

Fig. 20: Correlation of wnFC with UPDRS-III OFF in Data-PR. Scatter plots showing the relation between motor symptom severity (measured by part III of the unified PD Rating Scale in medical OFF-state, UPDRS-III OFF) and within-network functional connectivity (wnFC) of the default mode network (DMN). Significant Pearson's partial correlation to a *p*-level of < 0.05 at two different FC threshold levels: a) thr0 = positive edges retained, b) thr25 = weights above 0.25 retained. Pearson's r: thr0: $r = -0.53$; thr25: $r = -0.57$, both $p < 0.05$.

Another finding concerning the average FC measures was a positive correlation of bnFC between the DMN and MotorPerc with UPDRS-III OFF ($r = 0.542$, $p < 0.05$) at thrX. When using an FC threshold, this correlation was no longer significant (cf. Fig. 21).

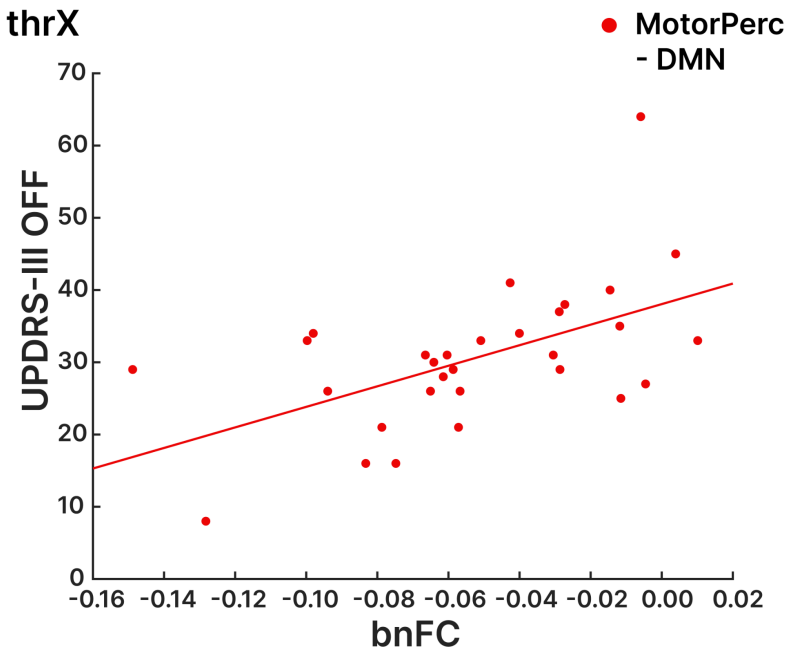

Fig. 21: Correlation of bnFC with UPDRS-III OFF in Data-PR. Scatter plot showing the relation between motor symptom severity (measured by part III of the unified PD Rating Scale in medical OFF-state, UPDRS-III OFF) and average between-network functional connectivity (bnFC) of the perceptuo-motor network (MotorPerc). Significant Pearson's partial correlation at a *p*-level of < 0.05. No FC threshold applied (thrX).

For the graph theory measures, the following correlations were significant: ST within the DMN correlated negatively with UPDRS-III OFF at all FC threshold levels (thrX: r = -0.53; thr0: r = -0.54; thr25: r = -0.56; all $p < 0.05$). Furthermore, at thr25 ST of several DMN-TPN combinations showed a significant correlation, too, namely combinations of DMN with CogAR (r = -0.45), emotional scene and face processing (EmoSF, r = -0.42), MotorEx (r = -0.48), MultiTask (r = -0.52), Rew (r = -0.42), eMDN (r = -0.43) and eSAD (r = -0.53, cf. Fig. 22).

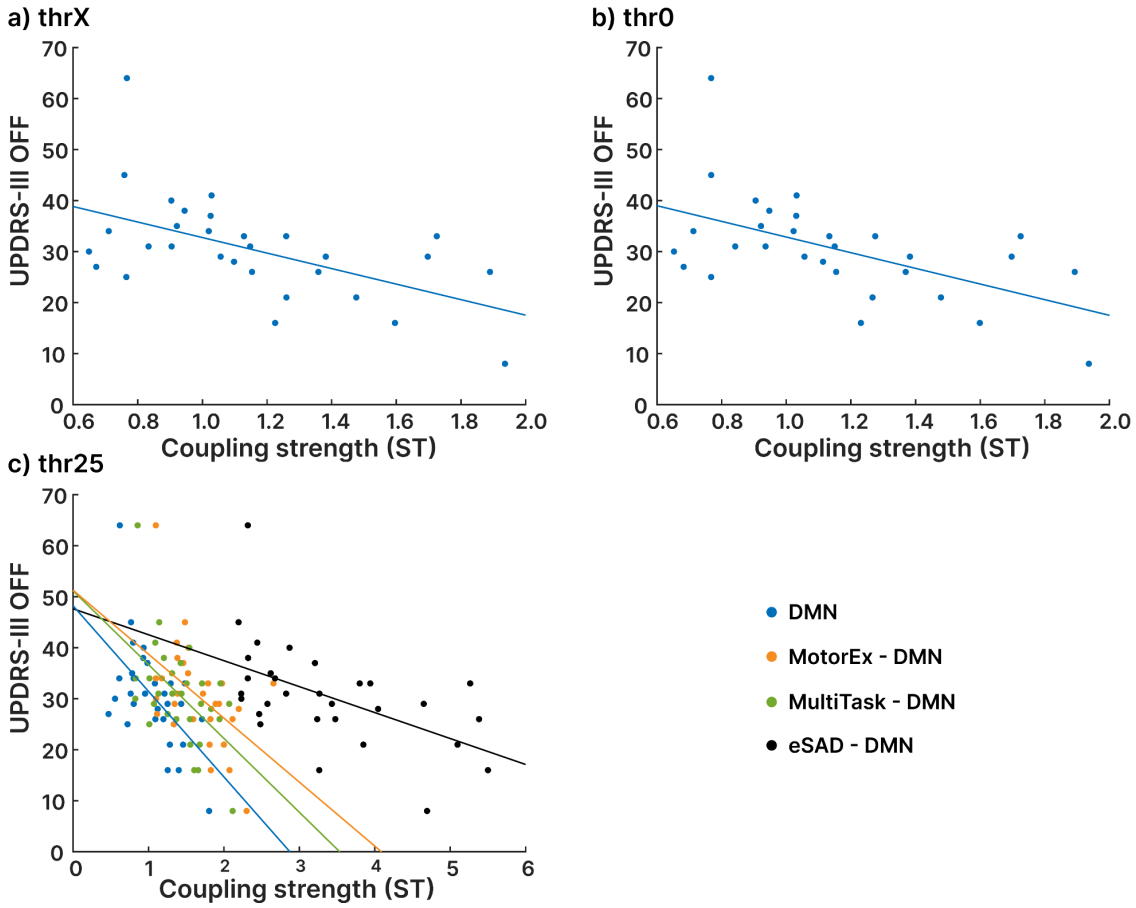

Fig. 22: Correlation of ST with UPDRS-III OFF in Data-PR. Scatter plots showing the relation between motor symptom severity (measured by part III of the unified PD Rating Scale in medical OFF-state, UPDRS-III OFF) and mean nodal strength (ST). Significant Pearson's partial correlation to a *p*-level of < 0.05). Analysis conducted for 3 functional connectivity threshold levels (thr): a) thrX = all weights included; b) thr0 = positive edges retained; c) thr25 = weights above 0.25 retained. For reasons of readability, the diagram showing the correlations of ST at thr25 does not contain all significant networks. Not displayed are ST of DMN-CogAR (r = -0.45), DMN-EmoSF (r = -0.42), DMN-Rew (r = -0.42) and DMN-eMDN (r = -0.43; all p < 0.05). Networks: Default mode network (DMN), cognitive action regulation network (CogAR), emotional scene and face processing network (EmoSF), motor execution network (MotorEx), multitasking network (MultiTask), extended multiple demand network (eMDN), extended social-affective default network (eSAD).

For the PPC, several DMN-TPN combinations correlated with motor symptom severity (cf. Fig. 23). At all FC thresholds, significant correlations were found for the DMN combined with MotorPerc (thrX: r = 0.49; thr0: r = 0.49; thr25: r = 0.59) and MultiTask (thrX: r = 0.54; thr0: r = 0.53; thr25: r = 0.50). At thr25, also the PPC of DMN combined with CogAC (r = 0.47) and MotorEx (r = 0.50) were positively

correlated with UPDRS-III OFF. The PPC of the DMN combined with the WBN however was negatively correlated with UPDRS-III OFF at thr25 (r = -0.44).

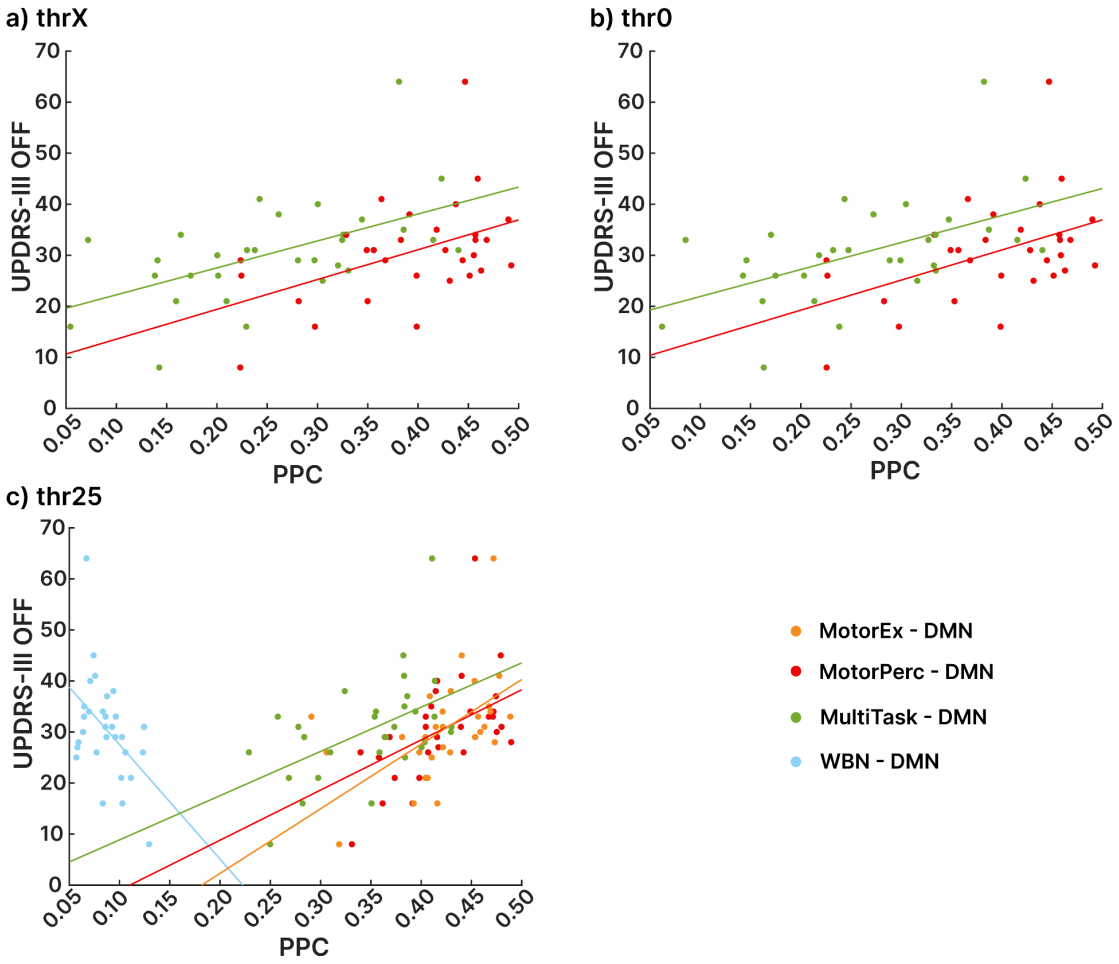

Fig. 23: Correlation of PPC with UPDRS-III OFF in Data-PR. Scatter plots showing the relation between motor symptom severity (measured by part III of the unified PD Rating Scale in medical OFF-state, UPDRS-III OFF) and mean positive participation coefficient (PPC) of the default mode network (DMN) combined with task-positive networks/whole-brain network. Significant Pearson's partial correlation (p < 0.05). Analysis conducted for 3 functional connectivity threshold levels (thr): a) thrX = all weights included; b) thr0 = positive edges retained; c) thr25 = weights above 0.25 retained. For reasons of readability, the correlation of the PPC of DMN-CogAC (r = 0.47) with UPDRS-III OFF is not displayed. Networks: multitasking network (MultiTask), perceptuo-motor network (MotorPerc), motor execution network (MotorEx), whole-brain network (WBN).

Finally, a negative correlation of GE of the DMN with UPDRS-III was observed at both tested FC threshold levels (thr0: r = -0.54 and thr25: r = -0.54), as well as a negative correlation of the GE of DMN-MultiTask at thr25 (r = -0.47, cf. Fig. 24).

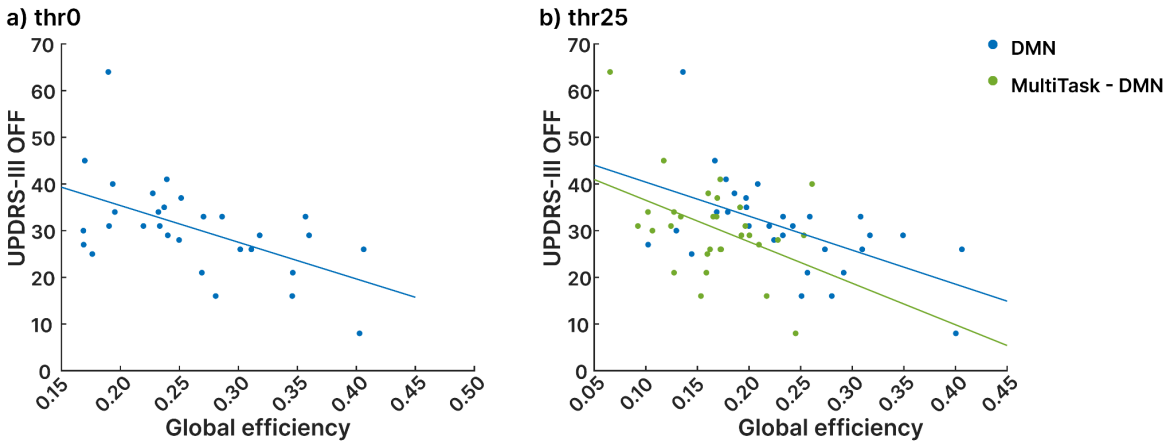

Fig. 24: Correlation of GE with UPDRS-III OFF in Data-PR. Scatter plots showing the relation between motor symptom severity (measured by part III of the unified PD Rating Scale in medical OFF-state, UPDRS-III OFF) and global efficiency (GE) of the default mode network (DMN) and the combination of the DMN with the multitasking network (MultiTask). Significant Pearson's partial correlation to a *p*-level of < 0.05 at two different FC threshold levels: a) thr0 = positive edges retained, b) thr25 = weights above 0.25 retained. Pearson's r: GE of DMN at thr0: r = -0.54 and thr25: r = -0.54, GE of DMN-MultiTask at thr24: r = -0.47, all $p < 0.05$.

3.3 Data-DU

3.3.1 Group differences

As in Data-PR, for every measure and every network, a group-wise comparison was performed between PD and HC. However, in Data-DU, only few significant group differences were observed. These appeared primarily when no FC threshold was applied.

Concerning the average FC measures, no significant group differences were found using a conservative significance criterion of $p < 0.05$. However, average within-network FC (wnFC) of the DMN ($p = 0.07$) and eMDN ($p = 0.09$) was lower in PD patients at a trend-level at thrX. The other networks that showed a significantly lower wnFC in Data-PR (CogAC, CogAR, MotorPerc, MotorEx, WBN, Rew, VigAtt) did not differ in Data-DU. For average combined FC (combFC), again only a trend-level decrease in PD patients was observed for several DMN-TPN combinations (CogAC, MotorPerc, MotorEx, MultiTask, eMDN, all $p < 0.1$).

For the graph theoretical measures, significant differences were found for DE and ECC. At thr0, DE of several DMN-TPN/WBN combinations was reduced in

PD-patients, namely the DMN combined with WBN, CogAC, Rew, VigAtt, WM, eMDN, eSAD, as well as in the DMN alone (all $p < 0.05$, cf. Fig. 25).

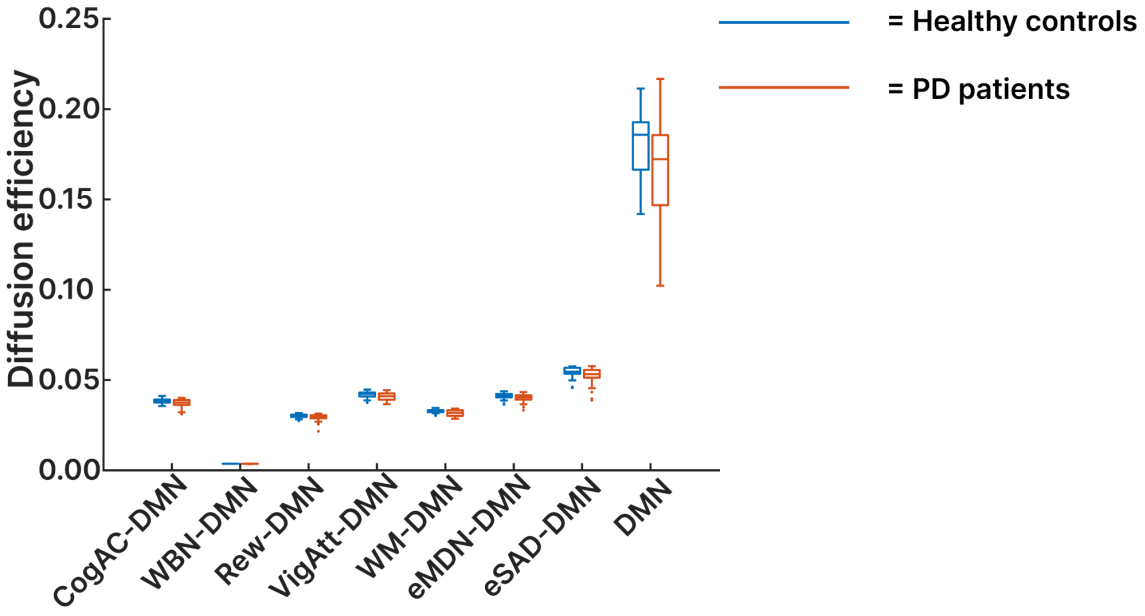

Fig. 25: Group differences in DE in Data-DU. Displayed are boxplots showing the data distribution for networks with significant differences in diffusion efficiency (DE). Conducted statistical analysis: Analysis of covariance (covariates: gender, age), false-discovery-rate-corrected *p*-level 0.05. Displayed are results from analysis at FC threshold level thr0 (only positive edges retained). Networks: Default mode network (DMN), cognitive action control network (CogAC), whole-brain network (WBN), reward-related decision-making network (Rew), vigilant attention network (VigAtt), working memory network (WM), extended multiple demand network (eMDN), extended social-affective default network (eSAD).

Finally, at thr0, the mean nodal eccentricity (ECC) showed a significant increase in PD patients for the combination of the DMN with MultiTask ($p = 0.038$, cf. Fig. 26).

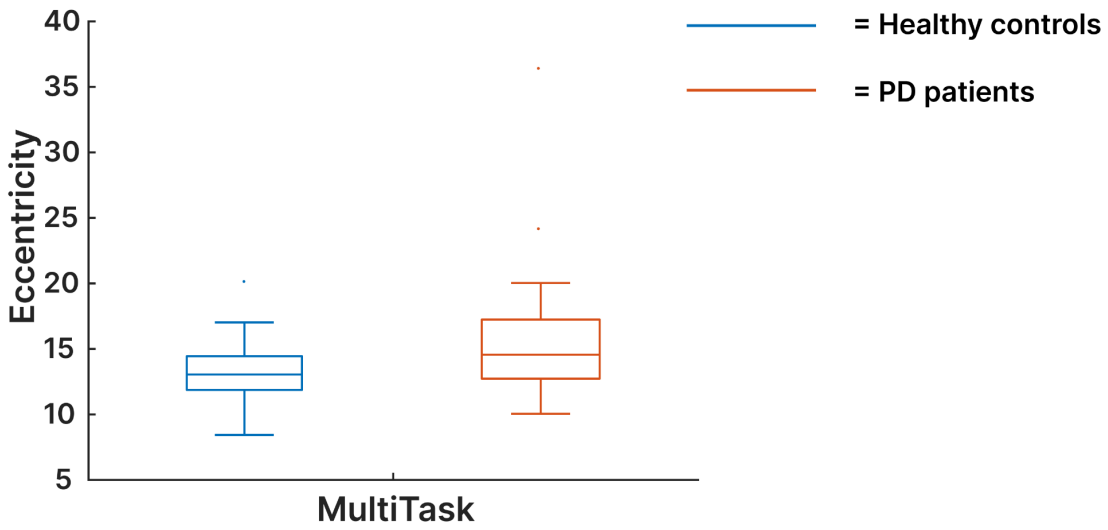

Fig. 26: Group differences in ECC in Data-DU. Displayed are boxplots showing the data distribution for group differences in mean nodal eccentricity (ECC) in the combination of the default mode network (DMN) with the multitasking network (MultiTask) at functional connectivity threshold level thr0 (only positive edges retained). Conducted statistical analysis: Analysis of covariance (covariates: gender, age), false-discovery-rate-corrected *p*-level 0.05.

3.3.2 Correlations with motor symptom severity

At a conservative *p*-level of 0.05, no significant correlations were found in Data-DU. However, at a trend-level, some observations could be made. Without the application of an FC threshold (thrX), wnFC of the DMN (r = -0.41) and combFC of the DMN combined with eSAD (r = -0.39) and the WBN (r = -0.40) correlated negatively with disease severity (all $p < 0.1$). Concerning graph theory measures, at thrX, ST of DMN combined with MotorPerc (r = -0.42), MotorEx (r = -0.48) and WBN (r = -0.40) was negatively correlated with motor symptoms (all $p < 0.1$). Similar correlations also appeared at thr0.

At thr25, some trend-level correlations of GE and BET were found. GE of the DMN combined with CogAC, MotorEx, WM and eSAD were negatively correlated with MDS-UPDRS-III (all $p < 0.1$). Finally, BET of the DMN together with CogAR and MotorEx showed a negative correlation with motor symptoms at thr25 (all $p < 0.1$).

3.4 Consistent findings across datasets

3.4.1 Group differences

At a significance level of $p < 0.05$, both datasets showed significant group differences for the DE within several DMN-TPN-combinations, i.e., the DMN combined with CogAC, WBN, Rew, VigAtt, WM, eMDN, eSAD, and the DMN alone (thr0). When considering a more lenient statistical significance of $p < 0.1$, a consistent finding was the decreased wnFC of the DMN at thrX ($p = 0.033$ in Data-PR and $p = 0.07$ in Data-DU). Similarly, combFC of several DMN-TPN combinations was decreased in both datasets (thr0; $p < 0.1$), namely the combinations of the DMN with CogAC, MotorPerc, MotorEx, MultiTask, WM and eMDN.

Overall, it can be said that a relatively large portion of the findings in Data-DU were also present in Data-PR, but in Data-PR, other significant differences were found, that were not present in Data-DU.

3.4.2 Correlations with motor symptom severity

When comparing the correlations with motor symptom severity in both datasets, the only consistent correlation was a negative correlation of wnFC of the DMN with UPDRS-III OFF. It should however be noted that this correlation was observed at different FC threshold levels (thrX in Data-DU and thr0 and thr25 in Data-PR). In Data-DU, the correlation was significant only at a trend level of $p < 0.1$.

In both datasets, the DMN and the two motor networks showed significant correlations with disease severity, albeit for different FC measures (significance level of $p < 0.1$ for Data-DU).

4 Discussion

In the present work, resting-state functional connectivity of predefined meta-analytic networks in PD patients was analyzed to study its potential of serving as a diagnostic or monitoring biomarker for PD. To find valuable biomarker candidates, a wide variety of functional networks and functional connectivity measures were included and analyzed. The computed measures comprised variations of average functional connectivity and graph theory measures and were used to characterize within- as well as between-network FC. Measures were statistically tested for group differences between PD patients and healthy controls and correlated with motor symptom severity.

In this discussion, the disease specific results will be reviewed in the context of the current literature and evaluated for their potential to serve as foundations for further biomarker research. Furthermore, the broader implications of functional connectivity in biomarker research will be considered. Then, the challenges and limitations will be addressed, followed by a conclusion that aims at guiding future research in this field.

4.1 Discussion of results

4.1.1 Functional connectivity of the DMN

The DMN was chosen as the central network for the present study. There are several factors that justify this choice. For instance, the DMN is arguably the most widely studied functional brain network, receiving significant attention in research on both healthy individuals and patients with various diseases. FC alterations have for example been described in the context of Alzheimer's disease, autism spectrum disorder, epilepsy, mood disorders and Parkinson's disease (e.g., Feng *et al.* 2024; Mohan *et al.* 2016; Tessitore *et al.* 2019). Furthermore, the DMN is involved in a wide range of brain functions. The DMN was first described as a set of brain regions that are suppressed when an individual is engaged in an external task and active in the absence of external stimuli (Shulman *et al.* 1997). The cognitive functions that were first discovered were therefore activities like self-referential thoughts, day-dreaming, thinking about future or past events and mind-wandering (Buckner *et al.* 2008; Menon 2023). More recently, it was

hypothesized that the DMN is also involved in other complex, goal-directed tasks like different planning scenarios, episodic or semantic memory and language (Menon 2023), for instance by coupling with other networks like the frontoparietal control network (Spreng 2012; Spreng *et al.* 2010). Considering this wide range of functions, it becomes clear why the interest in the DMN architecture in different neurological diseases is high.

In the present study, the average FC between all pairs of nodes in the DMN (wnFC) was significantly decreased in PD patients in Data-PR at thrX and thr0. Furthermore, in Data-PR, a decrease of global efficiency and diffusion efficiency of the DMN were observed in PD patients. WnFC, coupling strength (ST) and GE of the DMN were negatively correlated with motor symptom severity. Some of these observations were also made in Data-DU. There, a trend of decreased wnFC of the DMN was observed ($p = 0.07$) and DE of the DMN was significantly reduced. At a trend-level ($p < 0.1$), wnFC of the DMN was negatively correlated with symptom severity. Overall, these observations are hints for a less strongly and less efficiently connected DMN in PD patients compared to HC, especially in Data-PR. These functional abnormalities seem to increase with ongoing disease duration and worsening motor impairment. Several publications support the finding of decreased FC within the DMN in PD and found associations with lower cognitive performance (Baggio *et al.* 2015a; Disbrow *et al.* 2014; Hou *et al.* 2016; Jellinger 2023; Lucas-Jiménez *et al.* 2016; Tessitore *et al.* 2012; Wolters *et al.* 2019). The DMN is, as mentioned above, involved in memory processes (Mohan *et al.* 2016; Smallwood *et al.* 2021) and PD patients are prone to the development of cognitive impairments (Aarsland *et al.* 2021; Goldman & Sieg 2020; Litvan *et al.* 2012). The decreased wnFC of the DMN could therefore be interpreted as a sign of cognitive impairment. A reduction of within-network FC of the DMN is also well described in Alzheimer's disease, underlining the connection between the DMN-FC and cognitive performance (Mohan *et al.* 2016; Pini *et al.* 2021). Due to a lack of data on cognitive performance, the association with cognitive performance could not be directly tested here, however, correlations of DMN-FC measures with motor symptom severity were found in the present study. In PD, motor symptoms generally worsen with ongoing disease. As the likelihood of cognitive decline also increases with ongoing disease, it can be argued that motor symptom severity can to some extent serve as a proxy for cognitive symptoms. However, some studies

observed correlations of FC with cognitive performance but not motor performance (Disbrow *et al.* 2014; Olde Dubbelink *et al.* 2014), which shows that further testing with more information on patient phenotypes is needed in order to evaluate if the altered DMN architecture found here is also associated with cognitive decline.

Although the present data and several other studies suggest that the DMN is less efficiently organized in PD and loses some of its connectivity, it has to be noted that increased FC (e.g., Campbell *et al.* 2015; Chen *et al.* 2022) and increased GE (Fang *et al.* 2017) within the DMN is also described in the literature. There are several possible reasons for these discrepancies. In the study conducted by Campbell and colleagues, patients were scanned after an overnight withdrawal of their antiparkinsonian medication (Campbell *et al.* 2015) whereas in the present study, patients were scanned on their habitual medication regimen. Fang and colleagues investigated subjects with early PD, whereas the used samples in the present study are more heterogeneous in this regard (Fang *et al.* 2017). Similarly, the H&Y stage of the patients in the study conducted by Chen and colleagues was lower (1.41 ± 0.45) than in the present samples (Data-PR: 2.02 ± 0.54 and Data-DU: 2.59 ± 0.72) (Chen *et al.* 2022). Increased connectivity within the DMN in PD has been shown to be associated with visual hallucinations, suggesting that DMN connectivity has an impact on the development of specific symptoms or vice versa (Mohan *et al.* 2016), which might not have been frequently present in the investigated populations. Here again, more details on disease subtypes and specific symptoms are needed in order to understand the impact of changes in DMN FC.

Overall, because of its alterations and correlation with symptom severity, it can be argued that within-DMN FC has some potential as a starting point for the research for a disease-severity marker. This potential is underlined by the fact that significant FC changes could be observed in both datasets. Other studies also came to the conclusion that the DMN could be a valuable starting-point for further biomarker research in cognitively impaired PD patients (Tessitore *et al.* 2019; Wolters *et al.* 2019).

4.1.2 Functional connectivity changes within TPNs

In Data-PR, a decreased wnFC of both included motor networks was observed. This observation was however not replicated in Data-DU. The decreased wnFC of

the motor networks can be interpreted as a reflection of PD as a movement disorder. This finding is supported by previous studies that found decreased FC between brain regions involved in motor functions (e.g., Campbell *et al.* 2015; Caspers *et al.* 2021; Peraza *et al.* 2017; White *et al.* 2020). However, increased FC has also been described (de Schipper *et al.* 2018). As with the FC within the DMN, findings on motor network FC in the literature have often been seemingly contradictory. Still, several studies could relate FC changes of motor regions to different PD symptoms, e.g., motor symptoms (Dahmani *et al.* 2024; Hensel *et al.* 2019; Wu *et al.* 2009) or behavioral changes (Vervoort *et al.* 2016), highlighting its potential as a biomarker (Tessitore *et al.* 2019), i.e., to distinguish different PD subtypes. However, further research is needed.

Decreased wnFC was also found within the vigilant attention, cognitive action regulation (CogAR), cognitive action control (CogAC) and reward (Rew) networks in Data-PR. The vigilant attention network is based on a meta-analysis of fMRI-studies focusing on FC during continuous stimulus-detection and stimulus-discrimination tasks requiring attention over a prolonged period of time (Langner & Eickhoff 2013). CogAC and CogAR are both involved in action control, e.g., when a difficult action has to be favored over another, easier action, in order to achieve a certain goal (Cieslik *et al.* 2015; Langner *et al.* 2018). PD is often accompanied by cognitive impairment, including attention deficits (Aarsland *et al.* 2021). Therefore, alterations of FC in corresponding regions and networks are a plausible finding. Different studies have concentrated on the role of the dorsal and ventral attention network as well as the frontoparietal network defined by Yeo and colleagues (Yeo *et al.* 2011). These networks show a relevant overlap with the attention networks investigated here. FC alterations in these networks in PD have been observed and linked to specific symptoms, e.g., cognitive impairment (Baggio *et al.* 2015a; Bezdicek *et al.* 2018; Peraza *et al.* 2017; Yeager *et al.* 2024) or freezing of gait (Maidan *et al.* 2019), supporting the present findings.

The changes in the reward network found in the present study fit well together with the pathophysiology of PD, i.e., changes in the dopaminergic system, which is important for reward-related processes (Perry & Kramer 2015). Reward-processing is impaired in PD patients (Costello *et al.* 2022). This can for example lead to impaired impulse control, which can also be a side effect of the

dopamine replacement therapy or dopamine agonists, depression, or apathy (Costello *et al.* 2022; Perry & Kramer 2015).

4.1.3 Whole-brain functional connectivity

Besides the findings of decreased wnFC of different TPNs, the wnFC of the WBN was found to be decreased in PD patients in Data-PR, but not in Data-DU. This finding indicates the presence of FC alterations at the whole-brain level and underlines the perception of PD as a disconnection syndrome (Cronin-Golomb 2010). The concept helps to understand the variety of different symptoms that characterize PD. The decreased average FC at the whole-brain level shows that PD changes are not restricted to separate brain regions. The finding of altered whole-brain FC is for example supported by a meta-analysis that investigated changes in structural connectivity at the whole-brain level and found decreased global efficiency, clustering coefficient and an increased characteristic path length in PD (Zuo *et al.* 2023). They concluded that segregation and integration in PD patients are decreased at a structural level and that therefore the small-world-architecture is impaired (Zuo *et al.* 2023). In the present study, similar observations could be made, although the GE of the functional whole-brain network was only decreased at a trend-level.

The overall decrease of FC observed in the present study seems to be reflected or especially pronounced in several of the mentioned TPNs that are involved in functions that are impaired in PD, such as motor and cognitive processes.

4.1.4 Between-network functional connectivity

Alongside within-network FC, connectivity between networks (bnFC) was investigated, too. However, no significant group differences were found. When correlating bnFC with motor symptom severity, a significant positive correlation was found for the average FC between the perceptuo-motor network (MotorPerc) and the DMN in Data-PR (not in Data-DU). This finding suggests a shift in the relationship between these two networks with increasing disease severity.

Although no significant group differences in bnFC were found here, other studies could find alterations of FC between networks and link them to different PD symptoms. For instance, reduced FC between the right fronto-parietal network and the executive control network (Bharti *et al.* 2020) and reduced FC between the

dorsal attention network, the medial visual network and the sensory-motor network or an increase of negative FC between the dorsal attention network (Yu *et al.* 2021) were linked to freezing of gait. Furthermore, reduced FC between the DMN and regions of the dorsal attention and fronto-parietal network were associated with attention deficits (Boord *et al.* 2017). One observation that arises from the literature is that between-network FC has mostly been linked to specific symptoms and thus might be limited to specific subtypes of PD. This view is supported by the findings of Wang and colleagues, who hypothesized that between-network FC could be used to differentiate tremor dominant and postural instability dominant PD subtypes (Wang *et al.* 2023). Although no group differences of bnFC were observed in this study, it might have potential for a biomarker differentiating between subtypes, which could not be tested for in the present study due to a lack of phenotype data. Additionally, there might be potential as a disease monitoring biomarker, as correlations with disease severity were found in this study. A more detailed analysis of bnFC in different PD subtypes could help to solve this problem. It has moreover been reported, that bnFC varies with age (DeSerisy *et al.* 2021), even in healthy subjects, which may explain why no group differences were found in this study, as the results were controlled for age in all analyses.

4.1.5 Interaction of the DMN and TPNs

Several studies investigated the functional coupling and decoupling of resting-state networks in PD and suggested that changes in the coupling-behavior are associated with cognitive performance (Putcha *et al.* 2015, 2016; Tessitore *et al.* 2019; Yeager *et al.* 2024). Therefore, the investigation of network coupling and inter-network FC is an interesting approach for biomarker research and might offer valuable insights into brain architecture in the context of PD. Several of the calculated measures in this study, especially graph theory measures, aimed at characterizing the interaction of the DMN with task-positive networks. In PD patients, a decreased global efficiency of the DMN combined with the motor execution network and the vigilant attention network (as well as of the DMN alone) was observed in Data-PR, but not in Data-DU. This hints at a less efficient information flow between the DMN and the mentioned TPNs in PD. GE has only been used in a few studies in PD so far, but decreased GE of different brain networks in PD was observed (Novaes *et al.* 2021; Sang *et al.* 2015; Suo *et al.*

2017). One study found a decrease of GE within the motor circuit in PD. The decreased GE correlated with tremor severity (Novaes *et al.* 2021). Another study investigating GE of functional brain networks in PD found a decreased GE in the sensorimotor and the visual network but an increased GE within the DMN (Fang *et al.* 2017), which contradicts our finding of decreased GE within the DMN (cf. section 4.1.1). However, these results indicate that in general, GE can be useful for both the investigation of smaller functional networks and the whole-brain network. The present results indicate that GE can also help to characterize network coupling.

In both datasets, significant decreases of diffusion efficiency of several DMN-TPN-couples were found, however the absolute DE values were ranging between 0 and 0.05 and were thus very small. Only for the DMN alone, higher values were calculated. No other studies investigating diffusion efficiency in PD were found. The present results suggest that DE might be more suitable for the analysis of smaller networks rather than large or combined networks. A similar but less pronounced effect could be observed for GE, where the values of the DMN alone were higher than those of DMN-TPN-combinations. A possible explanation could be that TPNs and the DMN are often considered as being anticorrelated (Fox *et al.* 2005), which leads to negative weights of inter-network connections. However, DE and GE were only calculated at thr0 and thr25, where negative weights were set to zero. Both measures are based on path lengths (characteristic path length in GE and random paths in DE) between all nodes of the network. In the presence of negative edges (set to zero), these path lengths increase, which at the same time decreases the efficiency of information flow as measured by DE and GE.

Finally, significant correlations between the PPC of different DMN-TPN-couples and UPDRS-III OFF were observed in Data-PR (not in Data-DU). On the one hand, there was a positive correlation of the PPC of the DMN combined with MotorPerc, MotorEx and MultiTask networks. A higher PPC indicates that the edges are distributed more equally between the different communities (i.e., networks). The positive correlation with symptom severity indicates a reduction in segregation of the respective networks with increasing disease severity. On the other hand, the PPC of the DMN with the WBN correlated negatively with symptom severity, indicating that the DMN might segregate from the brain as a

whole while integrating increasingly with different TPNs. The increased integration with motor networks and the multitasking network could be interpreted as a compensation mechanism. The observations concerning PPC support the assumption made by Zuo and colleagues, who, as mentioned before, found signs of an altered small-world-architecture, which is normally characterized by high clustering and short path length, in PD patients (Zuo *et al.* 2023). Taken together, the PPC could deliver some valuable insights in the functional brain architecture in PD and might have potential as a starting point for biomarker research, especially as a disease monitoring biomarker.

4.1.6 Functional connectivity thresholds and negative weights

There is an ongoing controversy about the use of negative FC correlations. In the present study, FC was evaluated at three different threshold levels: first including both negative and positive weights (thrX), second including only positive weights (thr0) and third including only weights with a correlation coefficient above 0.25 (thr25). The used thresholds derived from the literature and were already used in other studies (Buckner *et al.* 2009; Holiga *et al.* 2019; Wagner *et al.* 2021), yet there is an ongoing debate about the usefulness of negative weights and the choice of the threshold levels is still partly arbitrary, requiring a more detailed analysis in the future.

In group-wise comparison, most significant differences were found, when negative weights were included, indicating that negative weights can indeed provide meaningful insights. Recently, several studies supported this hypothesis. For example, one study used a negative correlation matrix to classify patients with autism with a high accuracy (Kazeminejad & Sotero 2020). Another possibility to take negative weights into account is to use the absolute values of negative weights when analyzing FC, resulting in a measure of shared information between brain regions, whether it is positive correlation or anticorrelation. Using this approach, one study made the observation that FC changes based on absolute values were more often reproducible (Ran *et al.* 2020). On the other hand, it was argued that thresholding can lead to more noise and potentially falsify the assumptions made on network topology (Douw *et al.* 2019).

When it comes to the correlation of FC measures with symptom severity, a contrary effect concerning the different threshold levels was observed, especially

in Data-PR. More significant correlations, especially for the graph theory measures, were found, when only higher weights were included (thr25). So possibly, the focus on stronger connections enhances and highlights individual-specific signals, leading to a better correlation with individual symptom severity. This observation can potentially help future biomarker studies, especially for the measurement of disease severity. It has been shown that individual FC of resting-state networks is reproducible over time, underlining the general potential of rsFC as a disease monitoring biomarker (Tessitore *et al.* 2019).

4.2 Implications for biomarker research

One aim of this study was to help to elucidate whether the analysis of network FC could prove useful as a starting point for the research for biomarkers in PD. Some of the changes observed in this study are consistent (at least at a trend level) across the two datasets and the literature (e.g., the decreased within-network FC of DMN), but the discrepancies were predominant and in the second dataset, only few significant results were obtained.

The changes present in both datasets concerned primarily the DMN and the motor networks and concerning the FC measures, some consistency was found for combFC, DE and ST.

The goal of biomarkers is to standardize diagnosis and monitoring of disease severity and therapy. In some clinical contexts, fMRI is already used today, for example in neurosurgical planning of epilepsy surgeries or to evaluate operability of brain tumors (Voets 2021), however the translation of functional connectivity data as a diagnostic biomarker into the clinical setting is difficult.

The findings of the present study show that meta-analytic functional networks assessed via fMRI have the potential to fulfill some of the properties of ideal biomarkers as defined by Lesko and Atkinson (Lesko & Atkinson 2001). First, they measure clinically relevant features that partly correlate with disease severity and thus could help differentiate PD patients from healthy individuals and differentiate different PD subtypes. fMRI has a good spatial resolution, is available in many hospitals and is relatively straightforward to acquire for both, the patient and the health care professional (Glover 2011; Gore 2003). It therefore can be used in the clinical setting. However, although numerous studies used FC measured by fMRI,

it still is not regularly used in the clinical context. In order to evaluate sensitivity and specificity of the present results, further research is needed, and the results ideally need to be matched to other diagnostic methods and post-mortem analyses of the patient's brain tissue. It was proposed by Douw and colleagues to consistently include the report of reliability, reproducibility, sensitivity and specificity of new measures that are meant to differentiate between patients and healthy subjects (Douw *et al.* 2019). In comparison to only reporting on significant group differences, this could help the field to advance faster on the way to reliable FC biomarkers (Douw *et al.* 2019).

The biggest challenge that comes with fMRI-derived FC is the reliability (Tessitore *et al.* 2019). As already mentioned several times throughout the manuscript, the overlap between the results of both datasets was minimal despite identical processing and analysis pipelines. At a significance level of $p < 0.05$ only a reduction of diffusion efficiency in the DMN and several DMN-TPN-couples was significant in both datasets. The choice of the significance level of $p < 0.05$ is conservative, given that the statistical analyses of the two datasets were conducted separately. When considering a more lenient significance threshold of $p < 0.1$ the overlap is larger, nevertheless still only a small part of the findings in Data-PR appear again in Data-DU. In the past decades, fMRI was used widely to characterize FC patterns in PD. However, the literature on FC changes in PD is still inconclusive and the replication of results across different samples often failed (Badea *et al.* 2017; Jadavji *et al.* 2023). This challenge also becomes apparent in this study. There are different possible reasons for these replication difficulties that can be divided in two main categories: differences in methods, ranging from image acquisition to preprocessing choices and data analysis on the one hand and heterogeneity of the different samples, e.g., disease stage, disease subtype, or subject characteristics on the other hand. The first category was addressed in this study by using identical preprocessing and analysis pipelines on both datasets. The image acquisition parameters were also similar in both datasets (cf. methods), so these technical influences are probably not the main reason for the observed lack of replicability. It is however a general problem, that to date, no standardized analysis-pipelines exist for the analysis of resting-state fMRI-data, which in general makes replicability of results across samples difficult (Badea *et al.* 2017; Tessitore *et al.* 2019).

When comparing the patient characteristics of the two cohorts, the age and gender distribution was similar. Also, the motor symptom severity, although measured with two different versions of the UPDRS, was similar. Based on the available patient data, only the Hoehn & Yahr stage differed between the two datasets, being significantly higher in Data-DU, which possibly influenced the results. A lack of replicability of fMRI-based findings in different PD cohorts is a general issue that was for example addressed by Badea and colleagues, who specifically aimed at replicating results across three different PD samples (Badea *et al.* 2017). They concluded that the heterogeneous nature of PD is the most probable reason for this issue. This view is also supported by other studies (e.g., Berg *et al.* 2021; Greenland *et al.* 2019; Tahmasian *et al.* 2017). The cardinal symptoms of PD, namely tremor, rigor, akinesis and postural instability, can to some extent be found in every PD patient, but the degree or predominance of each symptom is highly variable. Based on the predominance of specific symptoms, several PD subtypes are differentiated (Tolosa *et al.* 2021). These subtypes are not only characterized by the different symptom manifestation but also by different disease progression speed, the presence or absence of cognitive impairment and by the degree of response to dopaminergic treatment (Armstrong & Okun 2020). Furthermore, it becomes more and more evident that FC alterations are also different between the subtypes (Baggio *et al.* 2015b; Filippi *et al.* 2019). As a reaction to these heterogeneous phenotypes, it is even questioned if PD is one single disease entity or if it is more suitable to view PD as a group of diseases with a similar pathogenesis (Rodríguez-Violante *et al.* 2017). Furthermore, dopaminergic treatment influences the intrinsic network FC and therefore can lead to more variable results (Achard & Bullmore 2007; Asendorf *et al.* 2024; Baggio *et al.* 2015a; Ballarini *et al.* 2018; Cole *et al.* 2013; Esposito *et al.* 2013; Krajcovicova *et al.* 2012).

Another challenge in fMRI-imaging that is often mentioned in the literature is that it appears to be more suitable to investigate group differences (as in the present study) compared to individual differences. It is often difficult or impossible to transfer the insights of fMRI studies from the group level to the individual level (Cerasa *et al.* 2016; Glover 2011). This makes the translation to the clinical setting very challenging (Tessitore *et al.* 2019).

There is an urgent need for publicly available large scale PD datasets, comprising detailed phenotype information, in order to systematically analyze FC patterns associated with PD subtypes and disease states. Furthermore, reproducibility and comparability across studies could be improved by defining standardized processing pipelines and sharing code.

4.3 Limitations

The present study yielded some meaningful and interesting insights on the architecture of functional brain networks in Parkinson's disease, however there are some limiting factors that should be addressed in further studies.

The present datasets were rather small. The used datasets are typical for clinical datasets used in PD FC-studies which tend to be small, inhomogeneous and thus non-representative (Baggio *et al.* 2015b; Khalili-Mahani *et al.* 2017; Tahmasian *et al.* 2017; Woo *et al.* 2017). Small samples are more vulnerable to outliers and individual deviations, for instance caused by other, not yet diagnosed diseases, potentially influence the mean of the cohort to a greater extent than in large samples.

Furthermore, there was not enough information on the disease subtype, disease duration, details on dopaminergic treatment or cognitive impairments and the influence of these factors on the results can only be hypothesized. The lack of information on cognitive performance is important for the results concerning the networks that are implicated in cognitive processes rather than motor processes. Especially, alterations within the DMN architecture have repeatedly been correlated with cognitive performance (e.g., Tessitore *et al.* 2012). A similar approach should be repeated using datasets with more information on the mentioned patient properties in order to evaluate their impact on the results.

The DMN was chosen as the central network of the study because of its prominent role in different cognitive processes and because of its often cited quality as a task-negative network. However, recent findings challenge the view of the DMN as task-negative, as it is also recruited for the execution of different complex tasks (for a review see Spreng 2012). Other studies also investigated the coupling of other resting-state networks, without directly including the DMN, and observed

interesting alterations in PD. The same additional analyses would be interesting for the used datasets and networks and should be investigated in the future.

The network coordinates used in this study were defined in prior coordinate-based meta-analyses. Another commonly used approach is the independent component analysis (ICA), which is especially useful in exploratory studies without a strong *a priori* hypothesis (Cerasa *et al.* 2016). However, meta-analytical networks were chosen here, because the coordinates are a good estimate for the location of functional brain regions that consistently and robustly show activation across similar tasks and therefore cognitive functions. This allowed it to include networks representing a large variety of functions. As some networks (e.g., CogAR and CogAC) were based on similar but still distinct tasks, we could test for consistency of results within datasets. However, it would be interesting to use a purely data-driven approach, such as ICA, with similar datasets to further investigate the influence of this methodological choice.

5 Conclusion

The present study aimed to evaluate the potential of the network-based analysis of resting-state functional connectivity of predefined meta-analytic networks for the development of biomarkers in Parkinson's disease.

In order to qualify as a potential biomarker, it first has to be established, that functional connectivity patterns in PD can be uncovered using meta-analytic networks instead of other, more popular approaches, such as independent component analysis. The present study showed that, indeed, FC alterations in PD patients could be found using meta-analytic networks. The significant findings were plausible and complement the existing literature on FC changes in PD. It became clear that the investigation of both, individual networks and combinations of networks, can deliver insights in disease specific connectivity patterns. The present work also shows, that both graph theory derived measures and simple variations of average FC can uncover PD specific FC alterations.

Several potentially interesting starting points for the development of biomarkers could be identified in the present study. The decreased wnFC (both datasets) and decreased GE (Data-PR) of the DMN both hint at a less efficiently organized DMN that correlates with disease severity and could therefore be investigated as a potential disease severity marker. Although no group differences were found for the between-network FC, there might be some potential as a biomarker for disease severity, as correlations with motor symptoms were found. The literature also suggests, that the analysis of between-network FC could have potential for the differentiation between disease subtypes. Additionally, the PPC of the DMN together with other communities is an interesting measure that should be further investigated in future studies. The networks with the most significant group differences and correlations were the DMN and the two motor networks, but cognitive networks, such as CogAC or VigAtt, were also altered in PD. In order to further evaluate the diagnostic potential of the architecture of cognitive networks, similar analyses should be repeated on larger datasets with phenotype data on cognitive performance. Longitudinal studies in a consistent set of patients could be conducted to evaluate the consistency of the results at an individual level over time, to facilitate the translation of the results into clinical practice.

Although several potential approaches for further biomarker research could be identified in the present study, the challenge of insufficient replicability of results across datasets remains. The application of the same analysis-pipeline to both datasets did not improve reliability of rs-fMRI-derived measures in Parkinson's disease, and the overlap between the results in the two datasets was small. Combined with the inconsistent literature in the field, the present results raise concerns about the reliability and generalizability of FC alterations in such a heterogeneous disease as PD. This could indicate that FC measures may be more suitable for the differentiation between disease subtypes and for the use as a disease-monitoring biomarker, rather than as a general diagnostic biomarker for Parkinson's disease. There is a need for further investigations of different PD subtypes and larger datasets to fully evaluate the potential of FC-based biomarkers in general and the mentioned measures specifically in the context of PD. Only if the shortcoming of lacking reliability of fMRI-derived FC patterns can be overcome, reliable biomarkers can be found and used in the clinical setting.

6 Reference list

Aarsland, D., Batzu, L., Halliday, G. M., … Weintraub, D. (2021). Parkinson disease-associated cognitive impairment. *Nature Reviews. Disease Primers*, **7**(1), 47.

Achard, S., & Bullmore, E. (2007). Efficiency and cost of economical brain functional networks. *PLoS Computational Biology*, **3**(2), e17.

Amft, M., Bzdok, D., Laird, A. R., Fox, P. T., Schilbach, L., & Eickhoff, S. B. (2015). Definition and characterization of an extended social-affective default network. *Brain Structure & Function*, **220**(2), 1031–1049.

Amick, M. M., Grace, J., & Chou, K. L. (2006). Body side of motor symptom onset in Parkinson's disease is associated with memory performance. *Journal of the International Neuropsychological Society*, **12**(5), 736–740.

Andrews-Hanna, J. R., Reidler, J. S., Sepulcre, J., Poulin, R., & Buckner, R. L. (2010). Functional-anatomic fractionation of the brain's default network. *Neuron*, **65**(4), 550–562.

Armstrong, M. J., & Okun, M. S. (2020). Diagnosis and treatment of parkinson disease: A review. *The Journal of the American Medical Association*, **323**(6), 548–560.

Asendorf, A. L., Theis, H., Tittgemeyer, M., … van Eimeren, T. (2024). Dynamic properties in functional connectivity changes and striatal dopamine deficiency in Parkinson's disease. *Human Brain Mapping*, **45**(10), e26776.

Baddeley, A. (2000). The episodic buffer: a new component of working memory? *Trends in Cognitive Sciences*, **4**(11), 417–423.

Baddeley, A. D., & Hitch, G. (1974). Working memory. In *Psychology of learning and motivation*, Vol. 8, Elsevier, pp. 47–89.

Badea, L., Onu, M., Wu, T., Roceanu, A., & Bajenaru, O. (2017). Exploring the reproducibility of functional connectivity alterations in Parkinson's disease. *Plos One*, **12**(11), e0188196.

Baggio, H.-C., Segura, B., Sala-Llonch, R., … Junqué, C. (2015a). Cognitive impairment and resting-state network connectivity in Parkinson's disease. *Human Brain Mapping*, **36**(1), 199–212.

Baggio, H. C., & Junqué, C. (2019). Functional MRI in parkinson's disease cognitive impairment. *International Review of Neurobiology*, **144**, 29–58.

Baggio, H. C., Segura, B., & Junque, C. (2015b). Resting-state functional brain networks in Parkinson's disease. *CNS Neuroscience & Therapeutics*, **21**(10), 793–801.

Ballarini, T., Růžička, F., Bezdicek, O., … Jech, R. (2018). Unraveling connectivity changes due to dopaminergic therapy in chronically treated Parkinson's disease patients. *Scientific Reports*, **8**(1), 14328.

Bandettini, P. A. (2009). What's new in neuroimaging methods? *Annals of the New York Academy of Sciences*, **1156**, 260–293.

Bassett, D. S., & Sporns, O. (2017). Network neuroscience. *Nature Neuroscience*, **20**(3), 353–364.

Ben-Shlomo, Y., Darweesh, S., Llibre-Guerra, J., Marras, C., San Luciano, M., & Tanner, C. (2024). The epidemiology of Parkinson's disease. *The Lancet*, **403**(10423), 283–292.

Benjamini, Y., & Hochberg, Y. (1995). Controlling the false discovery rate: a practical and powerful approach to multiple testing. *Journal of the Royal Statistical Society: Series B (Methodological)*, **57**(1), 289–300.

Berg, D., Borghammer, P., Fereshtehnejad, S.-M., … Postuma, R. B. (2021). Prodromal Parkinson disease subtypes - key to understanding heterogeneity. *Nature Reviews. Neurology*, **17**(6), 349–361.

Berman, B. D., Smucny, J., Wylie, K. P., … Tregellas, J. R. (2016). Levodopa modulates small-world architecture of functional brain networks in Parkinson's disease. *Movement Disorders*, **31**(11), 1676–1684.

Bezdicek, O., Ballarini, T., Růžička, F., … Schroeter, M. L. (2018). Mild cognitive impairment disrupts attention network connectivity in Parkinson's disease: A combined multimodal MRI and meta-analytical study. *Neuropsychologia*, **112**, 105–115.

Bharti, K., Suppa, A., Pietracupa, S., … Pantano, P. (2020). Aberrant functional connectivity in patients with Parkinson's disease and freezing of gait: a within- and between-network analysis. *Brain Imaging and Behavior*, **14**(5), 1543–1554.

Bin Yoo, H., Concha, E. O. de la, De Ridder, D., Pickut, B. A., & Vanneste, S. (2018). The Functional Alterations in Top-Down Attention Streams of Parkinson's disease Measured by EEG. *Scientific Reports*, **8**(1), 10609.

Biomarkers Definitions Working Group. (2001). Biomarkers and surrogate

endpoints: preferred definitions and conceptual framework. *Clinical Pharmacology and Therapeutics*, **69**(3), 89–95.

Biswal, B., Yetkin, F. Z., Haughton, V. M., & Hyde, J. S. (1995). Functional connectivity in the motor cortex of resting human brain using echo-planar MRI. *Magnetic Resonance in Medicine*, **34**(4), 537–541.

Biswal, B. B. (2012). Resting state fMRI: a personal history. *Neuroimage*, **62**(2), 938–944.

Blauwendraat, C., Nalls, M. A., & Singleton, A. B. (2020). The genetic architecture of Parkinson's disease. *Lancet Neurology*, **19**(2), 170–178.

Bloem, B. R., Okun, M. S., & Klein, C. (2021). Parkinson's disease. *The Lancet*, **397**(10291), 2284–2303.

Boon, L. I., Hepp, D. H., Douw, L., … Schoonheim, M. M. (2020). Functional connectivity between resting-state networks reflects decline in executive function in Parkinson's disease: A longitudinal fMRI study. *NeuroImage. Clinical*, **28**, 102468.

Boord, P., Madhyastha, T. M., Askren, M. K., & Grabowski, T. J. (2017). Executive attention networks show altered relationship with default mode network in PD. *NeuroImage. Clinical*, **13**, 1–8.

Braak, H., Del Tredici, K., Rüb, U., de Vos, R. A. I., Jansen Steur, E. N. H., & Braak, E. (2003). Staging of brain pathology related to sporadic Parkinson's disease. *Neurobiology of Aging*, **24**(2), 197–211.

Brandes, U. (2001). A faster algorithm for betweenness centrality*. *The Journal of Mathematical Sociology*, **25**(2), 163–177.

Brücke, T., & Brücke, C. (2022). Dopamine transporter (DAT) imaging in Parkinson's disease and related disorders. *Journal of Neural Transmission*, **129**(5–6), 581–594.

Buckner, R. L., Andrews-Hanna, J. R., & Schacter, D. L. (2008). The brain's default network: anatomy, function, and relevance to disease. *Annals of the New York Academy of Sciences*, **1124**, 1–38.

Buckner, R. L., Sepulcre, J., Talukdar, T., … Johnson, K. A. (2009). Cortical hubs revealed by intrinsic functional connectivity: mapping, assessment of stability, and relation to Alzheimer's disease. *The Journal of Neuroscience*, **29**(6), 1860–1873.

Bullmore, E., & Sporns, O. (2009). Complex brain networks: Graph theoretical

analysis of structural and functional systems. *Nature Reviews. Neuroscience*, **10**(3), 186–198.

Caballero-Gaudes, C., & Reynolds, R. C. (2017). Methods for cleaning the BOLD fMRI signal. *Neuroimage*, **154**, 128–149.

Camilleri, J. A., Müller, V. I., Fox, P., … Eickhoff, S. B. (2018). Definition and characterization of an extended multiple-demand network. *Neuroimage*, **165**, 138–147.

Campbell, M. C., Koller, J. M., Snyder, A. Z., Buddhala, C., Kotzbauer, P. T., & Perlmutter, J. S. (2015). CSF proteins and resting-state functional connectivity in Parkinson disease. *Neurology*, **84**(24), 2413–2421.

Caspers, J., Mathys, C., Hoffstaedter, F., … Eickhoff, S. B. (2017). Differential Functional Connectivity Alterations of Two Subdivisions within the Right dlPFC in Parkinson's Disease. *Frontiers in Human Neuroscience*, **11**, 288.

Caspers, J., Rubbert, C., Eickhoff, S. B., … Mathys, C. (2021). Within- and across-network alterations of the sensorimotor network in Parkinson's disease. *Neuroradiology*, **63**(12), 2073–2085.

Cerasa, A., Novellino, F., & Quattrone, A. (2016). Connectivity changes in parkinson's disease. *Current Neurology and Neuroscience Reports*, **16**(10), 91.

Chen, J., Müller, V. I., Dukart, J., … Patil, K. R. (2021). Intrinsic Connectivity Patterns of Task-Defined Brain Networks Allow Individual Prediction of Cognitive Symptom Dimension of Schizophrenia and Are Linked to Molecular Architecture. *Biological Psychiatry*, **89**(3), 308–319.

Chen, L., Huang, T., Ma, D., & Chen, Y.-C. (2022). Altered Default Mode Network Functional Connectivity in Parkinson's Disease: A Resting-State Functional Magnetic Resonance Imaging Study. *Frontiers in Neuroscience*, **16**, 905121.

Cieslik, E. C., Mueller, V. I., Eickhoff, C. R., Langner, R., & Eickhoff, S. B. (2015). Three key regions for supervisory attentional control: evidence from neuroimaging meta-analyses. *Neuroscience and Biobehavioral Reviews*, **48**, 22–34.

Cole, D. M., Beckmann, C. F., Oei, N. Y. L., Both, S., van Gerven, J. M. A., & Rombouts, S. A. R. B. (2013). Differential and distributed effects of dopamine neuromodulations on resting-state network connectivity. *Neuroimage*, **78**, 59–67.

Cools, R., Rogers, R., Barker, R. A., & Robbins, T. W. (2010). Top-down attentional control in Parkinson's disease: salient considerations. *Journal of Cognitive Neuroscience*, **22**(5), 848–859.

Corbetta, M., & Shulman, G. L. (2002). Control of goal-directed and stimulus-driven attention in the brain. *Nature Reviews. Neuroscience*, **3**(3), 201–215.

Costello, H., Berry, A. J., Reeves, S., … Roiser, J. P. (2022). Disrupted reward processing in Parkinson's disease and its relationship with dopamine state and neuropsychiatric syndromes: a systematic review and meta-analysis. *Journal of Neurology, Neurosurgery, and Psychiatry*, **93**(5), 555–562.

Cronin-Golomb, A. (2010). Parkinson's disease as a disconnection syndrome. *Neuropsychology Review*, **20**(2), 191–208.

Dahmani, L., Bai, Y., Zhang, W., … Wang, D. (2024). Individualized functional connectivity markers associated with motor and mood symptoms of Parkinson's disease. *BioRxiv*. doi:10.1101/2024.01.31.578238

Dang, L. C., O'Neil, J. P., & Jagust, W. J. (2012). Dopamine supports coupling of attention-related networks. *The Journal of Neuroscience*, **32**(28), 9582–9587.

Delgado-Alvarado, M., Ferrer-Gallardo, V. J., Paz-Alonso, P. M., Caballero-Gaudes, C., & Rodríguez-Oroz, M. C. (2023). Interactions between functional networks in Parkinson's disease mild cognitive impairment. *Scientific Reports*, **13**(1), 20162.

DeSerisy, M., Ramphal, B., Pagliaccio, D., … Margolis, A. E. (2021). Frontoparietal and default mode network connectivity varies with age and intelligence. *Developmental Cognitive Neuroscience*, **48**, 100928.

Deuschl, G., Oertel, W., & Reichmann, H. (2016). S3-Leitlinie Idiopathisches Parkinson-Syndrom. *AWMF-Leitlinien-Registernummer 020-010*.

de Schipper, L. J., Hafkemeijer, A., van der Grond, J., Marinus, J., Henselmans, J. M. L., & van Hilten, J. J. (2018). Altered Whole-Brain and Network-Based Functional Connectivity in Parkinson's Disease. *Frontiers in Neurology*, **9**, 419.

Diamond, A. (2013). Executive functions. *Annual Review of Psychology*, **64**, 135–168.

Dienel, G. A. (2019). Brain Glucose Metabolism: Integration of Energetics with Function. *Physiological Reviews*, **99**(1), 949–1045.

Disbrow, E. A., Carmichael, O., He, J., … Sigvardt, K. A. (2014). Resting state

functional connectivity is associated with cognitive dysfunction in non-demented people with Parkinson's disease. *Journal of Parkinson's Disease*, **4**(3), 453–465.

Dorsey, E. R., Sherer, T., Okun, M. S., & Bloem, B. R. (2018). The emerging evidence of the parkinson pandemic. *Journal of Parkinson's Disease*, **8**(s1), S3–S8.

Douw, L., van Dellen, E., Gouw, A. A., … Stam, C. J. (2019). The road ahead in clinical network neuroscience. *Network Neuroscience (Cambridge, Mass.)*, **3**(4), 969–993.

Dragomir, A., & Omurtag, A. (2023). Brain's networks and their functional significance in cognition. In N. V. Thakor, ed., *Handbook of Neuroengineering*, Singapore: Springer Nature Singapore, pp. 2703–2732.

Drakesmith, M., Caeyenberghs, K., Dutt, A., Lewis, G., David, A. S., & Jones, D. K. (2015). Overcoming the effects of false positives and threshold bias in graph theoretical analyses of neuroimaging data. *Neuroimage*, **118**, 313–333.

Drew, D. S., Muhammed, K., Baig, F., … Husain, M. (2020). Dopamine and reward hypersensitivity in Parkinson's disease with impulse control disorder. *Brain: A Journal of Neurology*, **143**(8), 2502–2518.

Duncan, J., & Owen, A. M. (2000). Common regions of the human frontal lobe recruited by diverse cognitive demands. *Trends in Neurosciences*, **23**(10), 475–483.

Eickhoff, S. B., Bzdok, D., Laird, A. R., Kurth, F., & Fox, P. T. (2012). Activation likelihood estimation meta-analysis revisited. *Neuroimage*, **59**(3), 2349–2361.

Eickhoff, S. B., Laird, A. R., Grefkes, C., Wang, L. E., Zilles, K., & Fox, P. T. (2009). Coordinate-based activation likelihood estimation meta-analysis of neuroimaging data: a random-effects approach based on empirical estimates of spatial uncertainty. *Human Brain Mapping*, **30**(9), 2907–2926.

Eickhoff, S. B., & Müller, V. I. (2015). Functional Connectivity. In *Brain Mapping*, Elsevier, pp. 187–201.

Ek, B., VerSchneider, C., & Narayan, D. A. (2015). Global efficiency of graphs. *AKCE International Journal of Graphs and Combinatorics*, **12**(1), 1–13.

Engelhardt, E., & Gomes, M. da M. (2017). Lewy and his inclusion bodies: Discovery and rejection. *Dementia & Neuropsychologia*, **11**(2), 198–201.

Esposito, F., Tessitore, A., Giordano, A., … Tedeschi, G. (2013). Rhythm-specific

modulation of the sensorimotor network in drug-naive patients with Parkinson's disease by levodopa. *Brain: A Journal of Neurology*, **136**(Pt 3), 710–725.

Fagiolo, G. (2007). Clustering in complex directed networks. *Physical Review. E, Statistical, Nonlinear, and Soft Matter Physics*, **76**(2 Pt 2), 026107.

Fang, J., Chen, H., Cao, Z., … Feng, T. (2017). Impaired brain network architecture in newly diagnosed Parkinson's disease based on graph theoretical analysis. *Neuroscience Letters*, **657**, 151–158.

Farahani, F. V., Karwowski, W., & Lighthall, N. R. (2019). Application of graph theory for identifying connectivity patterns in human brain networks: A systematic review. *Frontiers in Neuroscience*, **13**, 585.

Feng, X., Piper, R. J., Prentice, F., Clayden, J. D., & Baldeweg, T. (2024). Functional brain connectivity in children with focal epilepsy: A systematic review of functional MRI studies. *Seizure*, **117**, 164–173.

Filippi, M., Sarasso, E., & Agosta, F. (2019). Resting-state Functional MRI in Parkinsonian Syndromes. *Movement Disorders Clinical Practice (Hoboken, N.J.)*, **6**(2), 104–117.

Flowers, K. A., & Robertson, C. (1995). Perceptual abnormalities in Parkinson's disease: top-down or bottom-up processes? *Perception*, **24**(10), 1201–1221.

Fornito, A. (2016). CH4 Node degree and strength. In A. Fornito, A. Zalesky, & E. T. Bullmore, eds., *Fundamentals of brain network analysis*, Elsevier, pp. 115–136.

Fox, M. D., Snyder, A. Z., Vincent, J. L., Corbetta, M., Van Essen, D. C., & Raichle, M. E. (2005). The human brain is intrinsically organized into dynamic, anticorrelated functional networks. *Proceedings of the National Academy of Sciences of the United States of America*, **102**(27), 9673–9678.

Freeman, L. C. (1977). A set of measures of centrality based on betweenness. *Sociometry*, **40**(1), 35.

Friston, K. J., Williams, S., Howard, R., Frackowiak, R. S., & Turner, R. (1996). Movement-related effects in fMRI time-series. *Magnetic Resonance in Medicine*, **35**(3), 346–355.

Friston, K. J. (1994). Functional and effective connectivity in neuroimaging: A synthesis. *Human Brain Mapping*, **2**(1–2), 56–78.

GBD 2016 Neurology Collaborators. (2019). Global, regional, and national burden of neurological disorders, 1990-2016: a systematic analysis for the Global

Burden of Disease Study 2016. *Lancet Neurology*, **18**(5), 459–480.

GBD 2016 Parkinson's Disease Collaborators. (2018). Global, regional, and national burden of Parkinson's disease, 1990-2016: a systematic analysis for the Global Burden of Disease Study 2016. *Lancet Neurology*, **17**(11), 939–953.

Geschwind, N. (1965). Disconnexion syndromes in animals and man. I. *Brain: A Journal of Neurology*, **88**(2), 237–294.

Gibb, W. R., & Lees, A. J. (1988). The relevance of the Lewy body to the pathogenesis of idiopathic Parkinson's disease. *Journal of Neurology, Neurosurgery, and Psychiatry*, **51**(6), 745–752.

Glover, G. H. (2011). Overview of functional magnetic resonance imaging. *Neurosurgery Clinics of North America*, **22**(2), 133–9, vii.

Goedert, M., Spillantini, M. G., Del Tredici, K., & Braak, H. (2013). 100 years of Lewy pathology. *Nature Reviews. Neurology*, **9**(1), 13–24.

Goldman, J. G., & Sieg, E. (2020). Cognitive impairment and dementia in parkinson disease. *Clinics in Geriatric Medicine*, **36**(2), 365–377.

Goñi, J., Avena-Koenigsberger, A., Velez de Mendizabal, N., van den Heuvel, M. P., Betzel, R. F., & Sporns, O. (2013). Exploring the morphospace of communication efficiency in complex networks. *Plos One*, **8**(3), e58070.

González-Madruga, K., Staginnus, M., & Fairchild, G. (2022). Alterations in structural and functional connectivity in ADHD: implications for theories of ADHD. *Current Topics in Behavioral Neurosciences*, **57**, 445–481.

Gore, J. C. (2003). Principles and practice of functional MRI of the human brain. *The Journal of Clinical Investigation*, **112**(1), 4–9.

Göttlich, M., Münte, T. F., Heldmann, M., Kasten, M., Hagenah, J., & Krämer, U. M. (2013). Altered resting state brain networks in Parkinson's disease. *Plos One*, **8**(10), e77336.

Greenland, J. C., Williams-Gray, C. H., & Barker, R. A. (2019). The clinical heterogeneity of Parkinson's disease and its therapeutic implications. *The European Journal of Neuroscience*, **49**(3), 328–338.

Guimerà, R., & Nunes Amaral, L. A. (2005). Functional cartography of complex metabolic networks. *Nature*, **433**(7028), 895–900.

Hacker, C. D., Perlmutter, J. S., Criswell, S. R., Ances, B. M., & Snyder, A. Z. (2012). Resting state functional connectivity of the striatum in Parkinson's disease. *Brain: A Journal of Neurology*, **135**(Pt 12), 3699–3711.

Helmich, R. C., Derikx, L. C., Bakker, M., Scheeringa, R., Bloem, B. R., & Toni, I. (2010). Spatial remapping of cortico-striatal connectivity in Parkinson's disease. *Cerebral Cortex*, **20**(5), 1175–1186.

Hensel, L., Hoffstaedter, F., Caspers, J., … Eickhoff, S. B. (2019). Functional connectivity changes of key regions for motor initiation in parkinson's disease. *Cerebral Cortex*, **29**(1), 383–396.

He, Y., Byrge, L., & Kennedy, D. P. (2020). Nonreplication of functional connectivity differences in autism spectrum disorder across multiple sites and denoising strategies. *Human Brain Mapping*, **41**(5), 1334–1350.

Heckner, M. K., Cieslik, E. C., Küppers, V., Fox, P. T., Eickhoff, S. B., & Langner, R. (2021). Delineating visual, auditory and motor regions in the human brain with functional neuroimaging: a BrainMap-based meta-analytic synthesis. *Scientific Reports*, **11**(1), 9942.

Hof, P. R., & Bouras, C. (1991). Object recognition deficit in Alzheimer's disease: possible disconnection of the occipito-temporal component of the visual system. *Neuroscience Letters*, **122**(1), 53–56.

Hohenfeld, C., Werner, C. J., & Reetz, K. (2018). Resting-state connectivity in neurodegenerative disorders: Is there potential for an imaging biomarker? *NeuroImage. Clinical*, **18**, 849–870.

Holiga, Š., Hipp, J. F., Chatham, C. H., … Dukart, J. (2019). Patients with autism spectrum disorders display reproducible functional connectivity alterations. *Science Translational Medicine*, **11**(481). doi:10.1126/scitranslmed.aat9223

Hou, Y., Luo, C., Yang, J., … Shang, H. (2017). Default-mode network connectivity in cognitively unimpaired drug-naïve patients with rigidity-dominant Parkinson's disease. *Journal of Neurology*, **264**(1), 152–160.

Hou, Y., Yang, J., Luo, C., … Shang, H. (2016). Dysfunction of the Default Mode Network in Drug-Naïve Parkinson's Disease with Mild Cognitive Impairments: A Resting-State fMRI Study. *Frontiers in Aging Neuroscience*, **8**, 247.

Hughes, A. J., Daniel, S. E., Kilford, L., & Lees, A. J. (1992). Accuracy of clinical diagnosis of idiopathic Parkinson's disease: a clinico-pathological study of 100 cases. *Journal of Neurology, Neurosurgery, and Psychiatry*, **55**(3), 181–184.

Jadavji, N. M., Haelterman, N. A., Sud, R., & Antonietti, A. (2023). Editorial: Reproducibility in neuroscience. *Frontiers in Integrative Neuroscience*, **17**, 1271818.

Jankovic, J. (2008). Parkinson's disease: clinical features and diagnosis. *Journal of Neurology, Neurosurgery, and Psychiatry*, **79**(4), 368–376.

Jellinger, K. A. (2023). Pathobiology of cognitive impairment in parkinson disease: challenges and outlooks. *International Journal of Molecular Sciences*, **25**(1). doi:10.3390/ijms25010498

Karunanayaka, P. R., Lee, E.-Y., Lewis, M. M., … Huang, X. (2016). Default mode network differences between rigidity- and tremor-predominant Parkinson's disease. *Cortex*, **81**, 239–250.

Kazeminejad, A., & Sotero, R. C. (2020). The Importance of Anti-correlations in Graph Theory Based Classification of Autism Spectrum Disorder. *Frontiers in Neuroscience*, **14**, 676.

Khalili-Mahani, N., Rombouts, S. A. R. B., van Osch, M. J. P., … van Gerven, J. M. (2017). Biomarkers, designs, and interpretations of resting-state fMRI in translational pharmacological research: A review of state-of-the-Art, challenges, and opportunities for studying brain chemistry. *Human Brain Mapping*, **38**(4), 2276–2325.

Kiesel, A., Steinhauser, M., Wendt, M., … Koch, I. (2010). Control and interference in task switching--a review. *Psychological Bulletin*, **136**(5), 849–874.

Kim, B., Kim, H., Kim, S., & Hwang, Y.-R. (2021). A brief review of non-invasive brain imaging technologies and the near-infrared optical bioimaging. *Applied Microscopy*, **51**(1), 9.

Klann, E. M., Dissanayake, U., Gurrala, A., … Vedam-Mai, V. (2021). The Gut-Brain Axis and Its Relation to Parkinson's Disease: A Review. *Frontiers in Aging Neuroscience*, **13**, 782082.

Koch, I., Poljac, E., Müller, H., & Kiesel, A. (2018). Cognitive structure, flexibility, and plasticity in human multitasking-An integrative review of dual-task and task-switching research. *Psychological Bulletin*, **144**(6), 557–583.

Koh, J., Kaneoke, Y., Donishi, T., … Ito, H. (2020). Increased large-scale inter-network connectivity in relation to impulsivity in Parkinson's disease. *Scientific Reports*, **10**(1), 11418.

Krajcovicova, L., Mikl, M., Marecek, R., & Rektorova, I. (2012). The default mode network integrity in patients with Parkinson's disease is levodopa equivalent dose-dependent. *Journal of Neural Transmission*, **119**(4), 443–454.

Kwak, Y., Peltier, S., Bohnen, N. I., Müller, M. L. T. M., Dayalu, P., & Seidler, R. D.

(2010). Altered resting state cortico-striatal connectivity in mild to moderate stage Parkinson's disease. *Frontiers in Systems Neuroscience*, **4**, 143.

Lake, E. M. R., Bazzigaluppi, P., & Stefanovic, B. (2016). Functional magnetic resonance imaging in chronic ischaemic stroke. *Philosophical Transactions of the Royal Society of London. Series B, Biological Sciences*, **371**(1705). doi:10.1098/rstb.2015.0353

Langner, R., & Eickhoff, S. B. (2013). Sustaining attention to simple tasks: a meta-analytic review of the neural mechanisms of vigilant attention. *Psychological Bulletin*, **139**(4), 870–900.

Langner, R., Leiberg, S., Hoffstaedter, F., & Eickhoff, S. B. (2018). Towards a human self-regulation system: Common and distinct neural signatures of emotional and behavioural control. *Neuroscience and Biobehavioral Reviews*, **90**, 400–410.

Latora, V., & Marchiori, M. (2001). Efficient behavior of small-world networks. *Physical Review Letters*, **87**(19), 198701.

Lerma-Usabiaga, G., Mukherjee, P., Ren, Z., Perry, M. L., & Wandell, B. A. (2019). Replication and generalization in applied neuroimaging. *Neuroimage*, **202**, 116048.

Lesko, L. J., & Atkinson, A. J. (2001). Use of biomarkers and surrogate endpoints in drug development and regulatory decision making: criteria, validation, strategies. *Annual Review of Pharmacology and Toxicology*, **41**, 347–366.

Litvan, I., Goldman, J. G., Tröster, A. I., … Emre, M. (2012). Diagnostic criteria for mild cognitive impairment in Parkinson's disease: Movement Disorder Society Task Force guidelines. *Movement Disorders*, **27**(3), 349–356.

Liu, X., Hairston, J., Schrier, M., & Fan, J. (2011). Common and distinct networks underlying reward valence and processing stages: a meta-analysis of functional neuroimaging studies. *Neuroscience and Biobehavioral Reviews*, **35**(5), 1219–1236.

Lucas-Jiménez, O., Ojeda, N., Peña, J., … Ibarretxe-Bilbao, N. (2016). Altered functional connectivity in the default mode network is associated with cognitive impairment and brain anatomical changes in Parkinson's disease. *Parkinsonism & Related Disorders*, **33**, 58–64.

Lv, H., Wang, Z., Tong, E., … Wintermark, M. (2018). Resting-State Functional MRI: Everything That Nonexperts Have Always Wanted to Know. *American*

Journal of Neuroradiology, **39**(8), 1390–1399.

Mahlknecht, P., Seppi, K., & Poewe, W. (2015). The concept of prodromal parkinson's disease. *Journal of Parkinson's Disease*, **5**(4), 681–697.

Maidan, I., Jacob, Y., Giladi, N., Hausdorff, J. M., & Mirelman, A. (2019). Altered organization of the dorsal attention network is associated with freezing of gait in Parkinson's disease. *Parkinsonism & Related Disorders*, **63**, 77–82.

Mantini, D., & Vanduffel, W. (2013). Emerging roles of the brain's default network. *The Neuroscientist*, **19**(1), 76–87.

Menon, V. (2023). 20 years of the default mode network: A review and synthesis. *Neuron*, **111**(16), 2469–2487.

Merello, M., Gerschcovich, E. R., Ballesteros, D., & Cerquetti, D. (2011). Correlation between the Movement Disorders Society Unified Parkinson's Disease rating scale (MDS-UPDRS) and the Unified Parkinson's Disease rating scale (UPDRS) during L-dopa acute challenge. *Parkinsonism & Related Disorders*, **17**(9), 705–707.

Mohan, A., Roberto, A. J., Mohan, A., … Lapidus, K. A. B. (2016). The significance of the default mode network (DMN) in neurological and neuropsychiatric disorders: A review. *The Yale Journal of Biology and Medicine*, **89**(1), 49–57.

Novaes, N. P., Balardin, J. B., Hirata, F. C., … Cardoso, E. F. (2021). Global efficiency of the motor network is decreased in Parkinson's disease in comparison with essential tremor and healthy controls. *Brain and Behavior*, **11**(8), e02178.

Ogawa, S., Lee, T. M., Kay, A. R., & Tank, D. W. (1990a). Brain magnetic resonance imaging with contrast dependent on blood oxygenation. *Proceedings of the National Academy of Sciences of the United States of America*, **87**(24), 9868–9872.

Ogawa, S., Lee, T. M., Nayak, A. S., & Glynn, P. (1990b). Oxygenation-sensitive contrast in magnetic resonance image of rodent brain at high magnetic fields. *Magnetic Resonance in Medicine*, **14**(1), 68–78.

Olde Dubbelink, K. T. E., Schoonheim, M. M., Deijen, J. B., Twisk, J. W. R., Barkhof, F., & Berendse, H. W. (2014). Functional connectivity and cognitive decline over 3 years in Parkinson disease. *Neurology*, **83**(22), 2046–2053.

Onnela, J.-P., Saramäki, J., Kertész, J., & Kaski, K. (2005). Intensity and coherence of motifs in weighted complex networks. *Physical Review. E,*

Statistical, Nonlinear, and Soft Matter Physics, **71**(6 Pt 2), 065103.

Parkinson, J. (2002). An essay on the shaking palsy. 1817. *The Journal of Neuropsychiatry and Clinical Neurosciences*, **14**(2), 223–36; discussion 222.

Park, H.-J., & Friston, K. (2013). Structural and functional brain networks: from connections to cognition. *Science*, **342**(6158), 1238411.

Pashler, H. (1994). Dual-task interference in simple tasks: data and theory. *Psychological Bulletin*, **116**(2), 220–244.

Pauling, L., & Coryell, C. D. (1936). The magnetic properties and structure of hemoglobin, oxyhemoglobin and carbonmonoxyhemoglobin. *Proceedings of the National Academy of Sciences of the United States of America*, **22**(4), 210–216.

Peraza, L. R., Nesbitt, D., Lawson, R. A., … Taylor, J.-P. (2017). Intra- and inter-network functional alterations in Parkinson's disease with mild cognitive impairment. *Human Brain Mapping*, **38**(3), 1702–1715.

Péron, J., Dondaine, T., Le Jeune, F., Grandjean, D., & Vérin, M. (2012). Emotional processing in Parkinson's disease: a systematic review. *Movement Disorders*, **27**(2), 186–199.

Perry, D. C., & Kramer, J. H. (2015). Reward processing in neurodegenerative disease. *Neurocase: Case Studies in Neuropsychology, Neuropsychiatry, and Behavioural Neurology*, **21**(1), 120–133.

Pini, L., Wennberg, A. M., Salvalaggio, A., Vallesi, A., Pievani, M., & Corbetta, M. (2021). Breakdown of specific functional brain networks in clinical variants of Alzheimer's disease. *Ageing Research Reviews*, **72**, 101482.

Postuma, R. B., Berg, D., Stern, M., … Deuschl, G. (2015). MDS clinical diagnostic criteria for Parkinson's disease. *Movement Disorders*, **30**(12), 1591–1601.

Power, J. D., Schlaggar, B. L., Lessov-Schlaggar, C. N., & Petersen, S. E. (2013). Evidence for hubs in human functional brain networks. *Neuron*, **79**(4), 798–813.

Power, J. D., Schlaggar, B. L., & Petersen, S. E. (2014). Studying brain organization via spontaneous fMRI signal. *Neuron*, **84**(4), 681–696.

Prodoehl, J., Burciu, R. G., & Vaillancourt, D. E. (2014). Resting state functional magnetic resonance imaging in Parkinson's disease. *Current Neurology and Neuroscience Reports*, **14**(6), 448.

Putcha, D., Ross, R. S., Cronin-Golomb, A., Janes, A. C., & Stern, C. E. (2015). Altered intrinsic functional coupling between core neurocognitive networks in Parkinson's disease. *NeuroImage. Clinical*, **7**, 449–455.

Putcha, D., Ross, R. S., Cronin-Golomb, A., Janes, A. C., & Stern, C. E. (2016). Salience and default mode network coupling predicts cognition in aging and parkinson's disease. *Journal of the International Neuropsychological Society*, **22**(2), 205–215.

Raffegeau, T. E., Krehbiel, L. M., Kang, N., … Hass, C. J. (2019). A meta-analysis: Parkinson's disease and dual-task walking. *Parkinsonism & Related Disorders*, **62**, 28–35.

Raichle, M. E. (2015). The brain's default mode network. *Annual Review of Neuroscience*, **38**, 433–447.

Ramos, A. A., & Machado, L. (2021). A Comprehensive Meta-analysis on Short-term and Working Memory Dysfunction in Parkinson's Disease. *Neuropsychology Review*, **31**(2), 288–311.

Ran, Q., Jamoulle, T., Schaeverbeke, J., Meersmans, K., Vandenberghe, R., & Dupont, P. (2020). Reproducibility of graph measures at the subject level using resting-state fMRI. *Brain and Behavior*, **10**(8), 2336–2351.

Rizzo, G., Copetti, M., Arcuti, S., Martino, D., Fontana, A., & Logroscino, G. (2016). Accuracy of clinical diagnosis of Parkinson disease: A systematic review and meta-analysis. *Neurology*, **86**(6), 566–576.

Robertson, I., & Garavan, H. (2004). Vigilant Attention. In M. Gazzaniga, ed., *The Cognitive Neurosciences*, MIT Press.

Rodríguez-Violante, M., Cervantes-Arriaga, A., Fahn, S., & Tolosa, E. (2017). Two-hundred Years Later: Is Parkinson's Disease a Single Defined Entity? *Revista de Investigacion Clinica; Organo Del Hospital de Enfermedades de La Nutricion*, **69**(6), 308–313.

Rottschy, C., Langner, R., Dogan, I., … Eickhoff, S. B. (2012). Modelling neural correlates of working memory: a coordinate-based meta-analysis. *Neuroimage*, **60**(1), 830–846.

Rubbert, C., Mathys, C., Jockwitz, C., … Caspers, J. (2019). Machine-learning identifies Parkinson's disease patients based on resting-state between-network functional connectivity. *The British Journal of Radiology*, **92**(1101), 20180886.

Rubinov, M., & Sporns, O. (2010). Complex network measures of brain connectivity: uses and interpretations. *Neuroimage*, **52**(3), 1059–1069.

Sabatinelli, D., Fortune, E. E., Li, Q., … Jeffries, J. (2011). Emotional perception: meta-analyses of face and natural scene processing. *Neuroimage*, **54**(3), 2524–2533.

Sang, L., Zhang, J., Wang, L., … Qiu, M. (2015). Alteration of Brain Functional Networks in Early-Stage Parkinson's Disease: A Resting-State fMRI Study. *Plos One*, **10**(10), e0141815.

Schmitter-Edgecombe, M., Brown, K., Chilton, R. C., Whiteley, N., & Greeley, D. (2024). Naturalistic assessment of everyday multitasking in Parkinson's disease with and without mild cognitive impairment. *The Clinical Neuropsychologist*, 1–21.

Schrag, A., Ben-Shlomo, Y., & Quinn, N. (2002). How valid is the clinical diagnosis of Parkinson's disease in the community? *Journal of Neurology, Neurosurgery, and Psychiatry*, **73**(5), 529–534.

Sheffield, J. M., & Barch, D. M. (2016). Cognition and resting-state functional connectivity in schizophrenia. *Neuroscience and Biobehavioral Reviews*, **61**, 108–120.

Shine, J. M., Halliday, G. M., Gilat, M., … Lewis, S. J. G. (2014). The role of dysfunctional attentional control networks in visual misperceptions in Parkinson's disease. *Human Brain Mapping*, **35**(5), 2206–2219.

Shulman, G. L., Fiez, J. A., Corbetta, M., … Petersen, S. E. (1997). Common Blood Flow Changes across Visual Tasks: II. Decreases in Cerebral Cortex. *Journal of Cognitive Neuroscience*, **9**(5), 648–663.

Smallwood, J., Bernhardt, B. C., Leech, R., Bzdok, D., Jefferies, E., & Margulies, D. S. (2021). The default mode network in cognition: a topographical perspective. *Nature Reviews. Neuroscience*, **22**(8), 503–513.

Smitha, K. A., Akhil Raja, K., Arun, K. M., … Kesavadas, C. (2017). Resting state fMRI: A review on methods in resting state connectivity analysis and resting state networks. *The Neuroradiology Journal*, **30**(4), 305–317.

Specht, K. (2019). Current Challenges in Translational and Clinical fMRI and Future Directions. *Frontiers in Psychiatry*, **10**, 924.

Sporns, O., & Betzel, R. F. (2016). Modular Brain Networks. *Annual Review of Psychology*, **67**, 613–640.

Sporns, O. (2013). Structure and function of complex brain networks. *Dialogues in Clinical Neuroscience*, **15**(3), 247–262.

Sporns, O. (2018). Graph theory methods: applications in brain networks. *Dialogues in Clinical Neuroscience*, **20**(2), 111–121.

Spreng, R. N., Sepulcre, J., Turner, G. R., Stevens, W. D., & Schacter, D. L. (2013). Intrinsic architecture underlying the relations among the default, dorsal attention, and frontoparietal control networks of the human brain. *Journal of Cognitive Neuroscience*, **25**(1), 74–86.

Spreng, R. N., Stevens, W. D., Chamberlain, J. P., Gilmore, A. W., & Schacter, D. L. (2010). Default network activity, coupled with the frontoparietal control network, supports goal-directed cognition. *Neuroimage*, **53**(1), 303–317.

Spreng, R. N. (2012). The fallacy of a “task-negative” network. *Frontiers in Psychology*, **3**, 145.

Steiner, J. A., Quansah, E., & Brundin, P. (2018). The concept of alpha-synuclein as a prion-like protein: ten years after. *Cell and Tissue Research*, **373**(1), 161–173.

Suo, X., Lei, D., Li, N., … Gong, Q. (2017). Functional brain connectome and its relation to hoehn and yahr stage in parkinson disease. *Radiology*, **285**(3), 904–913.

Tahmasian, M., Eickhoff, S. B., Giehl, K., … Eickhoff, C. R. (2017). Resting-state functional reorganization in Parkinson’s disease: An activation likelihood estimation meta-analysis. *Cortex*, **92**, 119–138.

Tessitore, A., Cirillo, M., & De Micco, R. (2019). Functional connectivity signatures of parkinson’s disease. *Journal of Parkinson’s Disease*, **9**(4), 637–652.

Tessitore, A., Esposito, F., Vitale, C., … Tedeschi, G. (2012). Default-mode network connectivity in cognitively unimpaired patients with Parkinson disease. *Neurology*, **79**(23), 2226–2232.

Thulborn, K. R., Waterton, J. C., Matthews, P. M., & Radda, G. K. (1982). Oxygenation dependence of the transverse relaxation time of water protons in whole blood at high field. *Biochimica et Biophysica Acta*, **714**(2), 265–270.

Tolosa, E., Garrido, A., Scholz, S. W., & Poewe, W. (2021). Challenges in the diagnosis of Parkinson’s disease. *Lancet Neurology*, **20**(5), 385–397.

Tysnes, O.-B., & Storstein, A. (2017). Epidemiology of Parkinson’s disease. *Journal of Neural Transmission*, **124**(8), 901–905.

van den Heuvel, M. P., & Hulshoff Pol, H. E. (2010). Exploring the brain network: a review on resting-state fMRI functional connectivity. *European Neuropsychopharmacology*, **20**(8), 519–534.

van den Heuvel, M. P., & Sporns, O. (2013). An anatomical substrate for integration among functional networks in human cortex. *The Journal of Neuroscience*, **33**(36), 14489–14500.

Van Dijk, K. R. A., Hedden, T., Venkataraman, A., Evans, K. C., Lazar, S. W., & Buckner, R. L. (2010). Intrinsic functional connectivity as a tool for human connectomics: theory, properties, and optimization. *Journal of Neurophysiology*, **103**(1), 297–321.

Verhaeghen, P., Steitz, D. W., Sliwinski, M. J., & Cerella, J. (2003). Aging and dual-task performance: a meta-analysis. *Psychology and Aging*, **18**(3), 443–460.

Vervoort, G., Alaerts, K., Bengevoord, A., … Nieuwboer, A. (2016). Functional connectivity alterations in the motor and fronto-parietal network relate to behavioral heterogeneity in Parkinson's disease. *Parkinsonism & Related Disorders*, **24**, 48–55.

Voets, N. L. (2021). Clinical applications of functional MRI. In *Advanced neuro MR techniques and applications*, Vol. 4, Elsevier, pp. 277–292.

Wagner, G., Li, M., Sacchet, M. D., … Jollant, F. (2021). Functional network alterations differently associated with suicidal ideas and acts in depressed patients: an indirect support to the transition model. *Translational Psychiatry*, **11**(1), 100.

Wang, Q., Yu, M., Yan, L., … Liu, W. (2023). Aberrant inter-network functional connectivity in drug-naive Parkinson's disease patients with tremor dominant and postural instability and gait difficulty. *Frontiers in Human Neuroscience*, **17**, 1100431.

Wei, L., Zhang, J., Long, Z., … Wang, J. (2014). Reduced topological efficiency in cortical-basal Ganglia motor network of Parkinson's disease: a resting state fMRI study. *Plos One*, **9**(10), e108124.

White, R. L., Campbell, M. C., Yang, D., Shannon, W., Snyder, A. Z., & Perlmutter, J. S. (2020). Little Change in Functional Brain Networks Following Acute Levodopa in Drug-Naïve Parkinson's Disease. *Movement Disorders*, **35**(3), 499–503.

Witt, S. T., Laird, A. R., & Meyerand, M. E. (2008). Functional neuroimaging correlates of finger-tapping task variations: an ALE meta-analysis. *Neuroimage*, **42**(1), 343–356.

Wolters, A. F., van de Weijer, S. C. F., Leentjens, A. F. G., Duits, A. A., Jacobs, H. I. L., & Kuijf, M. L. (2019). Resting-state fMRI in Parkinson's disease patients with cognitive impairment: A meta-analysis. *Parkinsonism & Related Disorders*, **62**, 16–27.

Woo, C.-W., Chang, L. J., Lindquist, M. A., & Wager, T. D. (2017). Building better biomarkers: brain models in translational neuroimaging. *Nature Neuroscience*, **20**(3), 365–377.

Woods, S. P., & Tröster, A. I. (2003). Prodromal frontal/executive dysfunction predicts incident dementia in Parkinson's disease. *Journal of the International Neuropsychological Society*, **9**(1), 17–24.

Worringer, B., Langner, R., Koch, I., Eickhoff, S. B., Eickhoff, C. R., & Binkofski, F. C. (2019). Common and distinct neural correlates of dual-tasking and task-switching: a meta-analytic review and a neuro-cognitive processing model of human multitasking. *Brain Structure & Function*, **224**(5), 1845–1869.

Wu, T., Wang, L., Chen, Y., Zhao, C., Li, K., & Chan, P. (2009). Changes of functional connectivity of the motor network in the resting state in Parkinson's disease. *Neuroscience Letters*, **460**(1), 6–10.

Xia, M., Wang, J., & He, Y. (2013). BrainNet Viewer: a network visualization tool for human brain connectomics. *Plos One*, **8**(7), e68910.

Yamashita, K. Y., Bhoopatiraju, S., Silverglate, B. D., & Grossberg, G. T. (2023). Biomarkers in Parkinson's disease: A state of the art review. *Biomarkers in Neuropsychiatry*, **9**, 100074.

Yao, N., Shek-Kwan Chang, R., Cheung, C., … McAlonan, G. M. (2014). The default mode network is disrupted in Parkinson's disease with visual hallucinations. *Human Brain Mapping*, **35**(11), 5658–5666.

Yeager, B. E., Twedt, H. P., Bruss, J., Schultz, J., & Narayanan, N. S. (2024). Cortical and subcortical functional connectivity and cognitive impairment in Parkinson's disease. *NeuroImage. Clinical*, **42**, 103610.

Yeo, B. T. T., Krienen, F. M., Sepulcre, J., … Buckner, R. L. (2011). The organization of the human cerebral cortex estimated by intrinsic functional connectivity. *Journal of Neurophysiology*, **106**(3), 1125–1165.

Yu, Q., Li, Q., Fang, W., … Cheng, O. (2021). Disorganized resting-state functional connectivity between the dorsal attention network and intrinsic networks in Parkinson's disease with freezing of gait. *The European Journal of Neuroscience*, **54**(7), 6633–6645.

Zhu, X., Liu, L., Xiao, Y., … Pan, S. (2021). Abnormal Topological Network in Parkinson's Disease With Impulse Control Disorders: A Resting-State Functional Magnetic Resonance Imaging Study. *Frontiers in Neuroscience*, **15**, 651710.

Zimmermann, J., Griffiths, J., Schirner, M., Ritter, P., & McIntosh, A. R. (2019). Subject specificity of the correlation between large-scale structural and functional connectivity. *Network Neuroscience (Cambridge, Mass.)*, **3**(1), 90–106.

Zuo, C., Suo, X., Lan, H., … Gong, Q. (2023). Global Alterations of Whole Brain Structural Connectome in Parkinson's Disease: A Meta-analysis. *Neuropsychology Review*, **33**(4), 783–80

Appendix

Data-PR	Cog AC	Cog AR	Emo SF	Motor Perc	Motor Ex	Mult iTask	WBN	Rew	VigAtt	WM	eMDN	eSAD	DMN
						thrX							
bnFC	0.874	0.874	0.874	0.874	0.874	0.874	0.874	0.874	0.874	0.874	0.874	0.874	NaN
wnFC	0.034*	0.029*	0.230	0.001*	0.001*	0.278	0.001*	0.030*	0.006*	0.081°	0.051°	0.256	NaN
combFC	0.033*	0.034*	0.293	0.003*	0.017*	0.072°	0.003*	0.033*	0.010*	0.064°	0.033*	0.121	0.033*
PPC	0.965	0.815	0.508	0.664	0.652	0.958	0.179	0.328	0.664	0.664	0.664	0.179	NaN
ST	0.112	0.091°	0.312	0.245	0.115	0.073°	0.254	0.133	0.091°	0.112	0.133	0.112	0.086°
						thr0							
bnFC	0.836	0.862	0.836	0.836	0.862	0.836	0.836	0.836	0.836	0.836	0.862	0.836	NaN
wnFC	0.081°	0.080°	0.417	0.002*	0.008*	0.410	0.022*	0.419	0.022*	0.216	0.176	0.380	NaN
combFC	0.063°	0.079°	0.410	0.034*	0.034*	0.103	0.034*	0.289	0.034*	0.127	0.121	0.162	0.034*
GE	0.094°	0.090°	0.431	0.051°	0.041*	0.102	0.083°	0.351	0.041*	0.102	0.200	0.207	0.041*
DE	0.032*	0.499	0.595	0.031*	0.224	0.492	0.031*	0.029*	0.034*	0.047*	0.047*	0.029*	0.047*
ECC	0.109	0.249	0.197	0.313	0.249	0.249	0.487	0.249	0.109	0.197	0.164	0.222	0.313
BET	0.820	0.063°	0.768	0.584	0.063°	0.679	0.679	0.768	0.584	0.810	0.584	0.810	0.483
PPC	0.957	0.780	0.504	0.666	0.664	0.957	0.179	0.326	0.666	0.666	0.666	0.179	NaN
ST	0.113	0.092°	0.312	0.245	0.116	0.074°	0.254	0.134	0.092°	0.113	0.134	0.113	0.085°
						thr25							
bnFC	0.888	0.888	0.888	0.846	0.888	0.888	0.888	0.888	0.888	0.888	0.846	0.846	NaN
wnFC	0.157	0.157	0.548	0.045*	0.022*	0.548	0.120	0.937	0.120	0.391	0.521	0.548	NaN
combFC	0.163	0.163	0.577	0.111	0.111	0.273	0.111	0.684	0.111	0.273	0.441	0.310	0.111
GE	0.088°	0.088°	0.646	0.178	0.088°	0.201	0.088°	0.259	0.088°	0.088°	0.338	0.178	0.088°
DE	0.068°	0.887	0.887	0.402	0.402	0.402	0.006*	0.068°	0.175	0.068°	0.595	0.046*	0.174
ECC	0.323	0.151	0.795	0.432	0.432	0.396	0.432	0.617	0.432	0.432	0.770	0.282	0.227
BET	0.957	0.957	0.957	0.957	0.957	0.957	0.957	0.957	0.957	0.957	0.957	0.957	0.957
PPC	0.750	0.612	0.559	0.491	0.559	0.750	0.491	0.504	0.612	0.750	0.504	0.504	NaN
ST	0.226	0.226	0.458	0.439	0.229	0.226	0.458	0.282	0.226	0.226	0.337	0.226	0.226

Table S1. Group differences between patients with Parkinson's disease and healthy controls in Data-PR. Conducted statistical analysis: ANCOVA (covariates: gender, age), displayed are FDR-corrected p-values (* = $p < 0.05$; ° = $p < 0.1$). Analysis conducted for 3 threshold levels (X = all weights included; 0 = positive edges retained; 25 = weights above 0.25 retained). Networks: Cognitive action control (CogAC), cognitive action regulation (CogAR), emotional scene and face processing (EmoSF), perceptuo-motor (MotorPerc), motor execution (MotorEx), multitasking (MultiTask), whole-brain network (WBN), reward-related decision-making (Rew), vigilant attention (VigAtt), working memory (WM), extended multiple demand (eMDN), extended social-affective default (eSAD), default mode network (DMN). Functional connectivity (FC) measures: average between-network FC (bnFC), average within-network FC (wnFC), average combined network FC (combFC), mean positive participation coefficient (PPC), mean nodal strength (ST), global efficiency (GE), mean global diffusion efficiency (DE), mean nodal eccentricity (ECC), mean node betweenness centrality vector (BET).

Data-DU	Cog AC	Cog AR	Emo SF	Motor Perc	Motor Ex	Mult iTask	WBN	Rew	VigAtt	WM	eMDN	eSAD	DMN
						thrX							
bnFC	0.944	0.944	0.944	0.944	0.944	0.944	0.944	0.944	0.944	0.944	0.944	0.944	NaN
wnFC	0.150	0.150	0.374	0.182	0.150	0.183	0.183	0.401	0.410	0.150	0.091°	0.182	NaN
combFC	0.070°	0.113	0.637	0.070°	0.070°	0.070°	0.155	0.122	0.155	0.070°	0.070°	0.122	0.070°
PPC	0.966	0.316	0.316	0.966	0.316	0.349	0.242	0.316	0.966	0.966	0.327	0.316	NaN
ST	0.872	0.872	0.872	0.951	0.872	0.872	0.872	0.872	0.872	0.872	0.872	0.872	0.872
						thr0							
bnFC	0.691	0.691	0.691	0.691	0.691	0.691	0.691	0.691	0.691	0.691	0.691	0.691	NaN
wnFC	0.489	0.489	0.489	0.686	0.529	0.489	0.686	0.489	0.904	0.529	0.489	0.642	NaN
combFC	0.616	0.616	0.616	0.647	0.616	0.616	0.653	0.616	0.844	0.649	0.616	0.616	0.616
GE	0.683	0.683	0.683	0.683	0.683	0.683	0.683	0.683	0.738	0.764	0.738	0.738	0.683
DE	0.016*	0.146	0.752	0.169	0.092°	0.305	0.007*	0.044*	0.035*	0.007*	0.016*	0.043*	0.016*
ECC	0.269	0.431	0.148	0.461	0.463	0.038*	0.843	0.269	0.148	0.823	0.244	0.240	0.190
BET	0.986	0.919	0.992	0.992	0.480	0.992	0.992	0.480	0.986	0.480	0.992	0.480	0.992
PPC	0.972	0.308	0.308	0.972	0.308	0.345	0.242	0.308	0.972	0.972	0.336	0.308	NaN
ST	0.877	0.877	0.877	0.948	0.877	0.877	0.877	0.877	0.877	0.877	0.877	0.877	0.877
						thr25							
bnFC	0.485	0.505	0.485	0.116	0.485	0.774	0.343	0.485	0.606	0.485	0.192	0.745	NaN
wnFC	0.896	0.896	0.615	0.896	0.963	0.896	0.896	0.240	0.922	0.978	0.896	0.978	NaN
combFC	0.974	0.974	0.749	0.749	0.974	0.974	0.749	0.389	0.974	0.974	0.974	0.974	0.831
GE	0.856	0.934	0.856	0.856	0.922	0.902	0.856	0.856	0.934	0.934	0.934	0.934	0.856
DE	0.389	0.389	0.101	0.389	0.944	0.527	0.101	0.527	0.944	0.389	0.417	0.417	0.101
ECC	0.789	0.823	0.789	0.925	0.273	0.789	0.873	0.873	0.789	0.789	0.789	0.873	0.873
BET	0.986	0.986	0.986	0.950	0.986	0.986	0.986	0.679	0.968	0.986	0.986	0.986	0.986
PPC	0.837	0.497	0.497	0.526	0.497	0.526	0.497	0.502	0.659	0.837	0.502	0.497	NaN
ST	0.901	0.901	0.901	0.901	0.901	0.901	0.901	0.901	0.901	0.901	0.901	0.901	0.901

Table S2. Group differences between patients with Parkinson's disease and healthy controls in Data-DU. Conducted statistical analysis: ANCOVA (covariates: gender, age), displayed are FDR-corrected p-values (* = $p < 0.05$; ° = $p < 0.1$). Analysis conducted for 3 threshold levels (X = all weights included; 0 = positive edges retained; 25 = weights above 0.25 retained). Networks: Cognitive action control (CogAC), cognitive action regulation (CogAR), emotional scene and face processing (EmoSF), perceptuo-motor (MotorPerc), motor execution (MotorEx), multitasking (MultiTask), whole-brain network (WBN), reward-related decision-making (Rew), vigilant attention (VigAtt), working memory (WM), extended multiple demand (eMDN), extended social-affective default (eSAD), default mode network (DMN). Functional connectivity (FC) measures: average between-network FC (bnFC), average within-network FC (wnFC), average combined network FC (combFC), mean positive participation coefficient (PPC), mean nodal strength (ST), global efficiency (GE), mean global diffusion efficiency (DE), mean nodal eccentricity (ECC), mean node betweenness centrality vector (BET)

Data-PR	Cog AC	Cog AR	Emo SF	Motor Perc	Motor Ex	Multi Task	WBN	Rew	VigAtt	WM	eMDN	eSAD	DMN
						thrX							
bnFC	0.28	0.33	-0.01	0.54*	0.38	0.35	0.11	0.02	0.30	0.23	0.27	-0.42	NaN
wnFC	-0.13	-0.10	0.18	-0.34	-0.22	-0.28	0.01	0.14	-0.19	-0.06	-0.20	-0.35	NaN
combFC	-0.02	0.06	0.05	-0.02	-0.06	-0.07	0.01	0.03	0.01	0.01	-0.08	-0.41	-0.47
PPC	0.30	0.38°	-0.29	0.49*	0.40°	0.54*	-0.45°	-0.42°	0.35	0.33	0.33	-0.18	NaN
ST	-0.24	-0.39	-0.41	-0.16	-0.40	-0.37	-0.22	-0.36	-0.33	-0.20	-0.33	-0.49°	-0.53*
						thr0							
bnFC	0.12	0.15	-0.23	0.34	0.14	0.25	-0.19	-0.18	0.10	0.14	0.08	-0.45	NaN
wnFC	-0.18	-0.15	-0.01	-0.16	-0.13	-0.31	-0.07	-0.01	-0.13	-0.13	-0.19	-0.38	NaN
combFC	-0.17	-0.20	-0.18	-0.06	-0.21	-0.29	-0.08	-0.14	-0.16	-0.12	-0.21	-0.45	-0.53*
GE	-0.24	-0.30	-0.21	-0.10	-0.33	-0.41	-0.13	-0.25	-0.18	-0.18	-0.25	-0.45	-0.54*
DE	0.13	0.17	0.04	0.07	0.15	0.24	0.00	0.07	0.14	0.04	0.07	-0.12	-0.33
ECC	0.11	0.10	-0.05	-0.16	0.02	0.14	0.21	0.14	0.08	0.04	0.09	0.23	0.17
BET	-0.16	-0.03	-0.24	-0.12	0.11	-0.16	-0.02	-0.09	-0.10	0.06	-0.15	0.13	0.21
PPC	0.30	0.39°	-0.29	0.49*	0.40°	0.53*	-0.45°	-0.42°	0.35	0.34	0.33	-0.18	NaN
ST	-0.24	-0.39	-0.41	-0.16	-0.40	-0.37	-0.22	-0.36	-0.33	-0.20	-0.33	-0.49°	-0.54*
						thr25							
bnFC	0.00	0.04	-0.20	0.17	-0.03	0.01	-0.29	-0.26	0.05	0.05	0.01	-0.47	NaN
wnFC	-0.26	-0.14	0.00	-0.05	-0.14	-0.33	-0.07	-0.08	-0.08	-0.15	-0.19	-0.42	NaN
combFC	-0.27	-0.27	-0.16	-0.10	-0.31	-0.41	-0.09	-0.22	-0.16	-0.16	-0.24	-0.48°	-0.57*
GE	-0.33	-0.34	-0.24	-0.13	-0.36	-0.47*	-0.14	-0.39	-0.13	-0.23	-0.28	-0.44°	-0.54*
DE	-0.01	0.01	0.12	0.22	0.20	-0.02	-0.04	-0.23	0.07	-0.12	-0.05	-0.30	-0.40
ECC	0.30	0.11	0.03	-0.15	-0.41	0.25	-0.09	0.11	-0.04	0.15	0.30	0.38	0.31
BET	-0.07	-0.17	0.02	-0.04	-0.09	-0.20	0.00	-0.34	-0.03	-0.02	-0.08	0.08	-0.07
PPC	0.47*	0.40°	-0.21	0.59*	0.50*	0.50*	-0.44*	-0.37°	0.41°	0.32°	0.41°	-0.20	NaN
ST	-0.37°	-0.45*	-0.42*	-0.32	-0.48*	-0.52*	-0.32	-0.42*	-0.40°	-0.33	-0.43*	-0.53*	-0.56*

Table S3. Correlation of functional connectivity measures with symptom severity in Data-PR. Conducted statistical analysis: Pearson's partial correlations (covariates: gender, age) between functional connectivity (FC) measures and symptom severity measured by UPDRS-III OFF. Displayed are correlation coefficients (* = $p < 0.05$; ° = $p < 0.1$). Analysis conducted for all three FC threshold levels (X = all weights included; 0 = positive edges retained; 25 = weights above 0.25 retained). Networks: Cognitive action control (CogAC), cognitive action regulation (CogAR), emotional scene and face processing (EmoSF), perceptuo-motor (MotorPerc), motor execution (MotorEx), multitasking (MultiTask), whole-brain network (WBN), reward-related decision-making (Rew), vigilant attention (VigAtt), working memory (WM), extended multiple demand (eMDN), extended social-affective default (eSAD), default mode network (DMN). Functional connectivity (FC) measures: average between-network FC (bnFC), average within-network FC (wnFC), average combined network FC (combFC), mean positive participation coefficient (PPC), mean nodal strength (ST), global efficiency (GE), mean global diffusion efficiency (DE), mean nodal eccentricity (ECC), mean node betweenness centrality vector (BET).

Data-Du	Cog AC	Cog AR	Emo SF	Motor Perc	Motor Ex	Multi Task	WBN	Rew	VigAtt	WM	eMDN	eSAD	DMN
						thrX							
bnFC	0.18	0.06	-0.13	0.11	0.03	0.30	-0.32	-0.09	0.29	0.14	0.17	-0.40	NaN
wnFC	-0.29	-0.19	-0.19	0.02	-0.14	-0.27	-0.40	-0.03	-0.26	-0.19	-0.18	-0.31	NaN
combFC	-0.23	-0.28	-0.27	-0.01	-0.23	-0.16	-0.40°	-0.13	-0.18	-0.18	-0.15	-0.39°	-0.41°
PPC	0.10	0.15	-0.29	0.03	0.07	0.43	-0.12	-0.22	0.14	0.02	0.01	-0.23	NaN
ST	-0.19	-0.32	-0.25	-0.42°	-0.48°	-0.26	-0.40°	-0.23	-0.11	-0.19	-0.19	-0.35	-0.31
						thr0							
bnFC	0.01	-0.04	-0.09	-0.18	-0.20	0.07	-0.38	-0.12	0.15	-0.04	0.03	-0.34	NaN
wnFC	-0.35	-0.24	-0.19	-0.24	-0.27	-0.31	-0.38	-0.17	-0.32	-0.33	-0.25	-0.34	NaN
combFC	-0.31	-0.29	-0.23	-0.32	-0.39	-0.31	-0.38	-0.21	-0.24	-0.32	-0.24	-0.38	-0.31
GE	-0.37	-0.31	-0.25	-0.29	-0.38	-0.31	-0.31	-0.21	-0.33	-0.34	-0.29	-0.39	-0.32
DE	-0.24	-0.27	-0.12	0.16	-0.10	-0.02	-0.21	-0.12	0.03	-0.08	-0.12	-0.30	-0.36
ECC	0.39	0.01	0.12	0.21	0.30	0.09	0.26	0.34	0.33	0.31	0.30	0.34	0.23
BET	0.00	0.08	-0.17	-0.12	-0.03	-0.16	-0.22	-0.09	-0.08	0.14	0.06	0.27	0.12
PPC	0.10	0.15	-0.29	0.03	0.07	0.43	-0.12	-0.22	0.14	0.01	0.01	-0.23	NaN
ST	-0.19	-0.32	-0.25	-0.42°	-0.48°	-0.26	-0.40°	-0.23	-0.11	-0.19	-0.19	-0.35	-0.31
						thr25							
bnFC	-0.03	-0.03	-0.07	-0.24	-0.16	-0.10	-0.27	-0.09	0.08	-0.07	-0.02	-0.29	NaN
wnFC	-0.35	-0.22	-0.15	-0.28	-0.25	-0.34	-0.30	-0.20	-0.34	-0.34	-0.28	-0.32	NaN
combFC	-0.33	-0.23	-0.16	-0.33	-0.30	-0.39	-0.30	-0.21	-0.28	-0.34	-0.28	-0.33	-0.18
GE	-0.38°	-0.32	-0.22	-0.28	-0.37°	-0.33	-0.31	-0.21	-0.35	-0.37°	-0.25	-0.38°	-0.30
DE	-0.16	-0.08	0.02	0.24	-0.04	-0.07	-0.14	0.17	0.04	-0.17	-0.15	-0.25	-0.25
ECC	0.17	0.29	-0.08	0.17	0.22	0.22	-0.28	0.18	0.37	0.39	0.14	0.13	0.42
BET	-0.04	-0.42°	-0.14	-0.12	-0.44°	0.01	-0.22	-0.09	-0.12	0.23	0.06	0.11	-0.38
PPC	-0.07	0.14	-0.16	0.07	0.05	0.26	-0.05	-0.12	-0.02	-0.03	-0.02	-0.10	NaN
ST	-0.15	-0.20	-0.15	-0.33	-0.25	-0.22	-0.28	-0.15	-0.09	-0.16	-0.17	-0.27	-0.19

Table S4. Correlation of functional connectivity measures with symptom severity in Data-DU. Conducted statistical analysis: Pearson's partial correlations (covariates: gender, age) between functional connectivity (FC) measures and symptom severity measured by MDS-UPDRS-III OFF. Displayed are correlation coefficients (° = $p < 0.1$). Analysis conducted for 3 threshold levels (X = all weights included; 0 = positive edges retained; 25 = weights above 0.25 retained). Networks: Cognitive action control (CogAC), cognitive action regulation (CogAR), emotional scene and face processing (EmoSF), perceptuo-motor (MotorPerc), motor execution (MotorEx), multitasking (MultiTask), whole-brain network (WBN), reward-related decision-making (Rew), vigilant attention (VigAtt), working memory (WM), extended multiple demand (eMDN), extended social-affective default (eSAD), default mode network (DMN). Functional connectivity (FC) measures: average between-network FC (bnFC), average within-network FC (wnFC), average combined network FC (combFC), mean positive participation coefficient (PPC), mean nodal strength (ST), global efficiency (GE), mean global diffusion efficiency (DE), mean nodal eccentricity (ECC), mean node betweenness centrality vector (BET).

Default mode network (DMN)			
X	**Y**	**Z**	**Corresponding macroanatomical brain region**
0	-53	26	Posterior cingulate gyrus
0	52	-6	Superior frontal gyrus, medial orbital
-48	-62	36	Left angular gyrus
46	-62	32	Right angular gyrus
-24	-22	-20	Left parahippocampal gyrus
24	-22	-20	Right parahypppocampal gyrus
Cognitive action control (CogAC)			
X	**Y**	**Z**	**Corresponding macroanatomical brain region**
36	22	-4	Right insula
2	16	48	Left supplementary motor area
48	12	30	Right inferior frontal gyrus, opercular part
36	2	54	Right middle frontal gyrus
48	30	24	Right inferior frontal gyrus, triangular part
-38	-44	46	Left inferior parietal gyrus
-24	-66	48	Left superior parietal gyrus
40	-46	46	Right inferior parietal gyrus
60	-44	24	Right superior temporal gyrus
30	-62	52	Right superior parietal gyrus
-44	10	30	Left inferior frontal gyrus, opercular part
-34	20	-4	Left insula
-26	2	52	Left middle frontal gyrus
6	-18	-2	Right Thalamus
-40	-66	-10	Left inferior occipital gyrus
48	19	6	Right inferior frontal gyrus, opercular part
8	29	30	Right anterior cingulate cortex
-45	27	30	Left inferior frontal gyrus, triangular part
11	7	7	Right caudate nucleus
Cognitive action regulation (CogAR)			
X	**Y**	**Z**	**Corresponding macroanatomical brain region**
-40	-64	-12	Left fusiform gyrus
36	22	-4	Right insula
-44	10	32	Left precentral gyrus

60	-44	24	Right superior temporal gyrus
0	18	48	Supplementary motor area
-36	-46	46	Left inferior parietal gyrus
38	-46	44	Right inferior parietal gyrus
-26	0	54	Left middle frontal gyrus
Emotional scene and face processing (EmoSF)			
X	**Y**	**Z**	**Corresponding macroanatomical brain region**
4	47	7	Right anterior cingulate cortex
42	25	3	Right insula
-42	25	3	Left inferior frontal gyrus, triangular part
48	17	29	Right inferior frontal gyrus, opercular part
-42	13	27	Left inferior frontal gyrus, triangular part
-2	8	59	Left supplementary motor area
20	-4	-15	Right hippocampus
-20	-6	-15	Left amygdala
-20	-33	-4	Left hippocampus
14	-33	-7	Right lingual gyrus
53	-50	4	Right middle temporal gyrus
38	-55	-20	Right fusiform gyrus
-40	-55	-22	Left fusiform gyrus
38	-76	-16	Right inferior occipital gyrus
-40	-78	-21	Crus I of left cerebellar hemisphere
-4	52	31	Left superior frontal gyrus, medial
36	25	-3	Right insula
-38	25	-8	Left inferior frontal gyrus, pars orbitalis
2	19	25	Right anterior cingulate cortex
0	-15	10	Thalamus
-2	-31	-7	Pulvinar
-28	-70	-14	Left fusiform gyrus
46	-68	-4	Right inferior temporal gyrus
-48	-72	-4	Left inferior occipital gyrus
Perceptuo-motor network (MotorPerc)			
X	**Y**	**Z**	**Corresponding macroanatomical brain region**
20	-56	-22	Lobule VI of right cerebellar hemisphere
16	-74	-36	Crus II of right cerebellar hemisphere

14	-68	-48	Lobule VIII of right cerebellar hemisphere
-32	-50	-32	Lobule VI of left cerebellar hemisphere
0	-2	56	Supplementary motor area
26	0	2	Right putamen
-25.7	-3.3	2.1	Left putamen
-14	-18	4	Left thalamus
14	-18	4	Right thalamus
-36	18	2	Left insula
-36	-18	58	Left precentral gyrus
38	-18	58	Right precentral gyrus
-26	-4	62	Left superior frontal gyrus, dorsolateral
26	-4	56	Right superior frontal gyrus, dorsolateral
-18	-56	66	Left superior parietal gyrus
-56	4	38	Left precentral gyrus
-48	-28	20	Left rolandic operculum

Motor execution (MotorEx)

X	Y	Z	Corresponding macroanatomical brain region
-39	-21	54	Left postcentral gyrus
41	-16	57	Right precentral gyrus
-3	-2	54	Left supplementary motor area
-57	2	32	Left precentral gyrus
-53	-24	21	Left supramarginal gyrus
45	-38	48	Right inferior parietal gyrus
-23	-7	1	Left pallidum
25	-8	3	Right pallidum
-22	-52	26	Left Cerebellum
18	-54	-22	Lobule VI of right cerebellar hemisphere

Multitasking (MultiTask)

X	Y	Z	Corresponding macroanatomical brain region
-34	22	-4	Left insula
34	24	0	Right insula
-26	0	52	Left middle frontal gyrus
44	38	28	Right inferior frontal gyrus, triangular part
46	10	28	Right inferior frontal gyrus, opercular part
-6	18	50	Left supplementary motor area

-34	-52	56	Left inferior parietal gyrus
32	-52	50	Right inferior parietal gyrus
32	6	58	Right middle frontal gyrus

Reward-related decision-making (Rew)

X	Y	Z	Corresponding macroanatomical brain region
12	10	-6	Right caudate nucleus
-10	8	-4	Left caudate nucleus
36	20	-6	Right insula
-32	20	-4	Left insula
0	24	40	Superior frontal gyrus, medial
0	54	-8	Superior frontal gyrus, medial orbital
24	-2	-16	Right amygdala
6	-14	8	Right thalamus
-6	-16	8	Left thalamus
0	8	48	Supplementary motor area
8	-18	-10	Right brainstem
-6	-18	-10	Left brainstem
2	44	20	Right anterior cingulate cortex
-24	2	52	Left middle frontal gyrus
-38	-4	6	Left insula
24	40	-14	Right superior frontal gyrus, orbital part
-16	42	-14	Left superior frontal gyrus, orbital part
40	32	32	Right middle frontal gyrus
-28	-56	48	Left inferior parietal gyrus
28	-58	50	Right angular gyrus
0	-32	32	Posterior cingulate gyrus
-36	50	10	Left middle frontal gyrus
-46	42	-4	Left inferior frontal gyrus, orbital part
30	4	50	Right middle frontal gyrus
-22	30	48	Left superior frontal gyrus

Vigilant attention (VigAtt)

X	Y	Z	Corresponding macroanatomical brain region
-2	8	50	Left supplementary motor area
8	32	46	Right superior frontal gyrus, medial
0	26	34	Middle cingulate and paracingulate gyri

50	8	32	Right precentral gyrus
40	22	-4	Right insula
46	36	20	Right middle frontal gyrus
-40	-12	60	Left precentral gyrus
-46	-68	-6	Left inferior occipital gyrus
-48	8	30	Left inferior frontal gyrus, opercular part
62	-38	17	Right superior temporal gyrus
8	-12	6	Right thalamus
32	-90	4	Right middle occipital gyrus
-42	12	-2	Left insula
-10	-14	6	Left thalamus
6	-58	-18	Lobule IV, V of vermis
44	-44	46	Right inferior parietal gyrus

Working memory (WM)

X	**Y**	**Z**	**Corresponding macroanatomical brain region**
-32	22	-2	Left insula
-48	10	26	Left inferior frontal gyrus, opercular part
-46	26	24	Left inferior frontal gyrus, triangular part
-38	50	10	Left middle frontal gyrus
36	22	-6	Right insula
50	14	24	Right inferior frontal gyrus, opercular part
44	34	32	Right middle frontal gyrus
38	54	6	Right middle frontal gyrus
2	18	48	Supplementary motor area
-28	0	56	Left middle frontal gyrus
30	2	56	Right middle frontal gyrus
-42	-42	46	Left inferior parietal gyrus
-34	-52	48	Left inferior parietal gyrus
-24	-66	54	Left superior parietal gyrus
42	-44	44	Right inferior parietal gyrus
32	-58	48	Right angular gyrus
16	-66	56	Right superior parietal gyrus
-12	-12	12	Left thalamus
-16	2	14	Left caudate nucleus
-16	0	2	Left pallidum

12	-10	10	Right thalamus
-34	-66	-20	Lobule VI of left cerebellar hemisphere
32	-64	-18	Lobule VI of right cerebellar hemisphere
Extended multiple-demand network (eMDN)			
X	**Y**	**Z**	**Corresponding macroanatomical brain region**
-46	6	30	Left inferior frontal gyrus, opercular part
50	12	28	Right inferior frontal gyrus, opercular part
-32	20	2	Left insula
36	22	0	Right insula
-4	14	44	Left middle cingulate and paracingulate gyri
6	18	46	Right middle cingulate and paracingulate gyri
-32	-52	46	Left inferior parietal gyrus
32	-58	48	Right angular gyrus
44	36	20	Right middle frontal gyrus
-28	-4	52	Left middle frontal gyrus
-44	32	22	Left inferior frontal gyrus, triangular part
32	0	52	Right precentral gyrus
-20	6	4	Left pallidum
10	-12	8	Right thalamus
-46	-60	-10	Left inferior occipital gyrus
22	6	4	Right putamen
-10	-16	6	Left thalamus
Extended social-affective default (eSAD)			
X	**Y**	**Z**	**Corresponding macroanatomical brain region**
0	38	10	Anterior cingulate gyrus
-24	-10	-20	Left hippocampus
24	-8	-22	Right hippocampus
-2	-52	26	Posterior cingulate gyrus
-2	32	-8	Anterior cingulate and paracingulate gyri
-46	-66	18	Left middle temporal gyrus
50	-60	18	Right middle temporal gyrus
-2	52	14	Anterior cingulate and paracingulate gyri
-6	10	-8	Left caudate nucleus
6	10	-8	Right caudate nucleus
-2	50	-10	Superior frontal gyrus, medial orbital

-54	-10	-20	Left middle temporal gyrus

Table S5. Network coordinates and corresponding brain regions. The coordinates are reported in standard space of the Montreal Neurological Institute (MNI), labels are taken from the AAL atlas as provided by MRIcron (v1.0.20201102).

Acknowledgments

The completion of this thesis would not have been possible without the support of many individuals, for which I am deeply grateful.

First and foremost, I would like to express my gratitude to my supervisor Prof. Dr. Simon B. Eickhoff for his guidance and for providing me with the opportunity to work in such a great research environment.
A special thank you goes to Dr. Kaustubh R. Patil for his constant support, insightful feedback and expertise throughout the entire research project. I am also grateful to Dr. Robert Langner, Prof. Dr. Julian Caspers and Prof. Dr. Jürgen Dukart for their valuable contributions and participation in this project.

In addition to the academic challenges that I was able to overcome with the help of the individuals mentioned above, a project as extensive as a doctoral thesis also comes with its fair share of mental and emotional challenges. I would not have navigated these nearly as well without the support of my friends and family. A heartfelt thank you goes to Annika, Arne, Charlotte, Bahne, and Theresa for always having my back and for guiding me through moments of doubt. Max, thank you for being by my side every day, for always listening, and for standing by me through every challenge. Finally, I want to express my deepest gratitude to my parents. Thank you for allowing me to follow my path and for supporting me unconditionally, no matter what.